Effects of recombinant human erythropoietin in the cuprizone mouse model of de- and remyelination

Dissertation

for the award of the degree
“Doctor rerum naturalium”
Division of Mathematics and Natural Sciences
of the Georg-August-University Göttingen

submitted by

Nora Hagemeyer
from Göttingen

Göttingen 2012

Doctoral thesis committee

Prof. Dr. Dr. Hannelore Ehrenreich (Advisor, First Referee)
Division of Clinical Neuroscience
Max Planck Institute of Experimental Medicine
Hermann-Rein-Straße 3
37075 Göttingen

Prof. Dr. Thomas Bayer (Second Referee)
Division of Molecular Psychiatry
Department of Psychiatry
University of Göttingen
Von-Siebold-Straße 5
37075 Göttingen

Prof. Dr. Klaus-Armin Nave
Department of Neurogenetics
Max Planck Institute of Experimental Medicine
Hermann-Rein-Straße 3
37075 Göttingen

Date of submission of the thesis: March 31, 2012

Date of oral examination: May 18, 2012

Declaration

I hereby declare that this thesis has been written independently with no other sources or aids than quoted.

Göttingen, March 31, 2012 Nora Hagemeyer

Acknowledgements

I would like to thank everybody who has contributed to the success of my doctoral thesis.

First of all I would like to express my gratitude to Prof. Hannelore Ehrenreich for giving me the opportunity to work on very interesting projects under her supervision in her lab and for her continuous support and guidance during my whole PhD period. Furthermore I want to thank the additional members of my thesis committee, Prof. Thomas Bayer and Prof. Klaus-Armin Nave, for their important advice and constructive criticism.

I want to thank Susann Boretius for all her contributions to the studies and for the open minded conversations we always had.

I am particularly grateful to Swetlana Sperling, Anja Ronnenberg and Kathrin Hannke for their outstanding support during the last years, and Christoph Ott, Axel von Streitberg and Henrike Welpinghus for their great assistance of the analyses of the 'cuprizone project'. It was a pleasure for me to be your supervisor. Many thanks to Sergi Papiol as well as the entire behavior team; you all encouraged me a lot.

I very much enjoyed the friendly, supportive and helpful working atmosphere in our lab – therefore I would like to thank all the present and past members of the Division of Clinical Neuroscience, especially Liane Dahm, Sabrina Grube, Imam Hassouna, Erin Choi, Bartosz Adamcio and Derya Sargin.

Thanks to Anton Safer for his expertise concerning statistics.

I want to thank my family and friends for all their continuous motivation and encouragement during the last years.

And last, but not least, special thanks to Micha.

My utmost thanks to my parents Renate & Michael Hagemeyer
for their never-ending love, support and encouragement.

TABLE OF CONTENTS

SUMMARY 11
1 INTRODUCTION 12
1.1 Cuprizone 12
1.2 The cuprizone animal model 13
1.2.1 Early history and development of the animal model 13
1.2.2 The cuprizone model of demyelination and remyelination 18
1.2.2.1 Characterization of cuprizone-induced damage 18
1.2.3 Cuprizone model and treatment strategies 32
1.3 Erythropoietin 38
1.3.1 Properties and pathways 38
1.3.2 Erythropoietin and oligodendrocytes 39
1.4 Scope of the thesis 40
2 MATERIALS AND METHODS 42
2.1 Animals 42
2.2 Preparation of cuprizone containing food 42
2.3 Erythropoietin administration 42
2.4 Measurement of the haematocrit 43
2.5 Experimental design 43
2.5.1 Pilot experiments 43
2.5.2 Investigation of EPO on remyelination 44
2.5.3 Investigation of EPO on demyelination 45
2.6 Behavioral testing 46
2.6.1 Rota-rod 46
2.6.2 Beam balance 47
2.7 Assessment of hearing 48
2.7.1 Startle response of mice 48
2.7.2 Recording of auditory brain stem responses (ABRs) 49
2.8 MRI analysis 50
2.9 Staining of mouse brains 51
2.10 Intra- and Interrater reliability 54
2.11 Western blot analysis 54
2.12 Isolation of total RNA and quantitative real-time RT-PCR (qPCR) 57
2.13 Statistical analysis 59
3 RESULTS 60
3.1 Establishment of the cuprizone model 60
3.2 Effect of EPO on re- and demyelination 63
3.2.1 Overview of analyzed parameters 63

3.2.2 Effect of EPO on remyelination 64
3.2.2.1 Basic observations under cuprizone and EPO treatment 64
3.2.2.2 Motor coordination and balance under cuprizone and EPO treatment. 66
3.2.2.3 Startle response of mice 67
3.2.2.4 Analysis of myelin proteins in the hippocampus and cortex 69
3.2.2.5 Volumetrical analysis of cuprizone-fed mice 70
3.2.3 Effect of EPO on demyelination 72
3.2.3.1 Basic observations under cuprizone and EPO treatment 72
3.2.3.2 Motor coordination and balance under cuprizone and EPO treatment. 73
3.2.3.3 Startle response of mice 75
3.2.3.4 Volumetrical analysis of cuprizone-fed mice 76
3.2.3.5 Examination of mature and precursor oligodendrocytes at week 6 77
3.2.3.6 Analysis of microglia and axonal degeneration at week 6 79
3.2.3.7 Expression of cytokines and mircoglia activity markers at week 6 82
4 DISCUSSION 83
4.1 Establishment of the cuprizone model 83
4.2 Effect of EPO on remyelination 84
4.3 EPO effect on demyelination 87
4.4 Limitations of the model 89
4.5 Final conclusion 90
5 LITERATURE 91
6 SUPPLEMENT 99
6.1 Certificate of the toxicological analysis of cuprizone pellets 99
6.2 Accepted first-author and co-author publications 100
6.2.1 Publication of first-authorship 1 100
6.2.2 Publication of first-authorship 2 100
6.2.3 Publication of co-authorship 1 101
6.2.4 Publication of co-authorship 2 101
6.3 Curriculum vitae 102

ABBREVIATIONS

ABR	Auditory brain stem response
AEP	Acoustic evoked potential
APC	Adenomatous polyposis coli
APP	Amyloid precursor protein
AU	Arbitrary unit
BBB	Blood-brain-barrier
BrdU	Bromodeoxyuridine
C1qA	Complement component 1, q subcomponent, A chain
CC	Corpus callosum
CCL2	Chemokine (C-C motif) ligand 2
CCR2	Chemokine (C-C motif) receptor 2
CD	Cluster of differentiation
CGT	Ceramide galactosyl transferase
cm	Centimeter
CNP	2’,3’-cyclic nucleotide 3'-phosphodiesterase
CXCR2	CXC chemokine receptor-2
DAB	Diaminobenzidine
DBH	Dopamine beta hydroxylase
ddH_20	Double distilled water
$Dist_{ac}$	Accumulative distance in meters
D_{max}	Maximum run duration
DTI	Diffusion tensor imaging
EAE	Experimental autoimmune encephalomyelitis
EDTA	Ethylendiamin-tetraacetat
EEG	Electroencephalography
EGTA	Ethylene glycol tetraacetic acid
EM	Electron microscopy
EPM	Elevated plus maze
EPO	Erythropoietin
EPOR	Erythropoietin receptor
FAE	Fumaric acid esters
FGF2	Fibroblast-growth-factor 2
GAPDH	Glyceraldehyde-3-phosphate dehydrogenase
GFAP	Glial fibrillary acidic protein
GST-pi	Glutathione S-transferase-pi
H&E	Haematoxylin & Eosin

HPRT1	Hypoxanthin-Phosphoribosyltransferase 1
i.p.	Intra-peritoneal
IBA-1	Ionized calcium binding adapter molecule-1
IFN-γ	Interferon-gamma
IGF-1	Insulin-like growth factor-1
IL-1ß	Interleukin-1ß
IL-1α	Interleukin-1α
IU	International unit
Jak2	Janus kinase 2
kDa	Kilodalton
LFB-PAS	Luxol Fast Blue-periodic acid Schiff
MAG	Myelin associated glycoprotein
MAO	Monoamine oxidase
MBP	Myelin basic protein
MHC	Major histocompatibility complex
MIP-1α	Macrophage-inflammatory protein-1 alpha
mm	Millimeter
MOG	Myelin oligodendrocyte glycoprotein
MOSS	Motor skill sequence
MP	Methylprednisolone
MRI	Magnetic resonance imaging
MS	Multiple sclerosis
ms	Milliseconds
MTR	Magnetization transfer ratio
µl/µmol	Microliter/Micromole
Na_3VO_4	Sodium orthovanadat
NaCl	Natrium chloride
NAD	Nicotinamide adenine dinucleotide
NaF	Natriumfluoride
NaOH	Natriumhydroxid
NG2	Nerve/glial antigen 2
Nogo-A	Neurite outgrowth inhibitor-A
NOS (i;n;e)	Nitric oxide synthase (inducible; neuronal; endothelial)
N_{run}	Number of individual runs
Olig	Oligodendrocyte transcription factor
PBS	Phosphate buffered saline
PDGFRα	Platelet-derived growth factor receptor-alpha

PFA	Paraformaldehyde
PFC	Prefrontal cortex
PI3K	Phosphatidylinositol 3-kinase
PL	Placebo
PLP	Proteolipid protein
pmol	Picomol
PPI	Pre-pulse-inhibition
ppm	Parts per million
qPCR	Quantitative real-time RT-PCR
Ras-MAPK	Ras-mitogen-activated protein kinase
RCA-1	Ricinus communis agglutinin-1
RNA/mRNA	Ribonucleic acid/ messenger Ribonucleic acid
ROI	Region of interest
rpm	Resolutions per minute
s	Seconds
SDS	Sodium dodecyl sulfate
SEM	Standard error of the mean
Shh	Sonic hedgehog
SLM	Stratum lacunosum moleculare
SMI-32	Neurofilament H non-phosphorylated
Stat	Signal transducers and activators of transcription
T_3	Triiodothyronine
TBST	Tris-buffered saline + Tween20
TGF-β	Transforming growth factor-β
TNFR	Tumor necrosis factor receptor
TNFα	Tumor necrosis factor alpha
Trem-2	Triggering receptor expressed on myeloid cells-2
Tris HCL	Tris(hydroxymethyl)aminomethane hydrochloride
TWEAK	TNF-like weak inducer of apoptosis
U	Unit
v/v	Volume per volume
V_{max}	Maximum running velocity (resolutions/minute)
w/v	Weight per volume
WB	Western blot

SUMMARY

Erythropoietin (EPO) has potent neuroprotective/neuroregenerative properties in various forms of experimental autoimmune encephalomyelitis (EAE), i.e. established rodent models of acute multiple sclerosis (MS), and in patients suffering from chronic progressive MS. However, the mechanisms of EPO action in these conditions is still not clear. In particular, studies on potential effects of EPO on oligodendrocytes/myelin in the absence of immune-inflammatory components, which are characteristic for acute MS but not for the chronic progressive state of the disease, are lacking. Therefore, in this PhD thesis, the cuprizone mouse model was employed to investigate the effect of EPO on toxic demyelination. This model allows investigation of myelination processes independent of T-cell mediated inflammation. Feeding of mice with 0.2% cuprizone mixed into ground chow results in demyelination of the corpus callosum, whereas withdrawal of the toxin leads to spontaneous remyelination. The hypothesis of the present thesis was that EPO modulates both, cuprizone-induced demyelination and the remyelination upon toxin-withdrawal. Two study designs were chosen to investigate the effects of EPO in a clinically most relevant manner: (1) EPO treatment was started immediately after cessation of 6 weeks of cuprizone feeding, i.e. at the time point of full damage and initiation of recovery/remyelination, or (2) EPO was given after 3 weeks of toxin application and continued for 3 weeks until cessation of cuprizone feeding to catch the demyelination phase. For both study parts, a 'double-blind' (for food/injections), placebo-controlled, longitudinal 4-arm design, using 8 week old male C57BL/6 mice, was applied. Target parameters included behavioral analyses, magnetic resonance imaging, and histology, as well as measurement of protein and mRNA levels. The cuprizone mouse model emerged as a highly variable animal model, making deeper mechanistic analyses of EPO effects difficult. Despite these limitations and a lack of clear effects of EPO on remyelination, EPO showed surprisingly distinct results when applied during the demyelination phase. Immediately after termination of cuprizone feeding, EPO revealed beneficial effects on vestibulomotor function/coordination, magnetic resonance imaging readouts and inflammation, as reflected by the number of microglia in the corpus callosum. Importantly, for the first time, EPO was found to reduce axonal degeneration in brain white matter tracts. These findings are of high relevance with respect to novel treatment strategies for demyelinating diseases such as MS.

1 INTRODUCTION

My PhD thesis is based on two projects, which both resulted in first author publications enclosed in the supplement of this thesis. In the first paper, "Erythropoietin attenuates neurological and histological consequences of toxic demyelination in mice," consequences of cuprizone-induced demyelination and the effect of erythropoietin (EPO) as a potential treatment strategy on these parameters were investigated. The second study, "A myelin gene causative of a catatonia-depression syndrome upon aging," analyzed the pathophysiological consequences of an altered expression of the myelin gene 2',3'-cyclic nucleotide 3'-phosphodiesterase (CNP). Additionally, two co-author publications are enclosed.
In this PhD thesis, I would like to focus on my main project analyzing the effect of EPO on de- and remyelination processes. I will elaborate mainly upon unpublished data of this project and include the published data as well.

1.1 Cuprizone

The discovery of cuprizone (oxalic acid bis(cyclohexylidene hydrazide) as an agent with copper chelating properties dates back to the 1950s. Gustav Nilsson demonstrated that cuprizone reacts with copper to produce a stable blue color and that this reaction was very sensitive even at low concentrations of copper (Nilsson, 1950). The technique was further described as a tool to detect copper levels in pulp and paper, in iron, steel and ferrous alloys and even in serum (Peterson & Bollier, 1955; Wetlesen, 1957). The cuprizone-copper complex has a molar absorbance at 595 nm and is stable at a pH of 7-9 (Benetti et al, 2010; Messori et al, 2007; Peterson & Bollier, 1955). However, the exact chemical property of the cuprizone-copper complex that results in an intense blue color is still not completely understood and is described to be rather complex. On one hand, it is suggested that cuprizone in the cuprizone-copper complex stabilizes copper (III); on the other hand, it is shown that only copper (II) is present in the cuprizone-copper complex (Benetti et al, 2010; Messori et al, 2007; Zatta et al, 2005).

1.2 The cuprizone animal model

1.2.1 Early history and development of the animal model

The initial idea of the cuprizone model was to mimic copper deficiency in animals. Copper is an essential trace element and it was observed that copper deficit in the food of pregnant ewes can lead to neurological impairments and lesions of demyelination in offspring. However, the proper animal model to study the cause and pathogenesis of the disease was missing (Carlton, 1966). In 1966 Carlton had the idea to use copper-chelating agents in experimental animals to mimic a copper deficiency and to study its consequences (Carlton, 1966). He used weanling male mice or pregnant mice and fed them cuprizone in a dose of 0.1% or 0.5% mixed into a chicken mash diet for 7 weeks. Additionally, he analyzed the effect of 0.5% cuprizone supplemented with different concentrations of copper sulfate. The lower dose of cuprizone resulted in slightly reduced growth, cerebellar edema and demyelination in weanling mice but did not affect pregnancy. However, high-dose cuprizone led to an increased mortality in the offspring of pregnant mice and a severe decrease in growth, increased mortality, paresis, cerebellar edema, demyelination and hydrocephalus in weanling mice. In general, supplementation of copper sulfate did not change the effect of cuprizone. After this first report of cuprizone application in mice, several studies followed to further characterize the model. The first two subsequent studies were performed by Carlton himself, wherein he demonstrated that spongy degeneration, astrogliosis and hydrocephalus were present at early stages (weeks 2-5) of cuprizone intoxication; myelin loss was first present at week 9. Moreover, it was seen that with increasing age, mice were less susceptible to 0.5% cuprizone (Carlton, 1967). Interestingly, it was observed that rats and guinea pigs were less susceptible to cuprizone than mice, showing a difference between species (Carlton, 1969; Love, 1988). Other studies confirmed previous findings in cuprizone-fed mice of an elevated mortality rate, hydrocephalus, status spongiosus and reactive/hypertrophic astrocytes, which were mainly studied in cerebellar white matter but described as well e.g. in brain stem, cerebellar cortex, hippocampus and corpus callosum (Blakemore, 1972; Kesterson & Carlton, 1971; Pattison & Jebbett, 1971; Pattison & Jebbett, 1973; Suzuki & Kikkawa, 1969; Venturini, 1973). It was specified that the histopathological changes occured bilaterally (Pattison & Jebbett, 1971). The formation of vacuoles in myelin sheaths and swollen astrocytes were thought to be possible causes of spongy degeneration in the brain stem and both

cerebral and cerebellar white matter (Suzuki & Kikkawa, 1969; Venturini, 1973). Additionally, enlarged and giant mitochondria in the liver were found in the same two studies, revealing toxic adverse effects in the peripheral system under cuprizone treatment. Meanwhile, Pattison and Jebbett were the first to describe potential for recovery in the cuprizone model. Mice of the BSVS strain were repeatedly fed with 0.5% cuprizone, followed by a normal food diet after the first and second “cuprizone-cycle”. They found all known histopathological changes during the first and second cycle of cuprizone feeding. In both periods of normal food, mice recovered from the previous symptoms and only slightly enlarged ventricles could still be seen at the end of the recovery phase (Pattison & Jebbett, 1973). This finding was important for future studies. Up until this point, all investigators had mainly focused on the aspect of spongy degeneration, a common finding in neurological disorders like scrapie disease. Blakemore was the first to put attention on the degeneration of oligodendrocytes and reported an increase of microglia upon cuprizone intoxication (Blakemore, 1972). With electron microscopy he observed degenerated oligodendrocytes early after cuprizone intoxication, followed by demyelinated axons and the appearance of remyelinating oligodendrocytes in several brain regions. Since then, degeneration of oligodendrocytes became the main focus in the cuprizone model and it developed into a model which allows investigation of de- and remyelination processes.

A detailed description of these studies is presented in Table 1.

Table 1: Early history and development of the cuprizone model.

Author	Year	Species	Experimental set-up	Results	Remarks
Carlton	1966	Weanling male mice	Male weanling mice: 7 week feeding with ***Trial 1:*** 0.1% cuprizone ***Trial 2:*** 0.5% cuprizone ***Trial 3:*** 0.5% cuprizone + copper sulfate	***Trial 1:*** Slightly reduced growth; cerebellar edema and demyelination. ***Trial 2:*** Severely decreased growth; increased mortality; weakness in mice, paresis evident; cerebellar edema and demyelination; hydrocephalus. ***Trial 3:*** No effect of added copper on brain lesions.	Region analyzed: cerebellum
		Pregnant mice	Pregnant mice: cuprizone (0.1 or 0.5%) feeding started on day 3 or 9 of gestation ± copper sulfate	0.1% cuprizone did not affect pregnancy. 0.5% cuprizone: no delivery when feeding started on day 3; increased percentage of nonviable young when feeding started at day 9; increased number of viable young by supplementation of 130ppm copper.	
Carlton	1967	Weanling albino male mice	***Trial 1:*** Feeding of weanling mice with cyclohexanone & oxaldihydrazide (chemical precursors of cuprizone) for 7 weeks ***Trial 2:*** Supplementation of several vitamins and a vitamin mixture to 0.5% cuprizone diet for 7 weeks ***Trial 3:*** Supplementation of Diurill to 0.5% cuprizone diet for 7 weeks ***Trial 4:*** Supplementation of 130ppm/260ppm copper to 0.2% cuprizone diet for 7 weeks	***Trial 1:*** Feeding of the chemical precursors of cuprizone had no toxic effects. ***Trial 2:*** A vitamin mixture, riboflavin and vitamin A supplement reduced the mortality rate; no further effects. ***Trial 3:*** No effect of Diurill supplement. ***Trial 4:*** 130ppm copper reduced incidence of hydrocephalus.	Region analyzed: cerebellum
		4-8 week old male mice	***Trial 5:*** 4 or 8 week old male mice received 0.5% cuprizone diet for 8 weeks ***Trial 6:*** Time scale experiment, feeding of 0.3% cuprizone and weekly analysis of mice	***Trial 5:*** With increasing age at the start of cuprizone feeding fewer mice developed hydrocephalus. ***Trial 6:*** Spongy degeneration observed after 2 weeks; astrogliosis occurred at week 4; hydrocephalus observed at week 5; myelin loss apparent after 9 weeks.	

Carlton	1969	Weanling albino male rats	Rats: Feeding with 0.1, 0.5, 1 or 1.5% cuprizone over 8 weeks	0.5% cuprizone: increased mortality rate; enlarged and swollen astrocytes, edema and status spongiosus in several brain regions. 1 & 1.5% cuprizone: Death of half of the rats in weeks 3-4. No hydrocephalus observed.	Rats and guinea pigs used; effects in general milder than in mice
		Male albino guinea pigs	Guinea pigs: Feeding with 0.5, 0.75 or 1% cuprizone over 21 weeks	0.75% cuprizone: higher mortality rate. 1% cuprizone: mortality rate further increased; small lesions present; no hydrocephalus observed.	
Suzuki & Kikkawa	1969	Weanling Swiss-Webster male mice	Feeding of 0.5% cuprizone up to 3 weeks	CNS: Status spongiosus (most prominent in brain stem and cerebellar white matter) caused by formation of vacuoles in myelin sheaths and in the cytoplasm of glial cells. Liver: Giant mitochondria and proliferation of the smooth endoplasmic reticulum.	
Kesterson & Carlton	1970	Weanling Swiss albino male mice	Feeding of 0.3, 0.5 or 0.75% cuprizone up to 8 weeks	Induction of hydrocephalus occurred secondary to stenosis of the aqueduct of Sylvius. May have resulted due to pressure exerted by the surrounding edematous tissue. (Normal CSF secretion)	
Pattison & Jebbett	1971	4-6 week old BSVS mice	Feeding of 0.5% cuprizone up to 60 days	Increased mortality rate; extracellular vacuolation and hypertrophic astrocytes in cerebellar white matter, pons and midbrain (bilaterally)	
Kesterson & Carlton	1971	Weanling Swiss albino male mice	Feeding of 0.3% cuprizone up to 8 weeks	Status spongiosus (prominent in thalamus, cerebellar medulla, reticular formation, corpus callosum, cerebellar peduncle, internal capsule, pes pedunculi, medial geniculate body, cerebellar folia); edema (cerebral cortex, basal ganglia, hippocampus); reactive astrocytes (cerebral cortex, putamen, hippocampus, caudate putamen, corpus callosum, ventral thalamic nucleus, cerebellar folia, cerebellar nucleus). Increased activity of several enzymes in astrocytes, most prominently: glutamate dehydrogenase, NAD diaphorase	
Pattison & Jebbett	1973	3-6 week old BSVS female mice	Feeding of 0.5% cuprizone 1, 2, 3, 4, or 6 weeks followed by 60 days with normal food	Confirmation of previous studies: mortality rate increased; older mice less vulnerable to cuprizone. After 60 day recovery: no changes in mice fed for 1, 2 or 3 weeks with cuprizone before; rarefaction of tissue in vicinity to slightly dilated ventricles in mice fed with cuprizone for 4 and 6 weeks.	Variation noted Repeated treatment
			Repeated feeding: 37 days cuprizone followed by 52 days normal food, again cuprizone for 38 days followed by 52 days normal food	Repeated feeding: Spongiform vacuolation, dilatation of ventricles and increased number of astrocytes and microglia after 37days cuprizone, after 34 days on normal diet only slightly dilated ventricles detected. Histopathology in second cuprizone cycle similar to the first, no changes after second cycle of withdrawal of cuprizone. Fast physical recovery after cuprizone withdrawal.	

Venturini	1973	30 day old Swiss male mice	Feeding with 0.5% cuprizone or copper-chelated cuprizone up to 4 weeks	Growth retardation; impaired motility of hind limbs; status spongiosus (brain stem and cerebral and cerebellar white matter) due to vacuoles within the myelin sheaths and swollen astrocytes. Enlarged and giant mitochondria in liver cells. In brain and liver: Reduced activity of monoamine oxidase and cytochrome oxidase; increased activity of succinate dehydrogenase. Decreased dry weight of brains after cuprizone treatment; increased Na^+ levels, decreased K^+ and Cu^+ levels in brain tissue. Feeding of copper-chelated cuprizone: no degenerative effects.	

1.2.2 The cuprizone model of demyelination and remyelination

The first discovery of cuprizone-induced degeneration of oligodendrocytes and demyelination led to further characterization of the model. The first studies focused on the superior peduncle and found that feeding of weanling ICI male mice with 0.5% cuprizone resulted in a distinct time course of demyelination which started at week 2, peaked at week 5 and stayed constant until week 8; morphological changes in astrocytes and microglia were observed (Blakemore, 1973a). It was seen that withdrawal of cuprizone from the diet for 6 weeks led to remyelination, however, myelin sheaths were thinner compared to control mice (Blakemore, 1973b). Similar results from others confirmed the potential of remyelination by withdrawal of cuprizone (Blakemore, 1974; Ludwin, 1978) and made the model even more interesting to study not only the aspect of demyelination but also remyelination. However, some variations in the time course of de- and remyelination between different studies could be the result of a different susceptibility of older mice and different mouse strains to cuprizone, as well as variations in the cuprizone concentrations used (Blakemore, 1974; Carlton, 1967; Ludwin, 1978). Since it was discovered that 8-10 week old C57BL/6 mice fed with 0.2% cuprizone showed clear demyelination of the corpus callosum, but did not show liver toxicity, this strain was preferentially used in future studies (Hiremath et al, 1998). Moreover, the corpus callosum became the main target region for the analysis of myelination (for detailed descriptions of the studies please see Table 2). A generally important characteristic of the cuprizone model is to find an intact blood-brain-barrier (BBB) (Bakker & Ludwin, 1987; Kondo et al, 1987).

1.2.2.1 Characterization of cuprizone-induced damage

Demyelination and remyelination in the corpus callosum are mainly studied histologically using Luxol Fast Blue-periodic acid Schiff (LFB-PAS) and immunohistochemically using different markers for myelin proteins (e.g. myelin basic protein (MBP), proteolipid protein (PLP)). These techniques allow a subjective (observer blinded) semi-quantitative analysis by rating the staining on a scale of severity of demyelination. A more precise but labor intensive analysis of myelin via electron microscopy is less frequently performed. Consequences of cuprizone intoxication on myelin in the corpus callosum are studied after acute (6 weeks) or chronic (12-16 weeks) application. Figure 1 summarizes the morphological and

cellular changes in the corpus callosum after acute cuprizone feeding as described in detail below. Demyelination after acute administration of cuprizone starts at week 3 and is almost complete in weeks 5-6 (Gao et al, 2000; Hiremath et al, 1998; Mana et al, 2006; Matsushima & Morell, 2001; Merkler et al, 2005; Morell et al, 1998; Remington et al, 2007). Interestingly, intrinsic remyelination already starts at week 6 of cuprizone feeding (Irvine & Blakemore, 2006; Mason et al, 2000; Mason et al, 2001a). Long-term feeding of cuprizone induces episodic de- and remyelination within the corpus callosum, showing the potential of intrinsic remyelination by weeks 6 and 12 even during continuous application of cuprizone (Mason et al, 2001a). Withdrawal of cuprizone after acute demyelination leads to almost complete remyelination on an immunohistochemical level over 6 weeks, whereas remyelination after chronic cuprizone treatment leads to a slower and incomplete remyelination even after 12 weeks (Armstrong et al, 2006; Crawford et al, 2009; Lindner et al, 2008; Mason et al, 2001a; Matsushima & Morell, 2001; Morell et al, 1998). Based on electron microscopy, however, it is known that the recovery of myelin even 6 weeks after acute demyelination is also still incomplete (Crawford et al, 2009; Lindner et al, 2008; Merkler et al, 2005). During demyelination the expression levels of several myelin genes are altered; MBP, myelin associated glycoprotein (MAG), ceramide galactosyl transferase (CGT), and PLP are gradually downregulated starting at week 1 and reaching a minimal expression level in weeks 2-4. Interestingly, re-expression of the genes starts already at week 5, and at the beginning of the recovery phase, the gene expression is even higher compared to controls (Gao et al, 2000; Morell et al, 1998).

Oligodendrocytes are the myelinating cells in the central nervous system and of special interest for evaluation in the cuprizone model. The characterization of the effect of cuprizone on oligodendrocytes is mainly based on immunohistochemistry using the antibodies: glutathione S-transferase-pi (GST-pi), adenomatous polyposis coli (APC) CC-1 and Nogo-A, for mature oligodendrocytes and nerve/glial antigen 2 (NG2) or platelet-derived growth factor receptor-alpha (PDGFRα) for precursor oligodendrocytes. The number of mature oligodendrocytes gradually decreases upon acute cuprizone intoxication reaching the lowest levels in weeks 5-6 and an intrinsic reappearance of oligodendrocytes is observed at week 6. After 2 weeks of remyelination, oligodendrocytes are already further increased and reach control levels until week 10. The number of precursor oligodendrocytes increases until

weeks 3-5 and is followed by a slight decrease. However, the overall number remains elevated even at week 10 of recovery (Arnett et al, 2001; Crawford et al, 2009; Gudi et al, 2009; Mason et al, 2000; Matsushima & Morell, 2001). Chronic demyelination leads to a depletion of mature oligodendrocytes until weeks 5-6, however, a population of cells reappears until week 12 of cuprizone feeding. In this condition, precursor oligodendrocytes increase until week 5 but are progressively lost upon further intoxication (Mason et al, 2004). Oligodendrocytes are mainly depleted by apoptosis (Mason et al, 2000; Mason et al, 2004). Astrocytes are gradually upregulated and hypertrophic during acute demyelination and stay at a high level in the recovery phase (Crawford et al, 2009; Gudi et al, 2009; Hiremath et al, 1998). A similar pattern is observed under chronic conditions (Lindner et al, 2009). The number of microglia is highly upregulated with a peak in weeks 5-6 during acute and chronic demyelination. Removal of cuprizone after 6 weeks leads to a fast decline to control levels 2-5 weeks later (Arnett et al, 2001; Gudi et al, 2009; Hiremath et al, 1998; Lindner et al, 2009; Mason et al, 2004; Merkler et al, 2005; Morell et al, 1998). During chronic exposure, microglia decline but stay elevated after week 6, and during a following recovery phase, microglia are present at a very low level (Lindner et al, 2009; Mason et al, 2004). It is suggested that microglia increase their phagocytic activity during cuprizone-induced demyelination (Voss et al, 2012). Acute axonal degeneration (investigated with the antibody amyloid precursor protein (APP)) is present 3-6 weeks after cuprizone intoxication (Crawford et al, 2009; Lindner et al, 2009; Merkler et al, 2005; Song et al, 2005) and suggested to gradually decrease after weeks 3-4 (Lindner et al, 2009; Song et al, 2005). Results for an additional marker for axonal degeneration (Neurofilament H non-phosphorylated (SMI-32)) are rare and so far inconclusive (Lindner et al, 2009; Sun et al, 2006). Swollen and dystrophic axons are observed with electron microscopy 5-6 weeks after cuprizone feeding and can even be found in the first 2 weeks of recovery (Irvine & Blakemore, 2006; Stidworthy et al, 2003). Furthermore, functional axon damage is seen by a conduction deficit during demyelination, which is not fully recovered by a 6 week remyelination period (Crawford et al, 2009).

Cuprizone-induced demyelination is not restricted to the corpus callosum and additionally present in the cortex, hippocampus and cerebellum (Groebe et al, 2009; Hoffmann et al, 2008; Koutsoudaki et al, 2009; Norkute et al, 2009; Skripuletz et al,

2008; Skripuletz et al, 2010b). Please find a detailed summary of the main cuprizone articles in Table 2.

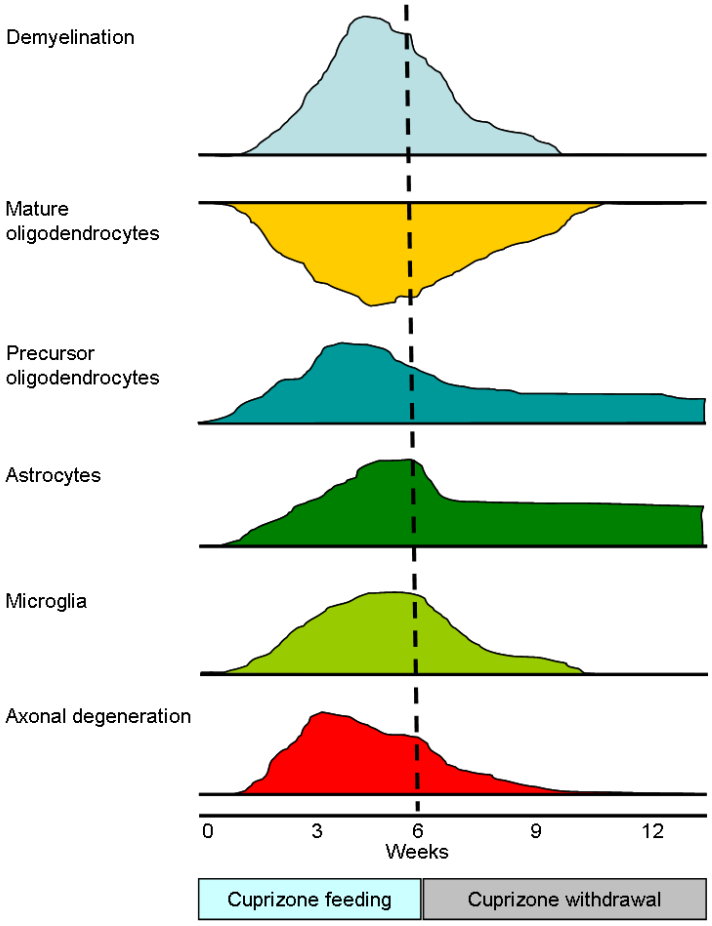

Figure 1: Overview of the morphological and cellular changes during acute cuprizone feeding for 6 weeks and within a 6 week recovery period.

Table 2: The cuprizone model of de- and remyelination. Studies are sorted chronologically within the subgroups. Antibodies and/or methods used are given in brackets.

Author	Year	Species	Experimental set-up	Results	Remarks
Blakemore	1972	Weanling albino ICI male mice	Feeding of 0.5% cuprizone for 1, 2, 4 and 5 weeks	From 1st week on: Astrocytosis (cerebral cortex, caudate-putamen, thalamus, midbrain); status spongiosus (internal capsule, anterior commissure, thalamus, midbrain, cerebellum, white matter of cerebellum); degenerated oligodendrocytes (cerebral cortex and white matter). Increased number of microglia at week 3. Remyelinating oligodendrocytes and a large number of demyelinated axons present at week 5.	First focus on oligodendrocytes
Analysis in the superior peduncle					
Blakemore	1973 a	Weanling albino ICI male mice	Feeding with 0.5% cuprizone up to 8 weeks	From 2nd week on: Degenerated oligodendrocytes. Demyelination peaked at week 5 and stayed constant until week 8; demyelination accompanied by morphological changes of astrocytes and microglia, cells described as remyelinating oligodendrocytes during demyelination.	
Blakemore	1973 b	Weanling male mice	Feeding with 0.5% cuprizone for 5 weeks followed by normal food up to 6 weeks	Withdrawal of cuprizone from the diet: Induction of remyelination. After 4-6 weeks almost all axons remyelinated (~ 88%). Remyelinated sheaths thinner, axon-fiber diameter ratio not back to control levels.	Remyelination capacity
Blakemore	1974	9 month old albino ICI male mice	Feeding of 0.75% cuprizone up to 10 weeks followed by normal food up to 12 weeks	Start of demyelination at week 7 of feeding, almost complete at week 10. Almost complete remyelination after 6 and 12 weeks on normal diet. Remyelinated sheaths thinner compared to controls.	
Ludwin	1978	Weanling Swiss male mice	Feeding of 0.6% cuprizone for 6-7 or up to 25 weeks. The 6-7 week feeding period was followed by normal feeding up to 18 weeks	Weeks 1-4 of cuprizone: Higher mortality rate. Hydrocephalus in most of the mice. Degeneration of oligodendrocytes from 2 weeks on; almost complete demyelination at week 7, no further change in the grade of demyelination thereafter. Peak of phagocytic macrophages at week 5 followed by a decrease. Reactive astrocytes and other undefined reactive and immature cells present at week 4. Recovery: Fast capacity of remyelination until week 4 but slow capacity until week 18. Myelin sheaths only reached ~ 50% of normal myelin thickness.	
Love	1988	Weanling male Wistar rats	Feeding of 0.5, 1 or 2% cuprizone up to 15 weeks. 3 rats fed with 0.1% cuprizone were returned to normal diet after 10 weeks.	Feeding of 1 or 2% cuprizone: higher mortality, weakness and wasting; intramyelinic edema (cerebral white matter, hilum of the dentate nucleus and superior cerebellar peduncle), rarely degenerated oligodendrocytes, no demyelination. Mild axonal degeneration in sciatic nerve. Complete recovery after 3 weeks of withdrawal of cuprizone.	Rats not severely affected by cuprizone

Analysis of the blood-brain-barrier (BBB)					
Bakker & Ludwin	1987	Weanling CD1 mice	Feeding of 0.5-0.6% cuprizone over 9 weeks	BBB proven to not be permeable by horseradish peroxidase tracer method & immunohistochemically using antisera to extravasated serum proteins. Mice with cortical lesions served as positive control.	Tracer studies
Kondo, Nakano & Suzuki	1987	3 week old Swiss-Webster male mice	Feeding of 0.5% cuprizone up to 9 weeks	BBB proven to not be permeable by the horseradish peroxidase tracer method (cerebrum, brainstem, spinal cord).	Tracer studies
Analysis in the corpus callosum (CC)					
Hiremath et al.	1998	8-10 week old C57BL/6J male mice	Feeding of 0.1 to 0.6% cuprizone for 6 weeks	Severe body weight loss with increasing cuprizone concentration. Liver only affected under 0.4% and 0.5% cuprizone. Complete demyelination (LFB, MBP) of the CC with 0.2-0.5% cuprizone at week 6.	C57BL/6 mice introduced & analysis of the corpus callosum
			Feeding of 0.2% cuprizone over 6 weeks; mice were sacrificed weekly	Start of demyelination at week 3; completion of demyelination at week 6; no further detrimental toxic effects. Astrocytosis paralleled to demyelination; microglia/macrophages (RCA-1) appeared in the 1st week & increased further.	
Morell et al.	1998	6 week old C57BL/6J mice	Feeding of 0.2% cuprizone up to 6 weeks followed by normal food up to 6 weeks	~20% body weight loss within 1st week; demyelination (LFB) in CC started at week 3, maximal in weeks 4-6. MBP, MAG & CGT-mRNA levels decreased at week 1, minimal at week 3, returned to normal levels until week 6; elevated expression levels at the beginning of recovery. Microglia (RCA-1; lysozyme) followed pattern of demyelination.	
Gao et al.	2000	8 week old C57BL/6 & IFN-γ transgenic male mice	Feeding of 0.2% cuprizone for up to 6 weeks	IFN-γ transgenic mice (very low level of IFN-γ expression): Resistant to cuprizone-induced demyelination in the CC; no changes on the number of astrocytes, microglia & apoptotic cells. MBP & PLP-mRNA levels decreased in weeks 2-4. IGF-1 increased.	Role of IFN-γ in demyelination
Mason et al.	2000	8 week old C57BL/6J male mice	Feeding of 0.2% cuprizone up to 6 weeks followed by normal food up to 6 weeks	Mature oligodendrocytes (GST-pi) almost completely depleted (largely by apoptosis) at week 6 and reappeared during remyelination phase. $NG2^+$ cell proliferation in the subventricular zone and accumulation in the CC upon demyelination (peak at week 4). $NG2^+$ cells switched from a bipolar to a branch-like phenotype in advance to the repopulation of GST-pi^+ cells. IGF-1 expression upregulated with a peak at week 4 and remained elevated until week 7 (potentially involved in remyelination).	
Mason et al.	2001 a	8 week old C57BL/6J mice	Feeding of 0.2% cuprizone up to 16 weeks or for 6 weeks followed by normal food up to 6 weeks	Long-term feeding induced episodic de- and remyelination (intrinsic remyelination at weeks 6 and 12); cuprizone feeding decreased axon diameter & thickness of myelin sheaths. 67% myelinated axons present at recovery week 4; average diameter of myelinated axons increased; myelin sheaths of remyelinated axons thinner than controls, high number of unmyelinated small caliber axons after recovery.	

McMahon et al.	2001	8-10 week old C57BL/6 & MIP-1α$^{-/-}$ male mice	Feeding of 0.2% cuprizone up to 6 weeks	Several cytokines up-regulated upon demyelination (TNF-α & IL-1β), MIP-1α and its receptor CCR-5 peaked in weeks 4-5. MIP-1α$^{-/-}$ mice: Delayed onset of demyelination in the CC (LFB; EM) correlated with a decreased number of astrocytes and microglia/ macrophages (RCA-1) in the CC; TNF-α level decreased.	
Mason et al.	2001 b	8 week old C57BL/6J & IL-1β$^{-/-}$ mice	Feeding of 0.2% cuprizone for 6 weeks followed by normal food for 6 weeks	During demyelination: IL-1β/IGF-1-mRNA upregulation in wild-type mice; mainly microglia express IL-1β & astrocytes IGF-1 (still elevated during remyelination). IL-1β$^{-/-}$ mice: Demyelination including depletion of mature and accumulation of precursor oligodendrocytes. Impaired remyelination: Decreased number of remyelinated axons & mature oligodendrocytes. NG2^{+} cells still elevated. No IGF-1^{+} cells detected in CC.	Suggests role for IL-1β & IGF-1 in normal oligodendrocyte regeneration
Arnett et al.	2001	6-8 week old C57BL/6J, TNFα$^{-/-}$, TNFR1$^{-/-}$& TNFR2$^{-/-}$ male mice	Feeding of 0.2% cuprizone for 6 weeks followed by normal food for 4 weeks	TNFα upregulated during demyelination in wild-type mice; TNFα^{+} cells co-localized with microglia (RCA-1) & astrocytes; TNFR2 but not TNFR1 upregulated during de-/remyelination. TNFα$^{-/-}$ mice: Delayed demyelination (LFB/GST-pi). TNFα$^{-/-}$ & TNFR2$^{-/-}$ mice: Impaired remyelination, reduced NG2^{+}/BrdU^{+} cells during demyelination; myelinated axons (EM), GST-pi^{+} & NG2^{+} cells decreased upon remyelination. No changes in TNFR1$^{-/-}$ mice.	Suggests role of TNFα via TNFR2 for oligodendrocyte regeneration/ proliferation
Stidworthy et al.	2003	10 week old C57BL/6 female and male mice	Feeding of 0.2% or 0.4% cuprizone for 5 weeks followed by normal food for 2 weeks	In 3rd week: all mice switched to 0.2% cuprizone due to the severe effect of 0.4% cuprizone. Caudal part of CC more susceptible to demyelination; cerebellar peduncle not affected. 2 weeks recovery: No change in G-ratio, relation of axon diameter & myelin sheath thickness not conclusive, swollen dystrophic axons present. High variability of all parameters even in control mice.	Variability reported; sex differences of mice not discussed
Mason et al.	2004	8 week old C57BL/6J mice	Feeding of 0.2% cuprizone up to 16 weeks or for 5 weeks followed by normal food for 6 weeks (Transplantation of O4^{+} cells)	Chronic demyelination in CC: Ongoing apoptosis of oligodendrocytes; little intrinsic remyelination; progenitor oligodendrocytes (NG2) increased in weeks 4-5, became progressively depleted until week 12. Peak of microglia/macrophages (RCA-1) at week 6, remained elevated afterwards. Transplantation of O4^{+} oligodendrocyte progenitors at week 12: increased number of myelinated axons & mature oligodendrocytes.	Suggests that chronically demyelinated axons retain remyelination capacity
Merkler et al.	2005	7-8 week old C57BL/6J male mice	Feeding of 0.2% cuprizone for 6 weeks followed by 6 weeks recovery with normal food	Week 6 of cuprizone: Demyelination (LFB, EM); G-ratio increased, acute axonal damage (APP), astrocytes & microglia (Mac-3) increased. 6 weeks recovery: G-ratio & astrocytes still elevated, microglia reduced. MRI analyses: The individual parameters T_1 & T_2 correlated with EM data. To differentiate regions of de-/remyelination, a discriminate function analysis using a combination of T_1, T_2 & MTR is necessary.	Development of MRI method to predict the myelin status in vivo

Irvine & Blakemore	2006	8-10 week & 6-7 month old C57BL/6 female mice	Feeding of 0.2% cuprizone for 6 weeks (young mice) & 0.4% cuprizone for 7 weeks (old mice) followed by 6 or 7 weeks on normal diet	Demyelination similarly distributed within the CC in both age groups but marginally greater in young mice; evidence of intrinsic remyelination in young but not old mice. More severe axonal degeneration (SMI32 & EM) in aged mice. Significant loss of axons in aged mice at 7 & 14 weeks. Higher number of microglia (CD11b) & astrocytes in old mice.	Suggests aged mice are more prone to axon degeneration
Linares et al.	2006	8-14 week old C57BL/6, nNOS$^{-/-}$ & eNOS$^{-/-}$ male mice	Feeding of 0.25% cuprizone for 4 weeks followed by 4 weeks recovery with normal food	Increased iNOS & nNOS-mRNA levels in wild-type mice. nNOS$^{-/-}$ vs. wild-type mice: Minor demyelination but slower remyelination; only slightly increased number of microglia (RCA-1), astrocytes, apoptotic cells; decreased NG2^{+} cells; decreased secretion of TNFα, IL-1β, IGF-1 & iNOS by cuprizone. eNOS$^{-/-}$ mice: Demyelination & cellular changes comparable to wild-type mice; only slightly delayed remyelination & reduced IGF-1 expression in cuprizone week 4.	Suggests that constitutive NOS isoforms play a role in demyelination
Armstrong et al.	2006	8 week old C57BL/6 male mice	Feeding of 0.2% cuprizone for 6 or 12 weeks followed by normal food for 6 weeks	Poorer recovery after chronic vs. acute demyelination in C57BL/6 mice; density of mature (PLP) & precursor (PDGFRα) oligodendrocytes severely decreased; compromised but continued precursor proliferation at week 12. FGF2 upregulated upon demyelination.	Characterization of slower recovery after chronic demyelination. Suggests role of FGF2 in remyelination
		FGF2$^{-/-}$ or FGF2$^{+/+}$ (129 Sv-Ev:Black Swiss) male mice		FGF2$^{-/-}$ mice susceptible to cuprizone-induced demyelination; better recovery rate compared to control mice; oligodendrocyte number returned to control levels after 6 weeks recovery. Number of precursor oligodendrocytes & proliferating cells not affected.	
Lin et al.	2006	6 week old DOX+(+doxycycline) DOX- (-doxycycline) (GFAP/tTA;TRE/IFNγ) male mice	Feeding of 0.2% cuprizone up to 6 weeks followed by normal food for 3 weeks	IFNγ had no effect on demyelination but remyelination in the CC: Lower number of APC^{+} cells, remyelinated axons & reduced myelin score, altered time course of NG2^{+} cell recruitment. Failure of remyelination associated with activation of the stress pathway of the endoplasmic reticulum.	Induction of high IFNγ levels impairs remyelination
Mana et al.	2006	8-14 week old C57BL/6 & IFNγR$^{-/-}$ male mice	Feeding of 0.25% cuprizone for 6 weeks followed by normal food for 4 weeks	Increased IFNγ expression level during cuprizone feeding in wild-type mice. IFNγR$^{-/-}$ vs. wild-type mice: Demyelination slightly delayed (LFB) but comparable at week 6; more myelinated axons at week 4, GST-pi^{+} cells higher at week 6; NG2^{+} cells peaked at week 3 but higher; delayed accumulation of microglia (RCA-1) until week 4; astrocyte number comparable; TNFα & IGF-1 increased (but less) during demyelination; faster remyelination.	Role of IFNγ in contrast to study of Gao et al.
Remington et al.	2007	8 week old C57BL/6J female mice, CCL2$^{-/-}$ & CCR2$^{-/-}$	Feeding of 0.2% cuprizone up to 6 weeks followed by normal food for 3 weeks	Increased cell number in demyelinated CC (peak at week 4.5); majority identified as parenchymal microglia (CD11b^{+}/CD45^{dim}), only few blood derived macrophages (CD45^{high}). Majority of cells show activation profile (B7.2/CD86, B7.1/CD80, MHC class I). A subpopulation of CD11c^{+} microglia/macrophages identified as antigen-presenting cells restricted to the demyelinated CC, higher activation level. Microglia expansion in CC by proliferation in CC and migration from blood stream.	Characterization of microglia response to cuprizone

Lindner et al.	2008	8 week old C57BL/6 male mice	Feeding of 0.2% or 0.3% cuprizone for 6 weeks followed by normal food for 10 weeks (just 0.3% cuprizone-treated mice)	Demyelination in CC incomplete by 0.2% & complete by 0.3% cuprizone at week 6. 0.3%cuprizone: G-ratio increased, percentage of myelinated axons decreased in weeks 4-6; fast remyelination started at day 4, almost complete at week 2 (LFB). Different re-expression pattern during remyelination of PLP, CNPase, MBP & MOG. Recovery rate highest in weeks 1-2 of remyelination phase.	Focus on early remyelination
Iocca et al.	2008	8-10 week old C57BL/6 & TWEAK$^{-/-}$ male mice	Feeding of 0.2% cuprizone for up to 6 weeks followed by normal food up to 8 weeks	Slight upregulation of TNF-like weak inducer of apoptosis (TWEAK) & its receptor Fn14 during demyelination in wild-types. TWEAK$^{-/-}$ mice: Slightly delayed demyelination (LFB, MBP) & accumulation of microglia/macrophages (RCA-1). No effect on astrocytes.	
Crawford et al.	2009	8 week old PLP-EGFP (C57BL/6) female mice	Feeding of 0.2% cuprizone for - 1.5 weeks + 3 weeks recovery - 3 weeks + 6 weeks recovery - 6 weeks + 6 weeks recovery	Gradual demyelination (CC) from weeks 1.5 to 6 (MOG); remyelination to normal levels in 1.5+3w & 3+6w group but incomplete in 6+6w group. Increase of precursor (PDGFRα) & decrease of mature (GST-pi) oligodendrocytes during demyelination, back to control levels in all remyelination groups. Microglia (CD45) increased during de- & remyelination. Astrocytes increased during demyelination & even higher upon remyelination. Functional axon damage in CC: Impaired amplitude, latency & refractoriness of compound action potentials even after remyelination (3+6w, 6+6w). Nodal protein disorganization & increased axonal damage (APP) at weeks 3 & 6 of demyelination & after remyelination (3+6w, 6+6w). Reduced G-ratio at all time points of demyelination & in 6+6w remyelination group.	Remyelination capacity
Gudi et al.	2009	8 week old C57BL/6 male mice	Feeding of 0.2% cuprizone up to 6 weeks	Regional differences in grey & white matter: Delayed demyelination in grey matter; all cell types analyzed less present & responsive in cortex than in CC; pattern of oligodendrocytes (Nogo-A, NG2) & astrocytes similar during demyelination; little microgliosis (Mac-3) in cortex; Peak of Nestin^{+}/GFAP^{+} cells at week 4 decline thereafter, increased number of proliferating cells mainly Ki67^{+}/Mac-3^{+} (for both: CC more pronounced).	Comparison of grey and white matter
Lindner et al.	2009	8 week old C57BL/6 male mice	Feeding of 0.2% cuprizone for: - 6 weeks + 6 weeks recovery - 12 weeks + 12 weeks recovery - 14 or 16 weeks + 4 weeks recovery	Demyelination of the CC at 6-12 weeks. 12 week cuprizone feeding: Reduced remyelination rate in weeks 1-2 of recovery, almost complete at the end of recovery. Data about mature (Nogo-A) oligodendrocytes inconclusive. Start of astrocyte accumulation at week 4, stayed constant until the end of recovery (acute & chronic model). Peak of microglia (Mac-3) accumulation at week 6, decreased thereafter (acute & chronic). Peak of acute axonal damage (APP) in weeks 4-6 and remained elevated (chronic). Correlation of microglia and APP^{+} axon number. SMI-32 present at week 8, most prominent at week 16 of chronic demyelination, not decreased during recovery.	Axonal degeneration

Liu et al.	2010	8-10 week old $Cxcr2^{-/-}$, $Cxcr2^{+/+}$ & $Cxcr2^{+/-}$ mice (backcrossed to C57BL/6)	Feeding of 0.2% cuprizone for up to 6 weeks	$Cxcr2^{-/-}$ mice: relatively resistant to cuprizone toxicity; decrease of mRNA levels of oligodendrocytes, only moderate loss of mature (GST-pi) & progenitor (PDGFRα) oligodendrocytes, no apoptosis; Cxcr2-positive neutrophils from bloodstream identified to be necessary for cuprizone-induced demyelination.	
Voß et al.	2012	8 week old C57BL/6 male mice	Feeding of 0.2% cuprizone for 5 weeks followed by normal food for 1 week	Peak of microglia (RCA-1) at week 3 in CC & cortex; new cell population with macrophage expression pattern appeared in CC. Increased phagocytic activity of microglia during demyelination, receptors involved in phagocytosis upregulated, especially TREM-2b. MHCII increased at peak of demyelination; TNFα; FGF-2, IGF-1 increased during demyelination	Role of microglia further analyzed
Analysis in the hippocampus, cortex and cerebellum					
Hoffmann et al.	2008	8 week old C57BL/6 male mice	Feeding of 0.2% cuprizone for up to 12 weeks followed by normal food for 5 weeks	Cuprizone-treated mice: Startle-induced generalized tonic-clonic seizures present (not visible in EEG). During 9 days after 12 weeks cuprizone, short but frequent spike discharges recorded (not associated with behavioral changes). Marked demyelination (PLP) & degenerated neurons (H&E, Fluoro-Jade C) in the hippocampus. Reduced neuron number & density in the hilus, 5 weeks after 12 weeks cuprizone.	Hippocampus
Norkute et al.	2009	8 week & 6 month old C57BL/6 male mice	Feeding of 0.2% (young mice) or 0.4% (old mice) cuprizone for up to 7 weeks	Characterization of grey & white matter demyelination in hippocampus: Grey (hilus of dentate gyrus, stratum lacunosum moleculare) & white matter (medial part of the alveus & dorsal hippocampal commissure) demyelinated by week 7 (LFB, PLP & CC-1, EM). MBP & PLP mRNA expression decreased upon demyelination. Increased number of hypertrophic astrocytes in grey matter. Microglia (Iba1) number not changed. Effects the same in old cuprizone-fed mice.	Hippocampus
Koutsoudaki et al.	2009	8 week old C57BL/6 male mice	Feeding of 0.2% cuprizone for up to 6 weeks	Complete demyelination (PLP, Nogo-A) of the hippocampus until week 6 (SLM, fimbria not affected); no change in precursor oligodendrocytes (NG2); accumulation of microglia (Mac-3) & astrocytes in most regions in weeks 3-4.5, declined thereafter. $Nestin^{+}$ cells upregulated upon cuprizone, 70% of these cells are $GFAP^{+}$. PSA expression (migration marker) reduced upon cuprizone.	Hippocampus
Skripuletz et al.	2008	8 week old C57BL/6 & BALB/cJ male mice	Feeding of 0.2% cuprizone for up to 6 or 12 weeks followed by normal food for 6 or 12 weeks	Complete cortical demyelination of C57BL/6 but not BALB/cJ mice after 6 & 12 weeks of cuprizone; complete remyelination after 6 or 12 weeks recovery but delayed remyelination in 12 weeks cuprizone-fed mice. Demyelination more severe than in CC; increased number of microglia (only in BALB/cJ mice). Increased hypertrophic astrocytes in both strains during demyelination and slow decline during remyelination.	Cortex Report strain differences

Groebe et al.	2009	8 week old C57BL/6 male mice	Feeding of 0.2% cuprizone up to 5 weeks	Demyelination (PLP, PLP-mRNA, MBP-mRNA) & reduced number of mature oligodendrocytes (CC-1) in the cerebellar marrow incl. the lateral cerebellar nucleus, medial cerebellar nucleus, interpositus nucleus. Increased number of hypertrophic astrocytes & microglia (Iba1) at week 5. Cortical cerebellar white matter not demyelinated but myelin sheaths swollen. Cortical cerebellar grey matter not affected.	Demyelination in distinct cerebellar regions
Skripuletz et al.	2010 a	8 week old C57BL/6 male mice	Feeding of 0.2% cuprizone for 12 weeks followed by normal food for 8 weeks	Peak of cerebellar grey & white matter demyelination at week 12; incomplete remyelination by week 8. Lowest level of oligodendrocytes (Nogo-A) at weeks 4 & 12, back to control levels after remyelination. Mac-3^+ cells increased (more prominent in white than grey matter) & peaked at week 6 (grey matter) & weeks 8-10 (white matter); peak of astrocytes at week 8, declined afterwards.	Cerebellum

Consequences of cuprizone-induced demyelination on a behavioral and cognitive level are not studied intensively. So far, impaired motor coordination in a complex running wheel, impaired social behavior and sensorimotor function, reduced anxiety and impaired spatial working memory are described (Franco-Pons et al, 2007; Hibbits et al, 2009; Liebetanz & Merkler, 2006; Makinodan et al, 2009; Xu et al, 2009). Some of these disturbances are shown to be recovered during remyelination (Franco-Pons et al, 2007; Hibbits et al, 2009; Liebetanz & Merkler, 2006; Makinodan et al, 2009). Please see Table 3.

The underlying mechanism of the action of cuprizone to induce demyelination is still under debate. The initial hypothesis was that a copper deficit in the central nervous system leads to disturbed mitochondrial enzyme function, such as for monoamine oxidase and cytochrome oxidase (Venturini, 1973). The idea of a copper deficit is supported by the finding that cuprizone and the cuprizone-copper complex cross neither the intestinal epithelium nor cell membranes and was therefore suggested to chelate copper already in the food to induce a copper deficit in mice (Benetti et al, 2010). A recent study, using proteomic analysis, demonstrated that mitochondrial function is the most altered cellular function induced by cuprizone (Werner et al, 2010), which may result by abnormal concentrations of copper and zinc (Benetti et al, 2010; Zatta et al, 2005). However, neither a deficit of copper in the brain could be shown by others (Zatta et al, 2005), nor did supplementation of copper to the diet inhibit the cuprizone-induced toxicity (Carlton, 1966; Carlton, 1967). Therefore, the action of cuprizone may involve a more complex mechanism. In vitro studies showed that application of cuprizone to primary oligodendrocytes results in metabolic stress without cell death unless cuprizone is applied together with inflammatory cytokines, suggesting that inflammatory mediators play a role in the cuprizone-induced toxicity (Cammer, 1999; Pasquini et al, 2007). So far, several in vivo studies have been conducted to investigate underlying mechanisms of cuprizone-induced de- and remyelination processes. These studies suggest a role for cytokines such as tumor necrosis factor alpha (TNFα), Interferon-gamma (IFN-γ), Interleukin-1ß (IL-1ß) and macrophage-inflammatory protein-1 alpha (MIP-1α) (Arnett et al, 2001; Gao et al, 2000; Iocca et al, 2008; Lin et al, 2006; Mana et al, 2006; Mason et al, 2001b; McMahon et al, 2001). Moreover, a role for nitric oxide and growth factors such as fibroblast-growth-factor 2 (FGF2) and insulin-like growth factor 1 (IGF-1) is under

discussion (Armstrong et al, 2006; Linares et al, 2006; Mason et al, 2001b). Recently it was found that type 2 CXC chemokine receptor-positive ($CXCR2^+$) neutrophils from the bloodstream are necessary for cuprizone-induced demyelination (Liu et al, 2010). These investigators suggest a two-hit process of cuprizone intoxication: First mitochondrial functions are disturbed and induce metabolic stress in oligodendrocytes and second, peripheral $CXCR2^+$-neutrophils are needed to induce demyelination.

To this day, the knowledge about the mechanism of cuprizone-induced demyelination has increased, but the process is still not completely understood. Moreover, it is still questionable why oligodendrocytes are preferentially affected by cuprizone.

Table 3: Effect of cuprizone on basic behavioral and cognitive readouts.

Author	Year	Species	Experimental set-up	Results	Remarks
Liebetanz & Merkler	2006	8 week old C57BL/6 female mice	Feeding of 0.2% cuprizone for 6 weeks followed by 7 weeks with normal food. Motor skill sequence (MOSS) test performed in weeks 4-6 of demyelination and weeks 5-7 of remyelination.	MOSS test performance obtained on a training and complex wheel. Training wheel: Significantly lower running distance of cuprizone-fed mice over 2 weeks; complex wheel: Influence of all parameters (V_{max}, N_{run}, D_{max}, $Dist_{ac}$) → worse performance of cuprizone-fed mice vs. controls during demyelination. Remyelination phase: Comparable performance of cuprizone and control mice except for a reduced V_{max}.	Introduced novel motor test Fitness of mice could influence the performance
Franco-Pons et al.	2007	8 week old C57BL/6 male mice	Feeding of 0.2% cuprizone for up to 6 weeks followed by normal food for 6 weeks	Hyperactive behavior in weeks 3-4 (climbing, center-area activity & rearing in open field), increased sensorimotor reactivity (freezing as response to an auditory click) & motor dysfunction at week 5 (gait abnormalities, higher frequency of falling on rota-rod); hyperactivity & motor deficits still present in recovery group.	
Xu et al.	2009	7-8 week old C57BL/6 male mice	Feeding of 0.2% cuprizone for up to 6 weeks	Temporal pattern of higher climbing activity (weeks 2-4), abnormalities in sensorimotor function (pre-pulse-inhibition: lower PPI in cuprizone-fed mice in weeks 2-3), impaired social behavior (social interaction in pairs: reduced in weeks 4-6), lower anxiety levels (EPM: cuprizone-fed mice spent more time in open arm & higher open arm entries in weeks 2-6) & impaired spatial working memory (Y-maze: lower % of spontaneous alternations in weeks 2-6). Reduced enzyme activity (MAO, DBH) at week 3 in PFC & hippocampus, higher dopamine levels at week 2, lower norepinephrine levels at week 3.	"Link" to schizophrenia PPI: startle response of cuprizone mice influenced at weeks 2 & 3.
Hibbits et al.	2009	8-9 week old C57BL/6 male mice	Feeding of 0.2% cuprizone either for 6 or 12 weeks; 6 weeks feeding followed by normal food for 6 weeks	Acute & chronic demyelination: reduced running velocity in the complex wheel not recovered by remyelination. Wheel test applicable for longitudinal studies. Frequency of interactive behavior of test mice increased after acute & chronic demyelination & remyelination.	
Makinodan et al.	2009	Postnatal day 29 or 57 C57BL/6 female mice	Feeding of 0.2% cuprizone from P29-P56 (ED) or P57-P84 (LD) followed by normal food up to day P126	Impaired spatial working memory (Y-maze; lower % of spontaneous alternations) directly after cuprizone termination in ED/LD mice & after remyelination in ED mice. After remyelination: Reduced distance traveled in the center (open field) & disturbed social interaction of ED mice. No effects in EPM or novel object recognition.	"Link" to schizophrenia

Many studies still focus on characterization of the cuprizone model to better understand the mechanism of de- and remyelination, as well as the involvement of the different cell types such as microglia and astrocytes. Moreover, the model has been used to develop a new magnetic resonance imaging (MRI) method to predict myelin status in vivo (Merkler et al, 2005). As outlined below, the model is additionally used for investigations of treatment strategies concerning de- and remyelination.

1.2.3 Cuprizone model and treatment strategies

The cuprizone model serves as a tool to investigate treatment strategies for demyelinating diseases such as MS (for an overview see Table 4). Fumaric acid esters (FAE) are considered for the treatment of patients with relapsing-remitting MS. The corticosteroid methylprednisolone (MP) is an established and commonly used drug for MS; both drugs were tested in the cuprizone model. Unfortunately, no effects were found in oligodendrocytes, microglia or astrocytes; only minor-effects were found on remyelination upon FAE treatment with even a slight delay in remyelination by MP treatment (Clarner et al, 2011; Moharregh-Khiabani et al, 2010).

Minocycline, a second generation tetracycline, reduced the severity of demyelination in corpus callosum and cortex. Additionally, microglia and proliferating cells were decreased in the cortex, whereas a reduced micoglial number in the corpus callosum was observed in just one of the studies. Some contradictory results concerning the corpus callosum in these studies could be based on a slightly different treatment protocols and different microglia markers used (Pasquini et al, 2007; Skripuletz et al, 2010a). Improved motor coordination of minocycline treated mice was found using the beam walking test (Skripuletz et al, 2010b).

Sex hormones are suggested to have an effect on disease progression in MS. Combined 17β-estradiol/progesterone treatment during cuprizone-induced demyelination reduced ventricle enlargement and demyelination and increased the number of mature and precursor oligodendrocytes, microglia, astrocytes and proliferating cells. The expression of IGF-1 was increased (Acs et al, 2009). No effect was found when the mice were treated with only one of the hormones. However, another trial using a lower dose of cuprizone and a higher dose of 17β-estradiol demonstrated reduced demyelination, increased number of oligodendrocytes and a delayed accumulation of microglia. Precursor oligodendrocytes and astrocytes were

not affected and IGF-1 and TNFα were decreased, representing different effects of combined or single treatment of these hormones (Taylor et al, 2010). Based on the geographic distribution of MS, one could assume that nutrients and the climate can play a role in the disease mechanism. Supplementation of the cuprizone diet with N-3 polysaturated fatty acids from salmon reduced the demyelination rate and the number of microglia in the corpus callosum. These mice showed an elevated activity level and were less anxious (Torkildsen et al, 2009a; Torkildsen et al, 2009b). In addition, high dose vitamin D_3 was found to be potent in reducing demyelination and microglia accumulation after 6 weeks cuprizone feeding; no effects could be detected after 2 weeks of recovery (Wergeland et al, 2011).

Thyroid hormones are necessary for normal axonal myelination. Treatment with triiodothyronine (T_3) after chronic demyelination resulted in gradually improved myelination, increased numbers of mature/precursor oligodendrocytes and proliferating cells upon recovery (Harsan et al, 2008).

Growth factors are shown to promote oligodendrocyte precursor proliferation, survival and/or differentiation. A growth factor mix of PDGF-AA, neurotrophin-3, basic FGF-1 and IGF-1 was applied into the lateral ventricle 3 weeks after cuprizone feeding, which was followed by improved remyelination, activation of oligodendrocyte precursor proliferation and maturation (Kumar et al, 2007).

Based on the behavioral changes observed during cuprizone feeding and accumulating findings of white matter abnormalities in schizophrenia (Kubicki et al, 2005; Lim et al, 1999; Mitelman et al, 2007; Uranova et al, 2011), the cuprizone model was suggested to serve as an animal model to study this disease (Yang et al, 2009). Quetiapine, clozapine and olanzapine (second generation antipsychotics) and haloperidol (a first generation antipsychotic) were tested in the cuprizone model. When these drugs were given during the recovery phase, there was no effect on the status of myelin but rather enhanced performance in working memory (Xu et al, 2011). Administration of the antipsychotics during cuprizone feeding increased the degree of myelination (Chandran et al, 2011; Xiao et al, 2008; Xu et al, 2010; Zhang et al, 2008) and the number of mature oligodendrocytes was elevated, whereas the number of microglia and astrocytes were decreased within the corpus callosum (Zhang et al, 2008). Quetiapine and clozapine improved spatial working memory and social interaction in the cuprizone-fed mice (Xiao et al, 2008; Xu et al, 2010).

Haloperidol itself already influenced the performance in some of the behavior tests in healthy mice, which made it difficult to draw strong conclusions from these experiments. The results of these studies are presented in Table 5.

Table 4: The cuprizone model and treatment trials related to multiple sclerosis. Antibodies and/or methods used are given in brackets.

Author	Year	Species	Experimental set-up	Results	Remarks
Moharregh-Khiabani et al.	2010	8 week old C57BL/6 male mice	Feeding of 0.2% cuprizone for 5 weeks combined with oral treatment of monomethylfumarate or dimethylfumaric acid (15mg/kg) twice daily followed by normal food for 1 week.	Only a minor effect of monomethylfumarate on remyelination in the CC but not cortex in weeks 5-6 (LFB, PLP, MOG, MBP). No effects on oligodendrocytes, microglia or axonal damage.	
Clarner et al.	2011	C57BL/6 male mice	Feeding of 0.2% cuprizone for 5 weeks followed by normal food for 9 or 21 days combined with daily injections (i.p.) of methylprednisolone (15mg/kg).	Early (day 9) and late (day 21) during recovery, methylprednisolone treatment reduced myelination index (PLP) compared to placebo-treated mice. Mature oligodendrocytes (APC), microglia (Iba1) & astrocytes not influenced.	
Acs et al.	2009	8 week old C57BL/6 male mice	Feeding of 0.2% cuprizone for 5 weeks combined with s.c. depot injections of progesterone (25µg), 17β-estradiol (50ng) or a mixture of both twice weekly.	No effect of progesterone & 17β-estradiol alone. Both hormones together: Reduced ventricle enlargement (MRI) and demyelination in CC (LFB, mRNA: MBP, PLP), increased number of mature/precursor oligodendrocytes (APC/PDGFRα), microglia (Iba1), proliferating cells (Ki67) & the mRNA expression of GFAP (astrocytes). IGF-1 expression also increased.	
Taylor et al.	2010	8 week old C57BL/6 male mice	Feeding of 0.125% cuprizone up to 6 weeks followed by normal food for 1 week. 17β-estradiol (0.42mg/day) pellets were implanted s.c. 5 days prior cuprizone feeding.	Demyelination in CC (LFB) less severe & higher number of mature oligodendrocytes (GST-pi) at weeks 3 & 5 of demyelination. No effect on precursor oligodendrocytes & astrocytes; delayed microglia accumulation (RCA-1); reduction of TNFα & IGF-1 expression at weeks 3 & 5 of demyelination. No effect on remyelination.	
Pasquini et al.	2007	8 week old C57BL/6 male mice	Feeding of 0.2% cuprizone for 5 weeks. Feeding was combined in the 2nd week with injections (i.p.) of minocycline (50 mg/kg twice daily at days 1-2; daily at days 3-7 & 25 mg/kg daily until the end of experiment).	Demyelination (LFB, MBP) in CC less pronounced after 5 weeks cuprizone. Number of microglia (CD11b) significantly reduced within the CC.	
Skripuletz et al.	2010 b	8 week old C57BL/6 male mice	Feeding of 0.2% cuprizone for 6 weeks combined with injections (i.p.) of minocycline (50 mg/kg twice daily at days 1-2; daily at days 3-7 & 25 mg/kg daily until the end of experiment).	Less severe demyelination by minocycline treatment in the cortex in weeks 5-6 & in the CC in weeks 4-5 (PLP,MBP,CNPase). No effect on myelin re-expression; no effect on mature (Nogo-A) or precursor (NG2) oligodendrocytes & astrocytes in cortex & CC; decreased microglia number (Mac-3, RCA-1) & proliferation (Ki67) at week 5 in cortex but not CC. Improved motor coordination (beam walking) in weeks 5-6.	

Torkildsen et al.	2009 b	4 week old C57BL/6 female mice	Feeding of mice with the same food but supplemented with different lipid sources (salmon, cod liver, soybean & olive oils). At 8 weeks of age 0.2% cuprizone was added to the food for 6 weeks followed by 1 week without cuprizone.	Salmon/cuprizone group: Reduced volume of hyperintense brain lesions measured in T2-weighted MRI images (correlated with increased water content in brain parenchyma) at cuprizone week 5; demyelination (LFB, PLP) of the CC less severe at week 6 & after 1 week recovery. Lowest number of microglia in CC at week 6 but no group differences after recovery. Soybean oil/cuprizone group: Tendency to improve remyelination. No effect on astrocytes in any group. BBB not disrupted.	
Torkildsen et al.	2009 a	4 week old C57BL/6 female mice	Feeding of mice with the same food but supplemented with different lipid sources (salmon, cod liver, soybean & olive oils). At 8 weeks of age 0.2% cuprizone was added to the food for 6 weeks.	Salmon/cuprizone group: Confirmed their previous finding of reduced demyelination. New: Less body weight loss and increased activity levels in the EPM, visits of open and closed arm increased without a preference to either of them (less anxious).	
Wergeland et al.	2011	6 week old C57BL/6 female mice	Feeding with food containing <50 IU/kg, 500 IU/kg, 6200 IU/kg or 12500 IU/kg vitamin D_3. After 2 weeks, diets were supplemented with 0.2% cuprizone for 6 weeks followed by 2 weeks without cuprizone.	Serum levels of vitamin D_3 increased or deceased according to the feeding. High dose of vitamin D_3: Decreased demyelination in the CC, no influence on remyelination (LFB, PLP); depletion of mature oligodendrocytes (Nogo-A) not influenced; reduced microglia accumulation (Mac-3) in CC. 2 weeks after recovery microglia further decreased in all groups, significantly only by low dose vitamin D_3.	
Harsan et al.	2008	8 week old C57BL/6 female mice	Feeding of 0.2% cuprizone for 12 weeks followed by normal food for 12 weeks +/- triiodothyronine hormone (T_3; 0.3µg/g body weight) daily for 3 weeks (i.p.).	Hyperthyroidism 3 weeks after treatment started but transient at week 6. T_3-effects: DTI: Fractional anisotropy back to normal levels at week 12 in all ROIs (e.g. genu, splenium & cerebellum); radial diffusivity gradually decreased, reached normal levels until week 3 (cerebellum), 6 (splenium) or 12 (genu). Gradual increase of carbonic anhydrase II^+-oligodendrocytes & MBP in the CC/cerebellum (weeks 3-12 of recovery) Higher number of $Olig2^+$, Shh^+, $NG2^+$ & proliferating cells from week 3 on, gradual decrease of $CD45^+$ microglia & increase of myelinated axons.	
Kumar et al.	2007	6-7 week old C57BL/6 & Nestin-GFP female mice	Feeding of 0.2% cuprizone for 3 weeks followed by normal food + a single injection of a growth factor mix (PDGF-AA, NT3, bFGF,IGF-1) into the lateral ventricle.	2-5 days post injection (dpi): Increased cell proliferation & migration in CC, rostral migratory stream, cortex & striatum in wild-type & cuprizone-fed mice; proliferating cells identified as $GFAP^+$ & $NG2^+$ cells. $NG2^+/BrdU^+$ cells partially differentiated into mature oligodendrocytes (GST-pi). More myelinated fibers & thicker myelin sheaths in growth factor-treated cuprizone mice 21 dpi. Increased apoptosis in wild-type and cuprizone mice upon growth factor treatment.	

Table 5: The cuprizone model and treatment trials related to schizophrenia. Antibodies and/or methods used are given in brackets.

Author	Year	Species	Experimental set-up	Results	Remarks
Xiao et al.	2008	8 week old C57BL/6 male mice	Feeding of normal chow for 1 week followed by feeding with 0.2% cuprizone for 4 weeks. Quetiapine (10mg/kg/day) via drinking water over all 5 weeks.	Prevention of myelin breakdown (MBP) in whole brain (especially cortex) and improvement of spatial working memory (Y-maze: spontaneous alternation, arm entries).	
Zhang et al.	2008	8 week old C57BL/6 mice	Treatment with quetiapine (10mg/kg/day) for 6 weeks via drinking water; feeding of 0.2% cuprizone started after 1st week of quetiapine treatment for 5 weeks.	Elevated degree of myelination (LFB,MBP IHC&WB) quantified in whole brain & GST-pi^{+} oligodendrocytes in CC by quetiapine. Decreased activity of superoxide dismutase 1 in the cortex of cuprizone mice and back to normal levels upon quetiapine treatment. Decreased number of CD11b^{+} microglia & GFAP^{+} astrocytes in CC.	
Xu et al.	2010	7-8 week old C57BL/6 male mice	Feeding of 0.2% cuprizone for 14-42 days combined with daily injections (i.p.) of haloperidol (1mg/kg), clozapine or quetiapine (10mg/kg).	All antipsychotics blocked cuprizone-induced PPI deficit & reduced cuprizone-induced levels of dopamine & norepinephrine in PFC (day14). Clozapine & quetiapine counteracted cuprizone-induced decrease in spontaneous alternation in Y-maze & impaired social interaction (day28). Clozapine & haloperidol increased myelination in PFC; clozapine & quetiapine in caudate putamen (day 43; MBP, WB).	Haloperidol influenced PPI, Y-maze & social interaction in healthy mice.
Xu et al.	2011	6 week old C57BL/6 male mice	Feeding of 0.2% cuprizone for 5 weeks followed by normal food for 3 weeks combined with daily injections (i.p.) of clozapine or quetiapine (10mg/kg), haloperidol (1mg/kg) or olanzapine (3mg/kg).	Cuprizone feeding influenced the performance in EPM (increased time in open arm), reduced social interaction & spatial working memory of mice. Fast spontaneous recovery within 14-21 days concerning EPM but social interaction & spatial working memory still reduced. Only clozapine, quetiapine & olanzapine promoted the recovery of spatial working memory. No effect of antipsychotics on other tests or the myelin status.	Haloperidol influenced social interaction & Y-maze in healthy mice.
Chandran et al.	2011	8 week old C57BL/6 female mice	Feeding of normal chow for 1 week followed by 0.2% cuprizone for 5 weeks. Quetiapine (10mg/kg) was administered via drinking water during the 6 weeks.	T2-weighted MRI images: Significant decrease in the signal intensity ratio counteracted by quetiapine. DTI: fractional anisotropy levels back to control levels under quetiapine treatment. Optical density of LFB & MBP significantly elevated by quetiapine.	

1.3 Erythropoietin

1.3.1 Properties and pathways

EPO is a hematopoietic growth factor regulating the survival, proliferation and differentiation of erythroid progenitor cells (Jelkmann, 1992; Klingmuller, 1997). In 1977, the human EPO molecule was purified from urine, opening the possibility for its characterization (Miyake et al, 1977). EPO is a 30.4 kDa glycoprotein which belongs to the class I cytokine superfamily and is mainly expressed in the fetal liver and adult kidney (Dame et al, 1998; Fried, 1972; Koury et al, 1988; Zanjani et al, 1977). Additionally, EPO is identified to be expressed in the brain (Bernaudin et al, 1999; Marti, 2004; Marti et al, 1996; Masuda et al, 1994). The expression of EPO and the EPO receptor (EPOR) peaks during mid-gestation, whereas both are expressed in low levels during adulthood (Juul et al, 1998; Liu et al, 1994; Siren et al, 2001). However, in both the hematopoietic system and in the brain, EPO expression is upregulated under hypoxic conditions (Brines & Cerami, 2005; Jelkmann, 2007; Noguchi et al, 2007; Sasaki et al, 2001; Siren & Ehrenreich, 2001). The importance of the EPO-EPOR system during normal brain development was shown in EPO and EPOR null mice. The lack of erythropoiesis led to death of mice at day E13.5. Brain development was already impaired at day E10.5 (Yu et al, 2002). Mice with a conditional knockout of the brain EPOR survived through adulthood but showed reduced neurogenesis (Tsai et al, 2006).

The EPOR is a cell surface receptor and belongs to the cytokine class I receptor superfamily (Klingmuller, 1997; Youssoufian et al, 1993). These receptors are characterized by a single hydrophobic transmembrane domain, an extracellular N-terminal domain with conserved cysteines and a WSXWS-motif and a cytosolic domain that lacks intrinsic kinase activity (Jelkmann, 2007). The cytoplasmic domain of the EPOR is associated with the Janus kinase 2 (Jak2). Binding of EPO to the pre-formed EPOR homodimer activates Jak2, which phosphorylates 8 tyrosines located in the cytoplasmic domain of EPOR. These serve as docking sites for downstream molecules, which can become phosphorylated and activate several intracellular pathways (Jelkmann, 2007). Signaling pathways involved are signal transducers and activators of transcription (Stat), phosphatidylinositol 3-kinase (PI3K) and ras-mitogen-activated protein kinase (Ras-MAPK) (Brines & Cerami, 2005; Siren & Ehrenreich, 2001).

For more than 20 years, EPO has been used to treat patients suffering from anemia and is therefore accepted as a well tolerated and safe therapy (Jelkmann, 1992). Some of the first observations of neuroprotective properties of EPO were the prevention of glutamate-induced neuronal cell death in vitro (Morishita et al, 1997), anti-apoptotic and neurotrophic effects of EPO after unilateral fimbria-fornix transection (Konishi et al, 1993) and reduced ischemia-induced neuronal damage (Sakanaka et al, 1998) in rodents. Ever since, several studies could demonstrate neuroprotective and neuroregenerative properties of EPO in preclinical and clinical studies ranging from cerebrovascular diseases and neuroinflammatory diseases to neurodegeneration (for an extensive review please see (Sargin et al, 2010)). In these studies, EPO has been shown to be anti-apoptotic, anti-oxidative, anti-inflammatory, neurotrophic, angiogenetic and stimulate stem cell differentiation (Bartels et al, 2008; Brines & Cerami, 2005; Byts & Siren, 2009; Chen et al, 2007; Shingo et al, 2001; Siren & Ehrenreich, 2001). To emphasize that these effects are independent of the hematopoietic action of EPO, it was important to investigate whether EPO is able to cross the BBB. Indeed, it has been shown that a small proportion of high doses of exogenous EPO is able to cross the BBB using biotinylated-EPO in rodents (Brines et al, 2000) and indium-labeled EPO in healthy subjects and schizophrenic patients (Ehrenreich et al, 2004). The exact mechanism of how EPO crosses the BBB is not yet known. Additionally, it is still questionable if the EPOR responsible for the neuroprotective effect of EPO in the brain is the same as for the hematopoietic system. Brines and colleagues suggested a heteromeric receptor complex consisting of one EPOR subunit and one ß-common receptor subunit which belongs to the interleukin-3 receptor family (Brines et al, 2004). Moreover, the identification of an EPO analogue with potent neuroprotective but no hematopoietic action is of major interest for clinical applications.

1.3.2 Erythropoietin and oligodendrocytes

Oligodendrocytes are the myelinating cells in the CNS. They allow fast saltatory conduction of signals along the axons and more recent investigations show a supportive function of oligodendrocytes for axon survival (Nave, 2010).

The expression of EPO and EPOR has been found in vitro in astrocytes, neurons, microglia and oligodendrocytes (Masuda et al, 1994; Morishita et al, 1997; Nagai et al, 2001; Sugawa et al, 2002). The effect of EPO on oligodendrocytes is not

extensively studied yet. The first who clearly showed the presence of EPO and EPOR mRNA expression in cultured rat oligodendrocytes were Sugawa and colleagues (Sugawa et al, 2002). Moreover, they claimed that EPO promotes differentiation/maturation of oligodendrocytes as shown by direct EPO treatment and by a co-culture experiment with astrocytes. In this study, the involvement of the classical EPO pathway Jak2/Stat5 could not be detected. In several different disease models, EPO has been found to preserve myelin sheaths (Gorio et al, 2002; Iwai et al, 2010; Kumral et al, 2007; Li et al, 2004; Liu et al, 2011; Vitellaro-Zuccarello et al, 2007; Yamada et al, 2011) and resulted in earlier and faster white matter reorganization after ischemia shown by MRI (Li et al, 2009). Direct preservation of oligodendrocytes was observed in a model of neurotrauma (Sargin et al, 2009). A very consistent finding so far is that EPO enhances proliferation of precursor oligodendrocytes and increases the maturation of oligodendrocytes, and is therefore suggested to enhance oligodendrogenesis (Iwai et al, 2010; Vitellaro-Zuccarello et al, 2007; Zhang et al, 2005; Zhang et al, 2010). In models for periventricular leukomalacia and traumatic spinal cord injury, it was shown that EPO reduced the apoptosis rate in the white matter (Arishima et al, 2006; Gorio et al, 2002; Kumral et al, 2007). In vitro, EPO decreased the cytotoxicity in oligodendrocyte cultures after interferon-γ and lipopolysaccharide or hydrogen peroxide administration (Genc et al, 2006; Mizuno et al, 2008). Furthermore, anti-inflammatory potential of EPO was shown by a decrease in nitrite production and reduced mRNA expression of inducible nitric oxide synthase in mature oligodendrocyte cultures, as well as by a reduction of cytokine levels in the developing rat brain (Genc et al, 2006; Kumral et al, 2007). Some discrepancies between studies may result from different study designs or different protocols of EPO application. Further studies are needed to clarify the effect of EPO on oligodendrocytes and myelin. In addition, this is of special interest concerning alternative treatment strategies for demyelinating diseases such as MS.

1.4 Scope of the thesis

As outlined above, EPO has been proven to bear neuroprotective and neuroregenerative properties shown in several disease models. With respect to oligodendrocytes, EPO is suggested to mainly promote oligodendrogenesis and preserve myelin under different pathological conditions. It is of major interest to understand the effect of EPO on oligodendrocytes in more detail concerning

alternative treatment strategies for demyelinating diseases such as MS. In the most commonly used animal model for MS, experimental autoimmune encephalomyelitis (EAE), EPO has been shown to delay the disease onset, has immune-modulatory capacity by reducing inflammatory cytokine production and improves electrophysiological and histological readouts of EAE ((Agnello et al, 2002; Brines et al, 2000; Chen et al, 2010; Diem et al, 2005; Kang et al, 2009; Leist et al, 2004; Li et al, 2004; Sattler et al, 2004; Savino et al, 2006; Thorne et al, 2009; Yuan et al, 2008; Zhang et al, 2005) and reviewed in (Bartels et al, 2008; Sargin et al, 2010)). The effect of EPO on demyelination in the EAE model is rarely investigated - so far it has been shown that EPO reduces demyelination and enhances proliferation of precursor oligodendrocytes in the central nervous system but not in the optic nerve (Dasgupta et al, 2011; Diem et al, 2005; Li et al, 2004; Sattler et al, 2004; Zhang et al, 2005). The aim of this thesis was to make use of the cuprizone mouse model to investigate the effect of EPO on demyelination and remyelination processes without direct influence of immune-inflammatory components. This was studied with different experimental designs:

1. Effect of EPO on remyelination

In this experimental set-up, the effect of EPO was investigated after a single and repeated exposure to cuprizone. The idea of repeated cuprizone intoxication was to apply an additional “demyelination-hit” after a partial recovery. This is related to disease conditions such as in the relapsing-remitting disease course in MS. EPO application started in the beginning of the recovery phase and therefore allowed investigation of the effect of EPO on the remyelination process.

2. Effect of EPO on demyelination

The experimental design included a single cuprizone exposure followed by a recovery phase. From weeks 4-6 of cuprizone feeding, EPO was applied to investigate the effect on demyelination.

The analyses of the experiments included behavioral tests, MRI, immunohistochemical staining, western blot analysis and quantitative RT-PCR. It was hypothesized that EPO improves cuprizone-induced changes in these readouts. So far, no study exists to investigate the effect of EPO in the cuprizone mouse model.

2 MATERIALS AND METHODS

2.1 Animals

All experiments were approved by and conducted in accordance with the regulations of the local Animal Care and Use Committee (Niedersächsisches Landesamt für Verbraucherschutz und Lebensmittelsicherheit; AZ 33.11.42502-04-040/08 and AZ 33.9-42502-04-10/0157). 4 week old C57BL/6 male mice were purchased from Charles River Laboratories (Sulzfeld, Germany) for all experiments. They were housed in groups of 5 in standard plastic cages and maintained in a temperature-controlled environment (21±2°C) on a 12 hour light/dark cycle with food (Sniff, Soest, Germany) and water available ad libitum. 8 week old C57BL/6 male mice were used in each experiment if not indicated otherwise. Body weight of mice was monitored over the whole experimental time. Moreover mice were carefully observed to see any adverse effects of the treatment.

2.2 Preparation of cuprizone containing food

2.2.1 Food pellets containing 0.2% cuprizone

Food pellets containing 0.2% cuprizone (weight/weight) (Sigma Aldrich, Taufkirchen, Germany) were customer made by Sniff (Soest, Germany).

2.2.2 Standard ground chow containing 0.2% or 0.3% cuprizone

A plastic container was used to carefully mix standard ground chow (Sniff, Soest, Germany) with cuprizone. Food was freshly prepared daily. Mice in the control groups were fed with the regular standard ground chow without cuprizone added.

2.3 Erythropoietin administration

Erythropoietin (NeoRecomon; 50000 IU/ml; Roche, Penzberg, Germany) was freshly prepared by dilution with EPREX solvent solution (Pharmacy at the University hospital, Göttingen, Germany). Mice received a dose of 5000 IU/kg body weight every other day over a 3 week period. Placebo mice were injected with the diluent of EPO.

2.4 Measurement of the haematocrit

To measure the haematocrit, blood was taken from the heart and collected in EDTA-coated-tubes (Sarstedt, Nümbrecht, Germany). The blood was taken up by micro-haematocrit capillaries that were sealed with a kit (Brand, Wertheim, Germany). The tubes were centrifuged for 10 minutes; 8000 rpm (Heraeus Biofuge haemo; Kendro; Osterode; Germany). The haematocrit was directly measured on a micro-haematocrit scale (Kendro, Osterode, Germany).

2.5 Experimental design

2.5.1 Pilot experiments

In the first pilot experiment, mice were divided into two groups (44 mice/group); one group received normal food pellets and the other food pellets containing 0.2% cuprizone over a period of 7 weeks (Figure 2). Body weight and motor performance (2.6.1) of mice was monitored over the whole experimental time.

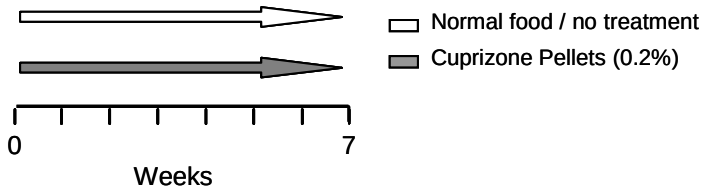

Figure 2: Experimental scheme of first pilot experiment. N=44/group

In the second pilot experiment, the difference of cuprizone administration via food pellets and rodent ground chow was tested. Over a period of 19 days, 7 week old mice (N=3) were exposed to 0.2% or 0.3% cuprizone mixed in rodent ground chow (Figure 3) and 6 week old mice (N=3) received food pellets containing 0.2% cuprizone (Figure 4). The body weight was measured over the whole experimental period.

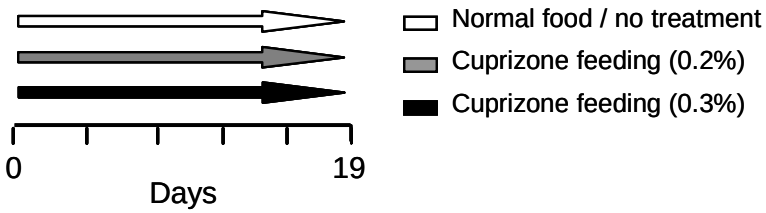

Figure 3: Experimental scheme of second pilot experiment.
Mice (N=3) received cuprizone mixed into ground chow.

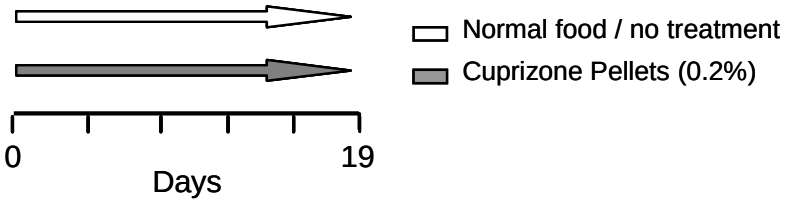

Figure 4: Experimental scheme of second pilot experiment.
Mice (N=3) received cuprizone via food pellets.

2.5.2 Investigation of EPO on remyelination

2.5.2.1 Single treatment of cuprizone

To investigate the effect of EPO on remyelination after an acute demyelination phase, a 4-arm design was used (N=20/group). Two groups served as control groups and received normal ground chow; the other two were fed with 0.2% cuprizone mixed into ground chow. After 6 weeks all mice were put on normal chow and one control and one cuprizone group received either placebo or EPO every other day over the next 3 weeks (Figure 5). Mice were sacrificed and used for protein analysis. During the experiment rota-rod was performed (see 2.6.1).

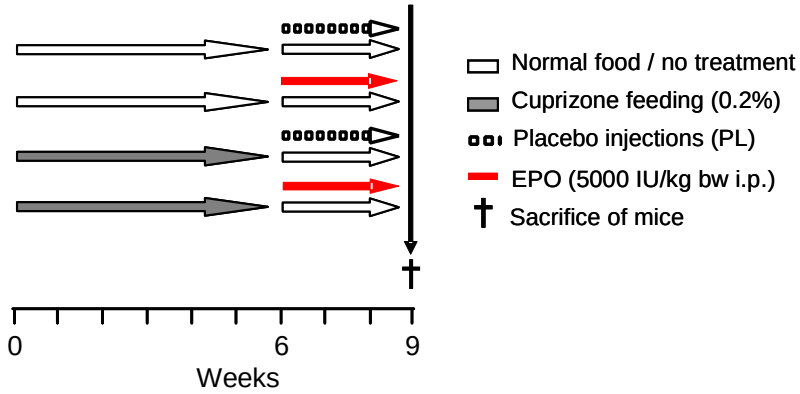

Figure 5: Experimental scheme of the single treatment group to investigate the effect of EPO on remyelination. N=20/group; i.p.=intra-peritoneal; bw=body weight; EPO=erythropoietin.

2.5.2.2 Repeated treatment of cuprizone

To investigate the effect of EPO on remyelination after a repeated exposure to cuprizone, a 4-arm design was used (N=25/group). Two groups served as control groups and received normal ground chow; the other two were fed with 0.2% cuprizone mixed into ground chow. After 6 weeks all mice were put on normal chow and one control and one cuprizone group received either placebo or EPO every other day over the next 3 weeks. This was followed by a second cycle of cuprizone feeding over 6 weeks and a second recovery phase for 3 weeks with placebo/EPO injections as described before (Figure 6). After the second demyelination phase (week 15) and at the end of the experiment (week 18) mice were tested on the beam balance test (see 2.6.2). Rota-rod was performed twice weekly during the whole experiment (see 2.6.1). At the end of the experiment (week 18) mice were used for MRI and the measurement of acoustic evoked potentials (AEPs) and sacrificed afterwards. Brain samples were used for protein analysis.

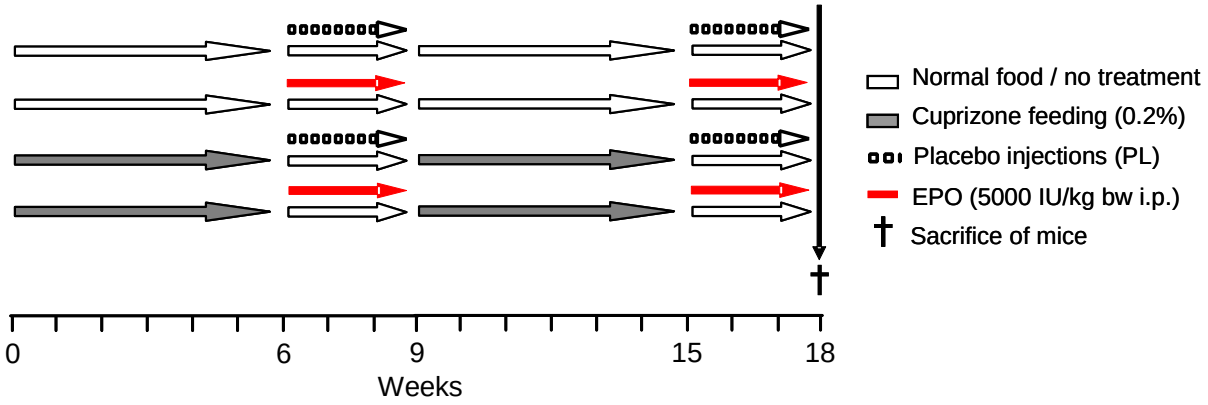

Figure 6: Experimental scheme of the repeated treatment group to investigate the effect of EPO on remyelination. N=25/group; i.p.=intra-peritoneal; bw=body weight; EPO=erythropoietin.

2.5.3 Investigation of EPO on demyelination

To investigate the effect of EPO on demyelination during an acute demyelination phase, a 4-arm design was used (N=26/group). Two groups received normal ground chow and the other two were exposed to 0.2% cuprizone over 6 weeks. From weeks 4 to 6 of this period, mice were injected intra-peritoneal (i.p.) with EPO or placebo (Figure 7). After 6 weeks, 8-11 mice/group were used for MRI and immunohistochemistry; whereas 15 mice/group received normal chow over the next 3 weeks. At week 9, mice were used for MRI and scarified afterwards. Additionally, at weeks 6 and 9 the beam balance test and rota-rod was performed (see 2.6).

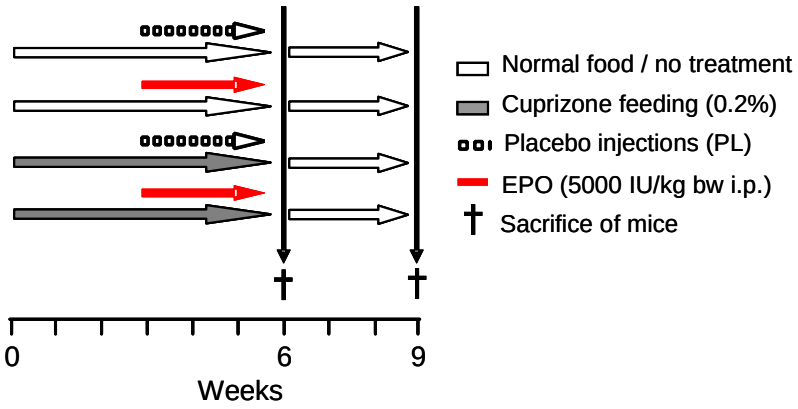

Figure 7: Experimental scheme to study the effect of EPO on demyelination. N= 26/group; i.p.=intra-peritoneal; bw=body weight; EPO=erythropoietin.

All tests and analyses were performed in a 'blinded' fashion. The experimenter was not aware of any group assignment until the end of the experiments.

2.6 Behavioral testing

The group size in the different behavioral experiments is stated in the respective figure legends.

2.6.1 Rota-rod

Rota-rod is a test for motor function, balance and coordination and comprises a rotating drum which is either at constant speed or accelerated from a lower to higher speed over a distinct time period. The protocols used are described before (Carter et al, 2001) and were modified in our laboratory (e.g. (Radyushkin et al, 2010)). Two protocols were used in these studies, first rota-rod with a constant speed of 16 resolutions per minute (rpm) and second an accelerated rota-rod of 4-40 rpm. Both protocols started with a habituation day which involved placing each mouse individually on the non-rotating drum for 5 minutes. The actual experiment started on the second day of testing.

2.6.1.1 Constant rota-rod

In the first pilot experiment, mice were tested twice every week throughout the whole experimental time. The rota-rod (Ugo Basile, Comerio, Varese, Italy) was set to a constant speed of 16 rpm and the time mice were able to stay on the rod (falling latency) was measured. Each mouse had 3 trials per day with an inter-trial interval of 5 minutes. A cut-off time was set to 5 minutes. After each trial, the rotating drum was cleaned. From week 5 on, all mice were switched to an accelerated rota-rod.

2.6.1.2 Accelerated rota-rod

In all experiments (except the first part of the first pilot experiment) an accelerated rota-rod protocol was used. The speed increased from 4-40 rpm within 5 minutes. Mice were placed on the rotating drum and the falling latency was recorded. For the second part of the first pilot experiment and for the experiment to investigate the effect of EPO on remyelination, all mice were tested twice every week with one trial per day over the whole experimental period.

In order for the experiment to investigate the effect of EPO on demyelination, the mice were first tested at baseline before cuprizone exposure. On the first day after the habituation, the mice were tested on the accelerated rota-rod (1 trial per day). To assess motor learning, the test was repeated 24 hours later. At both, week 6 and 9, the accelerated rota-rod was performed on 3 consecutive days.

2.6.2 Beam balance

Beam balance is a test for motor coordination and vestibulomotor function. The set-up consists of an elevated beam that has an enclosed escape platform including bedding on one end. The mice are trained to cross the beam towards the enclosed escape platform and the latency of mice to cross the beam is recorded (Carter et al, 2001). The protocol used in these studies are based on the common beam walking protocol but was further modified. All the beams were 59 cm long and varied in their diameter. The light in the experimental room was dimmed and the start side of the beam was illuminated. For habituation, a 25 mm diameter beam was used. On the first day of habituation, the mice were placed right in front of the enclosed escape platform; when the mouse entered the box they were allowed to stay there for 30 seconds (s). After a 5 minute inter-trial interval, mice were placed in the middle of the beam and the mice had to walk to and enter the escape box. The mouse was again

left there for 30 s. On the second day, habituation was performed by first placing the mouse in the middle of the beam followed by a 5 minute inter-trial interval and then starting again by placing the mouse at the start of the beam. The mouse then had to walk again to the escape box and stayed there for 30 s. After the habituation, the actual test was performed. The beam was exchanged to a 10 mm diameter beam, the mouse was placed at the start of the beam and the latency to reach the escape box was measured. On the third day the mice were tested on the 8 mm diameter beam and the latency to cross the beam was again recorded. If a mouse failed to stay on the beam, the test was repeated, maximum were 3 trials/mouse. If all trials failed, a cut-off time of 60 s was set for the analysis of data. This protocol including an intensive habituation phase was used at week 15 and at baseline to investigate the effect of EPO on remyelination and on demyelination respectively. At all other time points the beam balance test was performed on 2 consecutive days; on the first day a short habituation was applied by placing the mice again in the middle and start of the 25 mm beam. This was followed by testing the mice on the 10 mm beam. On the second day the latency to walk across the 8 mm beam was recorded. The same criteria for non-performer were used as described above. The performance of mice was calculated by the duration on the beam in % of control.

2.7 Assessment of hearing

2.7.1 Startle response of mice

To control for hearing of mice, a test using the startle response of mice as a response to acoustic stimuli can be used (Logue et al, 1997).

Each mouse was placed in a small metal cage (90x40x40 mm) to restrict major movements and exploratory behavior. The cages were equipped with a movable platform floor attached to a sensor that records vertical movements of the floor. The cages were placed in four sound-attenuating isolation cabinets (TSE GmbH, Bad Homburg, Germany). Startle reflexes were evoked by acoustic stimuli delivered from a loudspeaker that was suspended above the cage and connected to an acoustic generator. The startle reaction to an acoustic stimulus evokes a movement of the platform and a transient force results from this movement of the platform. This was recorded with a computer during a recording window of 100 ms and stored for further analysis. The recording window was defined from the onset of the acoustic stimulus.

An experimental session consisted of a 2 minutes habituation to 65 dB background white noise (continuous throughout the session), followed by a baseline recording for 1 minute at background noise. After baseline recording, stimuli of different intensity and fixed 40 ms duration were presented. Stimulus intensity was varied between 65 dB and 120 dB, such that 19 intensities from this range were used with 3 dB steps. Stimuli of each intensity were presented 10 times in a pseudorandom order with an interval ranging from 8 to 22 s. The amplitude of the startle response (expressed in arbitrary units; AU) was defined as the difference between the maximum force detected during a recording window and the force measured immediately before the stimulus onset. Amplitudes of responses for each stimulus intensity were averaged for individual animals. Mean values for each experimental group were used for analysis of the stimulus-response curves.

2.7.2 Recording of auditory brain stem responses (ABRs)

This measurement was done in collaboration with Nicola Strenzke, Department of Otorhynolaryngology, University hospital, Göttingen, Germany.

Animals were anaesthetized intra-peritoneally with a combination of ketamine (125 mg kg^{-1}) and xylazine (2.5 mg kg^{-1}) and the heart rate was constantly monitored to control the depth of anesthesia. The core temperature was maintained constant at 37°C using a rectal temperature-controlled heat blanket (Hugo Sachs Elektronik – Harvard Apparatus GmbH, March-Hugstetten, Germany). For stimulus generation, presentation, and data acquisition, the TDT III Systems was used (Tucker-Davis-Technologies, Ft Lauderdale, FL), run by custom-written Matlab software (The Mathworks). Clicks of 0.03 ms duration were calibrated using a ¼'' Brüel and Kjaer microphone (D 4039, Brüel & Kjaer GmbH, Bremen, Germany) and were presented at 20 and 90 Hertz in the free field ipsilaterally using a JBL 2402 speaker (JBL GmbH & Co., Neuhofen, Germany). The potential difference between vertex and mastoid subdermal needles was amplified 20 times and sampled at a rate of 50 kilohertz for 20 ms, 2x2000 times to obtain two mean ABRs for each sound intensity. Hearing threshold was determined with 10 dB precision as the lowest stimulus intensity that evoked a reproducible response waveform in both traces by visual inspection. Amplitudes and latencies of ABR waves I-V (Jewett & Williston, 1971) were analyzed using a semi-automatic custom-written Matlab routine.

2.8 MRI analysis

All MRI measurements and the analysis of the %MTR were performed in collaboration with Susann Boretius, Max Planck institute for biophysical chemistry, Göttingen, Germany. Volumetrical analysis of the data obtained was done by myself.

2.8.1 MRI measurements

6 mice per group underwent MRI at the time points described above. The animals were anesthetized with 1-1.5% isoflurane in a mixture of oxygen and ambient air and positive ventilated via endotracheal tube. The artificial respiration was controlled, by a homemade sensor placed on the chest of the mice. During the measurements the mice were fixed at the head and the body temperature (36±1°C) was kept constant by a rectal temperature-controlled heat blanket. 3D Fast Low-Angle Shot (FLASH) MRI (TR/TE = 14.9/3.9 ms, 45 minutes each) was performed at 9.4 T (Bruker Biospin, Ettlingen, Germany) with 110 µm isotropic spatial resolution using a 4-element phased-array surface coil (Bruker Biospin, Ettlingen, Germany) for signal reception. 3 data sets were obtained: a T-1 weighted data set with a flip angle of 12° and 2 proton-density (PD) weighted data sets with a flip angle of 5°. In addition, magnetization transfer (MT) weighted images were obtained by off-resonance irradiation (frequency offset 3 kilohertz, Gaussian pulse, duration 3.5 ms, flip angle 135°). The MT weighted data set together with the PD weighted image was used to calculate the magnetization transfer ratio (MTR) in percentage. %MTR=((PD-MT)/PD)x100%. To reduce the background noise the images were modified by a mild Gauß filter (s=1 Pixel, 3x3 Kernel) before. T1 maps were calculated by the T1- and PD-weighted data sets. In addition, multi-slice T2-weighted images were acquired with use of a fast spin-echo MRI sequence (TR/TE=5300/64 ms, 8 echoes, 26 sections) at an in-plane resolution of 80 µm and a section thickness of 300 µm (Boretius et al, 2009).

2.8.2 Volumetrical analysis

The brain volume (total brain, brain matter, hippocampi, ventricles) was determined by using Amira software (Visage Imaging GmbH, Berlin, Germany). In the T1 maps every second slice in the transversal layer was analyzed. The different regions were manually surrounded and labeled by going through the brain from superior to inferior. The coronal and sagittal layer was always consulted to reliably label the different

regions. The data obtained by Amira were non-dimensional and only represented the number of pixel within the regions. One pixel had a volume of 110*110*110 µm, therefore the data were multiplied by this volume and by 2 (because only every second brain slice was analyzed).

2.8.3 %MTR

%MTR was calculated pixel by pixel resulting in a 3-dimensional parameter map. From this MTR-map the corpus callosum as region of interest (ROI) was selected on a sagittal oriented slice, 4 slices away from the center. The corpus callosum was divided in 3 parts, rostral, central, and caudal allowing to separate between different regions within the corpus callosum.

2.9 Staining of mouse brains

2.9.1 Preparation of tissue

Animals were anesthetized with 0.25% tribromoethanol (Avertin; 0.125 mg/g, i.p.; Sigma Aldrich, Taufkirchen, Germany) and perfused transcardially with Ringer-solution (Braun, Melsungen, Germany) followed by 4% paraformaldehyde (PFA; Merck, Darmstadt, Germany). The brain, spinal cord, kidney and liver were removed, put in 4% PFA and post-fixed overnight at 4°C. On the next day the brains were placed in 30% sucrose (Merck, Darmstadt, Germany) diluted in phosphate buffered saline (PBS) for cryoprotection. After dehydration of the brains (2-4 days), the cerebellum and the brain were separately frozen on liquid nitrogen. The samples were stored at -80°C. Brains were cut by putting them vertically on a small metal plate with Tissue-tack (Sakura, Alphen aan den Rijn; Netherlands), surrounded by the tissue tack and placed in the cryostat (Leica, Wetzlar, Germany). When the tissue tack was fully frozen the whole mouse brain was cut into 30 µm thick coronal sections on a cryostat. The sections were kept in a 48 well plate (1 brain slice/well) in a storage solution (25% ethylene glycol (Sigma Aldrich, Taufkirchen, Germany) and 25% glycerol (Merck, Darmstadt, Germany) in PBS). The plates were stored at -20°C until the stainings were started.

2.9.2 Luxol Fast Blue staining

The LFB staining is a fast histological method to visualize myelin. The staining was done according to a well established protocol (http://library.med.utah.edu/WebPath/HISTHTML/MANUALS/LFB.PDF).

The cryostat-sections were washed 4 times 15 minutes in 1xPBS, mounted on Superfrost plus glass slides (Thermo Fisher Scientific, Braunschweig, Germany) and dried. Slides were then directly put into a 1:1 alcohol- (Sigma Aldrich, Taufkirchen, Germany) chloroform solution (Merck, Darmstadt, Germany) over night and hydrated back to 95% alcohol. On the next day, the slides were put in 0.1% LFB-solution (Serva, Heidelberg, Germany) containing ethyl alcohol 95% (Sigma Aldrich, Taufkirchen, Germany) and glacial acetic acid (Merck, Darmstadt, Germany) over night at 56°C. Slides were first rinsed with 95% ethanol (Sigma Aldrich, Taufkirchen, Germany) and then with ddH_2O. Slides were differentiated for 30 s by 0.05% lithium carbonate solution in ddH_2O (Sigma Aldrich, Taufkirchen, Germany), followed by 70% alcohol for 30 s. Slides were rinsed with ddH_2O, dehydrated and coverslipped using DePeX (Serva, Heidelberg, Germany).

2.9.3 Immunohistochemical staining

For immunohistochemistry, a series of every 10^{th} coronal section through the entire brain was taken for each marker under investigation. Free floating sections were washed with 1xPBS for 15 minutes 3 times, mounted on Superfrost plus glass slides (Thermo Fisher Scientific, Braunschweig, Germany) and dried over night. Slides were washed for 5 minutes 3 times in 1xPBS and then boiled in citrate buffer for 2 minutes 3 times (1.07 mM citric acid monohydrate and 11.9 mM trisodium citrate dehydrate; Merck, Darmstadt, Germany). Slides were cooled down in ddH_20 for 5 minutes, washed in 1xPBS (for 5 minutes 3 times) and then incubated in 0.5 % H_2O_2 in ddH_2O for 30 minutes. To prevent unspecific binding, the sections were incubated for 1 hour in a blocking solution containing 5% normal horse serum (Jackson Immunoresearch, West Grove, USA) and 0.5% Triton X-100 (Sigma-Aldrich, Taufkirchen, Germany) in 1xPBS. Afterwards the sections were incubated in the primary antibody solution containing 3% normal horse serum (Dianova, Hamburg, Germany) and 0.5% Triton X-100 in 1xPBS for 48 hours at 4°C. The primary antibodies used were rabbit anti-PDGFR-α antibody (1:2000; Cell signalling, Frankfurt a.M., Germany), mouse anti-APC (CC-1; 1:200; Merck, Darmstadt,

Germany), rabbit anti-ionized calcium-binding adapter molecule 1 (IBA1; 1:1000, Wako, Neuss, Germany) and rabbit anti-APP (1:850; Millipore, Schwalbach, Germany). Slides were washed for 5 minutes 5 times and then incubated in the secondary antibody solution containing 3% normal horse serum, 0.5% Triton X-100 and biotinylated goat anti-rabbit or anti-mouse antibody (1:200; Vector Laboratories, BA-1000) in 1xPBS. Incubation took place for 1.5 hours at room temperature followed by 3 washing steps for 5 minutes with 1xPBS. Next, 1.5 hour incubation at room temperature in the peroxidase-labeled avidin-biotin kit (Vectastain ABC Kit, Vector Laboratories, Burlingame, USA) followed. The solutions had to be prepared 30 minutes prior using (ABC-Complex dilution: 2 drops of solution A + 2 drops of solution B in 10 ml 1xPBS). Slides were again washed for 5 minutes 3 times in 1xPBS and then incubated in diaminobenzidine (DAB) solution (2 ml DAB + 36 µl H_2O_2 in 100 ml PBS; Sigma-Aldrich, Taufkirchen, Germany) for 1-2.5 minutes. Slides were washed in dd$H_2$0 and air-dried over night. Slides were put in xylol for 5 minutes (Chemie-Vertrieb Hannover GmbH, Hannover, Germany) and then mounted with non-aqueous DePeX (Serva, Heidelberg, Germany).

For the APP staining a counterstaining with haematoxylin was performed. Immediately after the DAB reaction, the slides were incubated in haematoxylin (Sigma Aldrich, Taufkirchen, Germany) for 30 s followed by washing for 5 minutes in $H_2$0. Slides were dried and coverslipped as described above.

2.9.4 Quantification of the cell numbers

Two ROIs within the corpus callosum were defined. The ‘rostral region’ encompassed bregma 1.10 to -0.10; it began with the section where the corpus callosum is connecting the two hemispheres and the lateral ventricle appears beneath and ended with the appearance of the 3rd dorsal ventricle (Figure 8A). The ‘caudal region’ included all sections of bregma 0.94 to -2.46 and started with the section where the dentate gyrus is visible for the first time and ended when the corpus callosum is separated again (Figure 8B). Images of the corpus callosum in these regions were taken by a digital camera on a Zeiss light microscope (Zeiss, Oberkochen, Germany) connected to a computer with the Kappa imaging software (Kappa Optronics GmbH, Gleichen, Germany). A 40x oil objective was used for all images. The single images of one brain section were merged to a continuous image using Adobe Photoshop CS2 (Adobe Systems, San Jose, USA) and the tool

'photomerge'. In these images the area of the corpus callosum was measured and the cell counting was performed using Image J software (http://rsbweb.nih.gov/ij/) and the tool 'cell count'. The results were calculated as cells per mm^2.

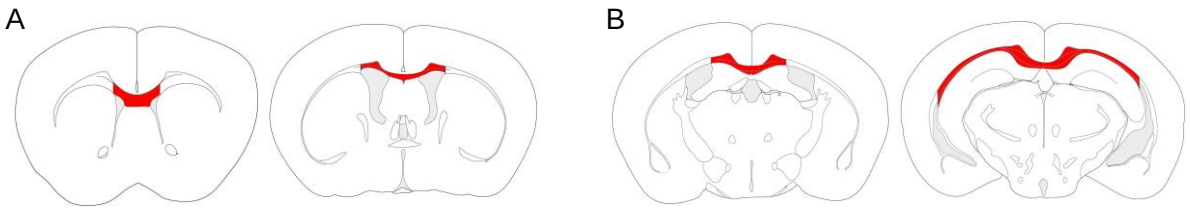

Figure 8: Illustration of the area of the corpus callosum used for quantification analysis. (A) rostral region bregma 1.10 to -0.10 and (B) caudal region from bregma 0.94 to -2.46.

2.10 Intra- and Interrater reliability

Intra- and interrater reliability was conducted to ensure the accuracy of the analyses of the MRI and cell counting data. All comparisons revealed significant correlations and were always ≥95%. SPSS for Windows version 17.0 (https://www.spss.com/de) was used for this analysis.

2.11 Western blot analysis

For western blot analysis the mice were deeply anesthetized with 0.25% tribromoethanol (Avertin) and sacrificed by decapitation. The brains were dissected out and the cortex, hippocampus and cerebellum of both hemispheres were separately quick frozen on dry ice. Additionally, kidney and liver were taken as possible control organs. Samples were stored at -80°C until use.

2.11.1 Protein extraction from brain tissue

All chemicals from Sigma Aldrich, Taufkirchen, Germany if not otherwise stated.

The lysis buffer (pH 8.3) for protein extraction contained: 50 mM Tris HCL ((tris(hydroxymethyl)aminomethane hydrochloride); pH 7.4), 150 mM Natrium chloride (NaCl; Merck, Darmstadt, Germany), 40 mM Natriumfluoride (NaF), 5 mM Ethylendiamin-tetraacetat (EDTA), 5 mM ethylene glycol tetraacetic acid (EGTA), 1 mM sodium orthovanadat (Na_3VO_4), 1% (v/v) Igepal, 0.1% (w/v) Natriumdesoxycholat and 0.1% Sodium dodecyl sulfate (SDS).

Just before use protease inhibitors were added: 1 mM Phenylmethylsulfonylfluoride, 10 µg/ml Aprotinin and 1 mM Leupeptin (both Roche, Penzberg, Germany).
Either 200 µl lysis buffer for cortex samples or 150 µl for hippocampus samples was used for each sample. Each sample was put into a glass homogenizer (VWR, Darmstadt, Germany) and the lysis buffer was added, the tissue was smashed immediately and then put on dry ice to freeze the sample. A cycle of freezing and thawing was repeated 4 times which was then followed by sucking the lysed material up and down with a heparin syringe (10 times). The material was transferred to a 2 ml tube (Eppendorf, Hamburg, Germany) and centrifuged (Thermo Fisher Scientific, Walldorf, Germany) at 12000 rpm at 4°C for 45 minutes. The supernatant was transferred to a fresh 2 ml tube (Eppendorf, Hamburg, Germany) and the volume was estimated, 10 µl were stored for protein estimation and 1/3 of 4x Laemmli (1 M Tris HCL (pH 8.3), 8% SDS, 40% Glycin, 20% ß-Mercaptoethanol, 0.04% Pyronin Y in ddH_20) was added to the rest followed by a heating step for 5 minutes at 95°C or 55°C (for PLP). Samples were stored at -80°C until use.

2.11.2 Protein estimation

The protein estimation was done using the Lowry-method. First a standard curve was prepared using a stock solution of albumin (1 mg/ml; Thermo Fisher Scientific, Walldorf, Germany) and ddH_20. The final albumin concentrations were 0, 2.5, 7.5, 10, 12.5, 15, and 20 µg/150 µl. For the samples, a dilution of 1:50 or 1:25 in ddH_20 was prepared. 1 ml of freshly prepared Copper solution (100 parts 2% Na_2CO_3 in 0.1 M NaOH (Roth, Lauterbourg, France), 1 part 2% K-Na-Tartrat in H_20 (Merck, Darmstadt, Germany), 1 part 1% $CuSO_4$ in H_20 (Merck, Darmstadt, Germany)) was added to each sample and the standard curve. Incubation time was 15 minutes. Next, 100 µl of Folin-Ciocalteu phenol reagent (Merck, Darmstadt, Germany) was added to each tube, immediately mixed and incubated for 45 minutes. To measure the protein concentration, a triplicate of every sample was created by 200 µl/well in a 96 well plate. The absorbance at 595 nm was determined in the plate reader (Dynex, Denkendorf, Germany). The final concentration of samples was calculated.

2.11.3 Quantification of myelin proteins

For MBP 16% Tris-Glycine precast gels and for all other proteins 4-12% Bis-Tris precast gels (all Invitrogen, Darmstadt, Germany) were used.

Solutions:

(1) 16% Tris-Glycine gels: 1x Tris Glycine SDS running buffer (for a 10x stock solution: 25 mM Tris Base, 195 mM Glycine, 0.1% SDS in ddH_20; pH 8.3) and Tris-Glycine transfer buffer (Tris Base 12 mM, 96 mM Glycine, 20% Methanol (J.T. Baker, Griesheim, Germany) in ddH_20) were used. Running time was set to 2.5 hours, 125 Volt; transfer time was set for 90 minutes, 25 Volt.

(2) 4-12% gels: 1x MES-Running buffer (Invitrogen, Darmstadt, Germany) and Bis-Tris transfer buffer (25 mM Bicine, 25 mM Bis-Tris, 1 mM EDTA in ddH_20, add 20% of methanol; pH 7.2) were used. Running time was set to ~45-60 minutes, 200 Volt; transfer time was set for 90 minutes, 30 Volt.

Procedure:

Precast gels were rinsed with ddH_20; tape at the bottom was removed and placed into the western blot chamber (Invitrogen, Darmstadt, Germany). The notched side of the gels faced inward of the chamber. Running buffer was filled to the whole chamber, the samples (15 µg/well) and SeeBlue™Plus2 Pre-Stained Protein Standard (10 µl; Invitrogen, Darmstadt, Germany) was loaded and the run started.

For the transfer, the pads and nitrocellulose membrane including filter paper (Invitrogen, Darmstadt, Germany) were soaked in transfer buffer at least 15 minutes before use. When the run was completed, the gels were removed from the plastic tray and a sandwich of 3 pads, 1 filter paper, the gel, membrane, filter paper and 2 pads was created. The blot module was placed in the western blot chamber and the transfer buffer was filled into the center until the gel-membrane sandwich was covered. The outer chamber was filled with H_20. The transfer was started.

When transfer was completed, the membranes were stained with Ponceau-S (Serva, Heidelberg, Germany) for 2-5 minutes to control the quality of the transfer. Membranes were rinsed with ddH_20, washed with TBST (50 mM Tris, 150 mM NaCl and 0.5 ml/1 liter Tween20; pH 7.4) for 5 minutes 3 times and placed in 5% (w/v) non-fat milk in TBST for 1 hour at room temperature. Primary antibodies were diluted

in 5% non-fat milk in TBST and put in a 50 ml Falcon tube (Greiner, Frickenhausen, Germany). The antibodies used were: PLP (1:5000 (Jung et al, 1996)), CNPase 1:1000, MBP 1:2000 (Dako, Hamburg, Germany), MOG 1:2500 (kindly provided by Prof. Nave). GAPDH (1:5000; Assay design; Lörrach, Germany) served as a loading control. Membranes were incubated in the primary antibodies over night at 4°C.
On the next day, membranes were washed for 15 minutes 3 times in TBST and incubated in anti-rabbit or anti-mouse secondary antibody coupled to horseradish peroxidase (1:2000; Vector Laboratories, Burlingame, USA) for 1 hour at room temperature. Membranes were again washed for 15 minutes 3 times. Immunoreactive bands were visualized by incubation of membranes in a chemiluminescence solution containing HRP Substrate Peroxide Solution and HRP Substrate Luminol Reagent in a 1:1 dilution (Millipore, Billerica, MA, USA) for 5 minutes. To detect the chemiluminescence signal, a Bio-Rad GelDoc set-up (Bio-Rad, Munich, Germany) was used. Densitometrical analysis were done using the Quality One 4.6.9. software (Bio-Rad, Munich, Germany).

2.12 Isolation of total RNA and quantitative real-time RT-PCR (qPCR)

2.12.1 Isolation of RNA from frozen brain sections

Two coronal brain sections per mouse, including the rostral and caudal part of the corpus callosum, were used to isolate total RNA according to the RNeasy FFPE kit (Qiagen, Hilden, Germany). First the sections were washed 3 times 5 minutes in 1xPBS, then the two sections per mouse were pooled in a 2 ml tube (Eppendorf, Hamburg, Germany), 150 µl PKD buffer was added and mixed by vortexing followed by centrifugation for 1 minute at 10000 rpm (Eppendorf, Hamburg, Germany). 10 µl of proteinase K was added to the lower, clear phase and mixed by pipetting up and down. Samples were incubated first at 56°C for 15 minutes and then at 80°C for 15 minutes followed by 3 minutes on ice before centrifugation for 15 minutes, 13500 rpm. 16 µl of DNase Booster buffer and 10 µl of DNase I stock solution were added, mixed and incubated for 15 minutes at room temperature. A volume of 320 µl RBC buffer was added and mixed, followed by addition of 720 µl ethanol (100%). After samples were well mixed, 700 µl were put on an RNeasy MinElute spin column placed in a 2 ml collection tube. Centrifugation took place for 15 s, 10000 rpm. The flow-through was discarded; this step was repeated until the entire sample was used. Next, 500 µl RPE buffer was added to the spin column and centrifuged at 10000 rpm

for 15 s. The flow-through was again discarded. Again 500 µl RPE buffer was added to the spin column and centrifuged at 10000 rpm for 2 minutes. The spin column was placed in a new 2 ml collection tube and centrifuged at 10000 rpm for 5 minutes. The collection tube and flow-through were discarded. The spin column was placed in a new 1.5 ml collection tube, 30 µl RNase-free water was added and the RNA was eluted by centrifugation at 10000 rpm for 1 minute. RNA concentration was measured with a UV-spectrometer (GeneQuant II, Pharmacia Biotech, Piscataway, NJ,. USA) at an absorbance of λ=260 nm. The RNA concentration ranged from 36-140 ng/µl. First strand cDNA was generated from total RNA using 10 µl RNA and 2 µl N6 random primers (50 µmol). Annealing took place at 70°C for 2 minutes, samples were cooled down on ice and the master mix containing 4 µl 5x 1st strand buffer, 2 µl 0.1 M DTT, 1 µl dNTPs (20 mM each) and 1 µl Superskript III (200 U/µm) (all from Invitrogen, Darmstadt, Germany) was added. Cycling was done for 10 minutes at 26°C, followed by 45 minutes at 50°C and 45 minutes at 55°C (UNO Thermoblock, Biometra, Göttingen, Germany). The cDNA was diluted 1:10 with ddH_2O.

2.12.2 Quantitative RT-PCR

The relative concentrations of mRNAs of interest in different cDNA samples were measured out of 3 replicates using the threshold cycle method (delta Ct) for each dilution and were normalized to a normalization factor derived from levels of 'housekeepers', GAPDH, beta-actin and HPRT1 mRNA, calculated with geNorm_win_3.5 (Vandesompele et al, 2002). Reactions were performed using 4 µl of diluted cDNA and 6 µl master mix containing SYBR green (ABgene, Foster City, CA, USA) and 5 pmol of the forward and reverse primer, respectively.

Cycling was done for 2 minutes at 50°C, followed by denaturation at 95°C for 10 minutes. The amplification was carried out with 45 cycles of 95°C for 15 s and 60°C for 60 s (Light Cycler480, Roche, Penzberg, Germany). The specificity of each primer pair was controlled with a melting curve analysis. For qPCR, the following primers were used: Mouse interleukin-1α (IL-1α) forward: 5'-TCA ACC AAA CTA TAT ATC AGG ATG TGG-3', reverse: 5'-CGA GTA GGC ATA CAT GTC AAA TTT TAC-3'; mouse interleukin-1β (IL-1β) forward: 5'-AAG GGC TGC TTC CAA ACC TTT GAC-3', reverse: 5'-ATA CTG CCT GCC TGA AGC TCT TGT-3'; mouse transforming growth factor-β (TGF-β) forward: 5'-TGA CGT CAC TGG AGT TGT ACG-3', reverse: 5'-GGT TCA TGT CAT GGA TGG TGC-3'; mouse complement component 1, q

subcomponent, A chain (C1qA) forward: 5' CGG GTC TCA AAG GAG AGA GA 3', reverse: 5' CCT TTA AAA CCT CGG ATA CCA GT 3'; mouse triggering receptor expressed on myeloid cells-2 (Trem-2) forward: 5'-ACA GCA CCT CCA GGA ATC AAG-3', reverse: 5'-CCA CAG CCC AGA GGA TGC-3'; mouse GAPDH forward: 5'-CAA TGA ATA CGG CTA CAG CAA C-3', reverse: 5'-TTA CTC CTT GGA GGC CAT GT-3'; mouse beta-actin forward: 5'-CTT CCT CCC TGG AGA AGA GC-3', reverse: 5'- ATG CCA CAG GAT TCC ATA CC-3'; mouse HPRT1 forward: 5'-GCT TGC TGG TGA AAA GGA CCT CTC GAA G-3', reverse: 5'-ATG CCC TTG ACT ATA ATG AGT ACT TCA GGG-3'.

2.13 Statistical analysis

Data were compared using 2-way or 3-way ANOVA for repeated measures including Bonferroni testing if applicable, and the Mann-Whitney-U-test for inter-group comparisons. Because the analyses concerning EPO were highly hypothesis driven, a one-sided Mann-Whitney-U-test was used. Significance level was set to $p<0.05$. Data are presented as mean±SEM if not stated otherwise. The data were analyzed using Prism5 (Graphpad Software, San Diego, CS, USA) and SPSS for Windows version 17.0 (https://www.spss.com/de).

3 RESULTS

3.1 Establishment of the cuprizone model

To establish the cuprizone model, a pilot experiment was performed. As described in detail in the Materials and Methods section, 8 week old C57BL/6 male mice were fed with either normal food pellets or food pellets containing 0.2% cuprizone over a period of 7 weeks. The body weight of mice and the motor performance on a rota-rod (constant speed 16 rpm) were monitored. Both experimental groups gained weight over the 7 weeks (Figure 9; 2-way ANOVA for repeated measures, $F_{6,492}$=746,14, P<0.001). Until week 4 the mice were not impaired in their motor performance (Figure 10A), to make the motor task more difficult the rota-rod protocol was changed; the rotation of the rotating drum started with a speed of 4 rpm and accelerated to 40 rpm within 5 minutes. Based on the challenge of the new rota-rod protocol a decrease in the performance in both groups was observed (Figure 10B). However, there was no difference between the groups. To check for demyelination a LFB staining was performed. The cuprizone-fed mice had a normal myelinated corpus callosum (Figure 11). Based on the histology and data for the body weight of mice a second pilot experiment was designed. Cuprizone was administered via food pellets or mixed into standard rodent ground chow.

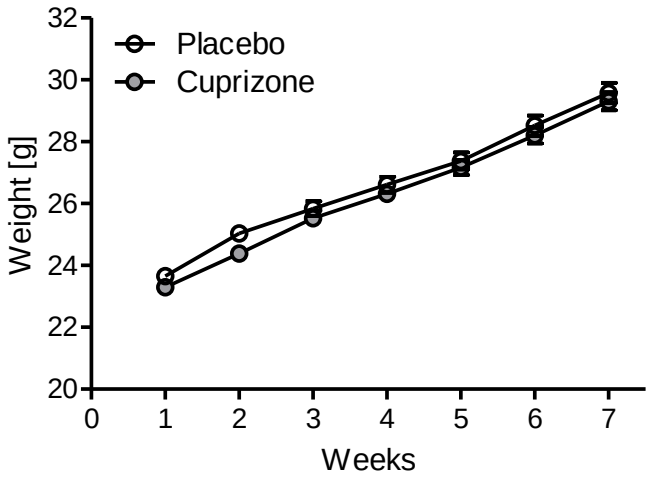

Figure 9: First pilot experiment. Body weight of mice fed with normal food pellets (Placebo) or food pellets containing 0.2% cuprizone over the whole experimental time. Mean±SEM presented; N= 42-44/group.

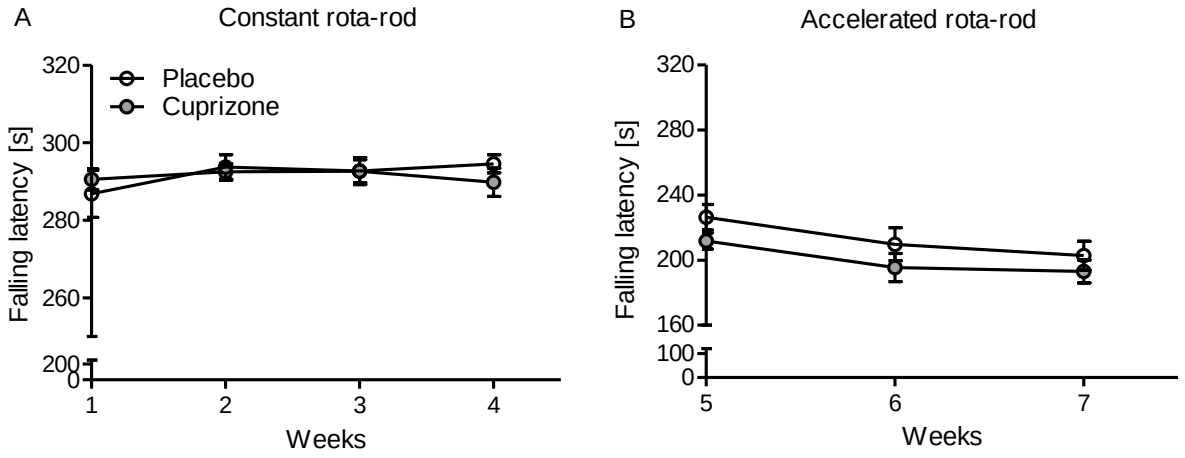

Figure 10: First pilot experiment. (A) Rota-rod performance of mice from weeks 1 to 4 with a constant speed of 16 rpm. (B) Rota-rod performance of mice from weeks 5 to 7 with accelerated speed from 4 to 40 rpm. Mean±SEM presented; N= 42-44/group.

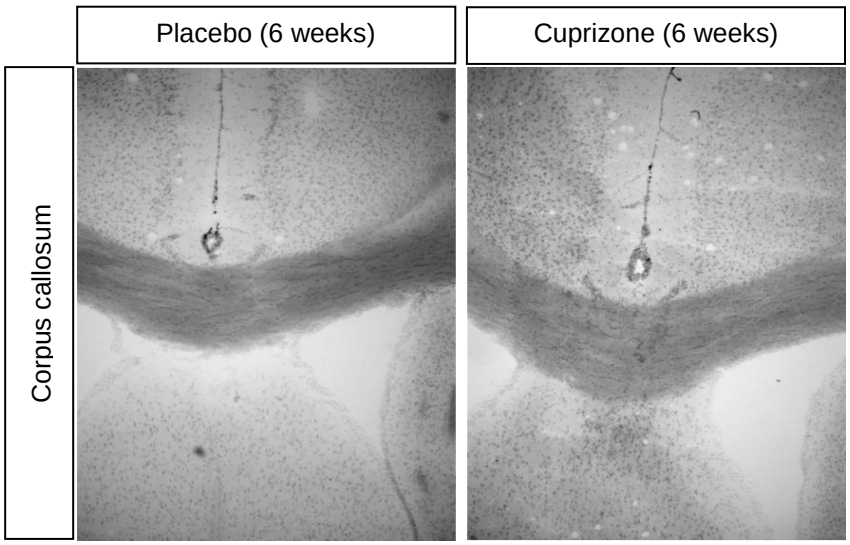

Figure 11: First pilot experiment. Presentation of a LFB-staining in the corpus callosum of a mouse fed for 6 weeks with normal food pellets (Placebo) and a mouse fed with food pellets containing 0.2% cuprizone.

In the second pilot experiment, the application of cuprizone via pellets or ground chow was compared (for the experimental design see Materials and Methods section 2.5.1). The main readout was body weight of mice. This parameter was significantly influenced by the cuprizone feeding of mice via ground chow (3-way ANOVA for repeated measures, $F_{(2,3)}$=55,80, P=0.004). Already 4 days after the application of 0.2 or 0.3% cuprizone mixed into ground chow these mice lost weight. The body weight further decreased and stayed on a constantly lower level until the end of the experiment (Figure 12A). Two mice fed with 0.3% cuprizone and one mouse of the 0.2% diet-group died on day 19. In comparison no weight loss and even a gain of weight over time was observed in mice fed 0.2% cuprizone via food pellets (Figure 12B; 2-way ANOVA for repeated measures, $F_{(6,24)}$=131,75, P<0.001). Toxicological analysis of the food pellets confirmed that cuprizone was present, intact and active (see Supplement 6.1; performed in the Department of Pharmacology and Toxicology at the University hospital Göttingen, Germany). Based on these findings all future experiments were performed with 0.2% cuprizone mixed into standard rodent chow.

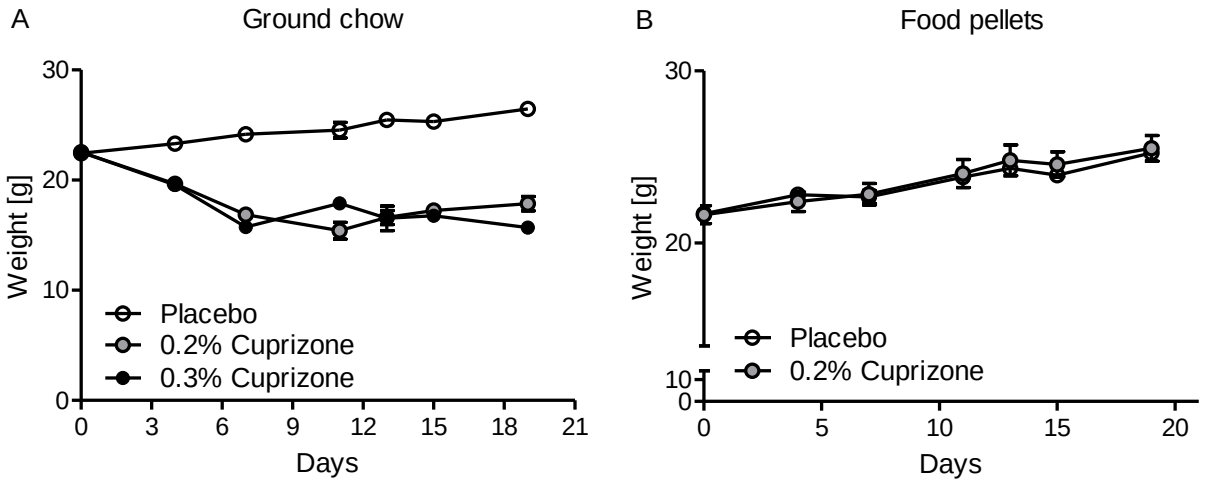

Figure 12: Second pilot experiment. (A) Body weight of mice fed with normal ground chow (Placebo) or cuprizone mixed into ground chow. Cuprizone feeding significantly influenced the body weight of mice (3-way ANOVA $F_{(2,3)}$=55,80, P=0.004). (B) Body weight of mice fed with normal food pellets (Placebo) or food pellets containing 0.2% cuprizone. No effect of feeding. Mean±SEM presented; N= 3/group.

3.2 Effect of EPO on re- and demyelination

3.2.1 Overview of analyzed parameters

In the following tables, an overview of the analyzed parameters in the two studies investigating the effect of EPO on remyelination (Table 6) and demyelination (Table 7) is presented. In the study which analyzed the effect of EPO on remyelination (Table 6) mice were not sacrificed at weeks 6 and 15, therefore only behavioral analyses were performed at these time points. The lack of data at some of the other time points in both studies is due to the results obtained from previous time points or the other parameters at that time. Additional analyses were not thought to give further insight into the EPO effect under the given experimental conditions.

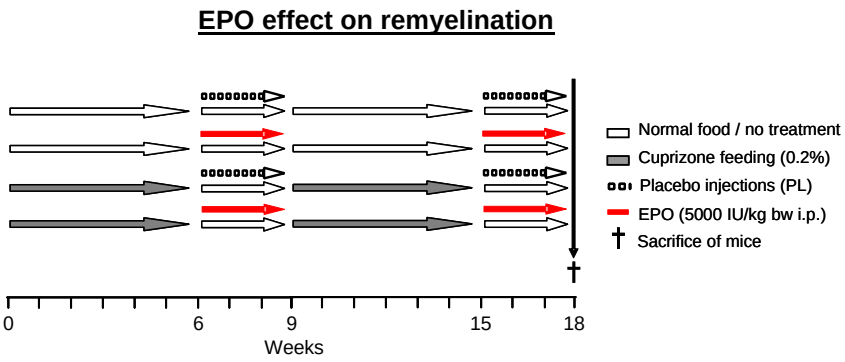

Table 6: Effect of EPO on remyelination. Overview of the parameters analyzed at different time points. (ABR: auditory brain stem response; WB: western blot; MTR: magnetization transfer ratio)

Parameters analyzed		Week 6	Week 9	Week 15	Week 18
Rota-rod		Done	Done	Done	Done
Beam balance		Not performed	Not performed	Done	Done
Startle response		Done	Done	Done	Done
ABRs		-	Not performed	-	Done
Protein analysis (WB)		-	Done	-	Done
MRI analysis	Volumetry	-	Not performed	-	Done
	%MTR	-	Not performed	-	Not performed
Haematocrit		-	Done	-	Done
Immunohistochemistry		-	Not performed	-	Not performed

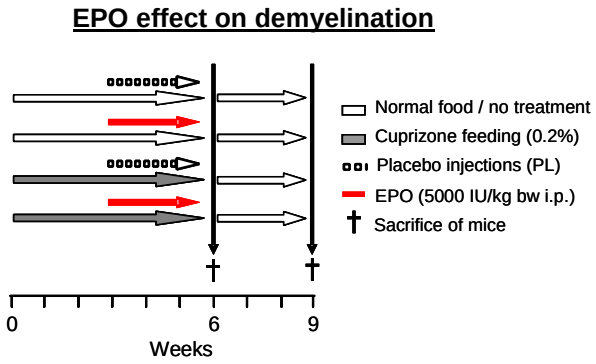

Table 7: Effect of EPO on demyelination. Overview of the parameters analyzed at different time points. (ABR: auditory brain stem response; WB: western blot; MTR: magnetization transfer ratio)

Parameters analyzed		Week 6	Week 9
Rota-rod		Done	Done
Beam balance		Done	Done
Startle response		Done	Done
ABRs		Not performed	Not performed
Protein analysis (WB)		Not performed	Not performed
MRI analysis	Volumetry	Done	Done
	%MTR	Done	Done
Haematocrit		Done	Done
Immunohistochemistry		Done	Not performed

3.2.2 Effect of EPO on remyelination

3.2.2.1 Basic observations under cuprizone and EPO treatment

Cuprizone application took place either once over 6 weeks followed by a remyelination phase of 3 weeks combined with intra-peritoneal placebo or EPO injections or repeatedly; a second cycle of cuprizone feeding and a second remyelination phase combined with placebo/EPO injections occurred after the first recovery phase (see Materials and Methods section 2.5.2.2). Cuprizone feeding significantly decreased the body weight over time (3-way ANOVA for repeated measures, $F_{(1,55)}$=212,28, P<0.001). A fast recovery in the first and even second remyelination phase was observable (Figure 13A and B). However, even in the third recovery week (weeks 9 and 18) the body weight of cuprizone-fed mice was always below the control groups. Interestingly, in the second demyelination phase (weeks 10-15) the body weight of EPO-treated cuprizone mice did not decline as much as

compared to the placebo-treated cuprizone mice. However, this difference did not reach significance levels.

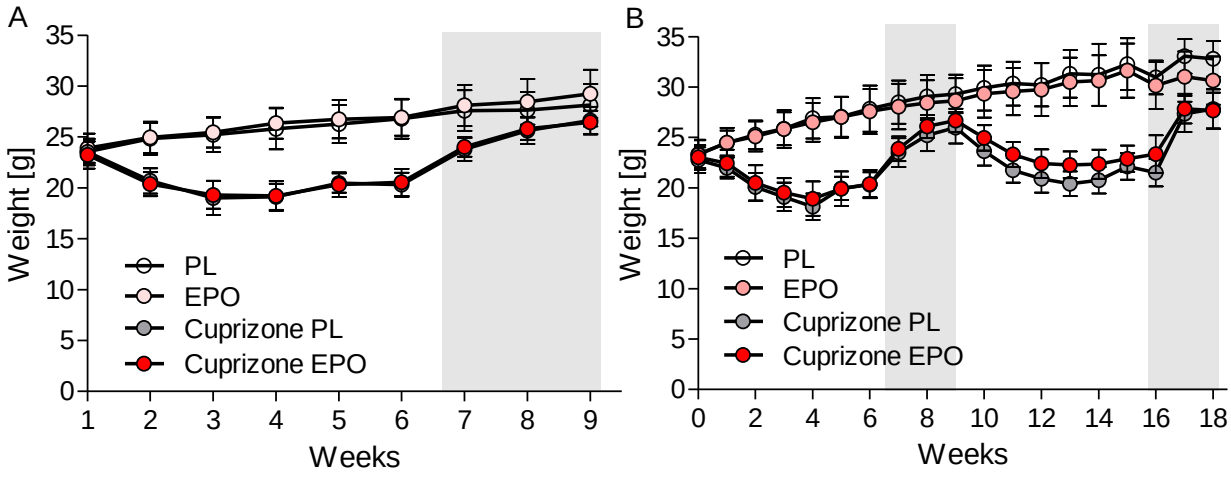

Figure 13: Effect of EPO on remyelination. (A) Body weight of mice in the single feeding group; N=20; (B) body weight of mice in the repeated feeding group; N=15-25. The cuprizone mice showed a significantly lower body weight over time compared to the controls (3-way ANOVA for repeated measures, $F_{(1,55)}$=212,28, P<0.001). Grey boxes indicate the recovery phases. Mean±SD presented; PL=placebo; EPO=erythropoietin.

Evaluation of the haematocrit at weeks 9 and 18 revealed a significant increase by EPO treatment in both the control and cuprizone group (Figure 14; Mann-Whitey U-test, P<0.001).

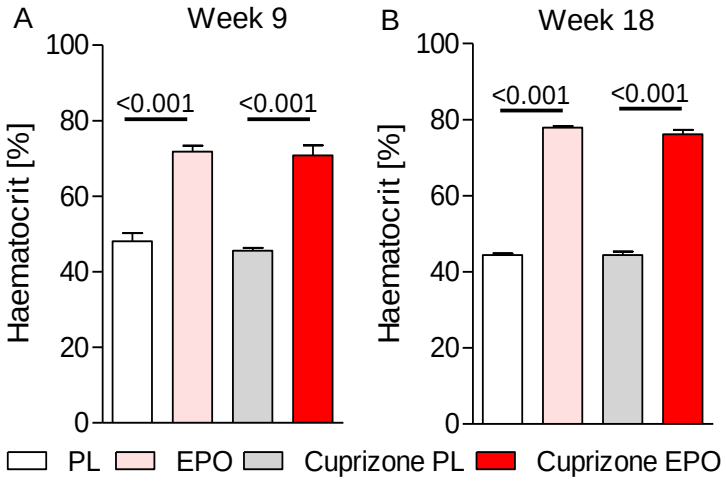

Figure 14: Effect of EPO on remyelination. Haematocrit of mice at (A) week 9; N=11-15 and (B) week 18; N=7-10. Mean±SEM presented; PL=placebo; EPO=erythropoietin.

3.2.2.2 Motor coordination and balance under cuprizone and EPO treatment

The results of the accelerated rota-rod, which is a relatively crude test for motor function, showed that all mice improved their performance over time (Figure 15; 3-way ANOVA for repeated measures, $F_{(18,990)}$=35.97, P<0.001). Cuprizone did not influence the performance of the mice in this test either had EPO any effect.

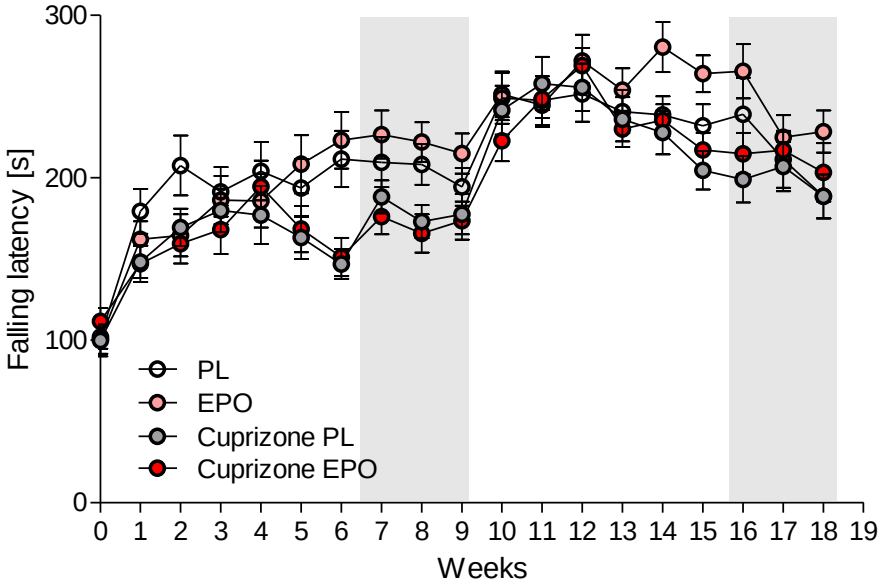

Figure 15: Effect of EPO on remyelination. Falling latency on the accelerated rota-rod (4-40 rpm). Grey boxes indicate the recovery phases. N=14-25; mean ±SEM presented; PL=placebo; EPO=erythropoietin.

Beam balance is a test for vestibulomotor function in mice. At week 15, directly after the second cycle of demyelination, cuprizone/placebo mice needed significantly more time to cross the 10 and 8 mm beam compared to the control group (Mann-Whitey U-test, P≤0.003). EPO treatment of cuprizone mice significantly improved the performance on the 8 mm beam (Figure 16; Mann-Whitey U-test, P=0.015). After the second recovery phase, cuprizone-fed mice had a higher duration to cross the beam compared to controls without an additional effect of EPO.

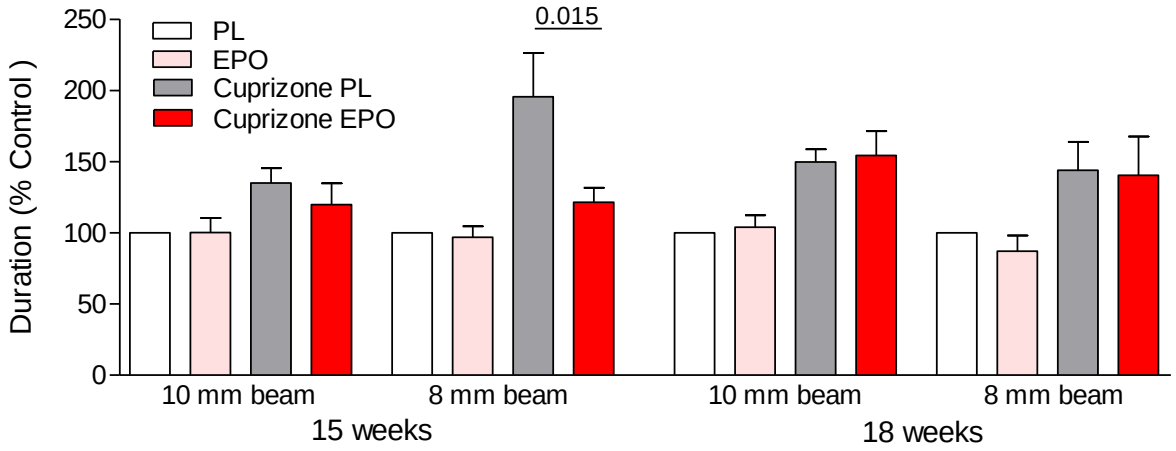

Figure 16: Effect of EPO on remyelination. The beam balance test was performed at weeks 15 and 18. A 10 and 8 mm diameter beam was used and the time to cross the beam (duration) was recorded. N= 14-15; mean ±SEM presented; PL=placebo; EPO=erythropoietin.

3.2.2.3 Startle response of mice

The observation of a disturbed behavior in the pre-pulse-inhibition test excluded the analysis of these data (therefore data not shown), and led to the assessment of hearing using the startle response test. This test measures the startle response of mice to acoustic stimuli in a range of 65 to 120 dB. At weeks 6, 15, and 18, both cuprizone groups showed a significantly reduced startle response without any further influence of EPO (Figure 17; 2- or 3-way ANOVA for repeated measures, $P \leq 0.001$). To further analyze whether this is in fact a result of an impaired hearing ability of the mice, acoustic evoked potentials were measured (collaboration with Nicola Strenzke, Department of Otorhynolaryngology, University hospital Göttingen, Germany). However, no group differences were observed in the amplitude or latency of the recorded ABRs at week 18 (Figure 18).

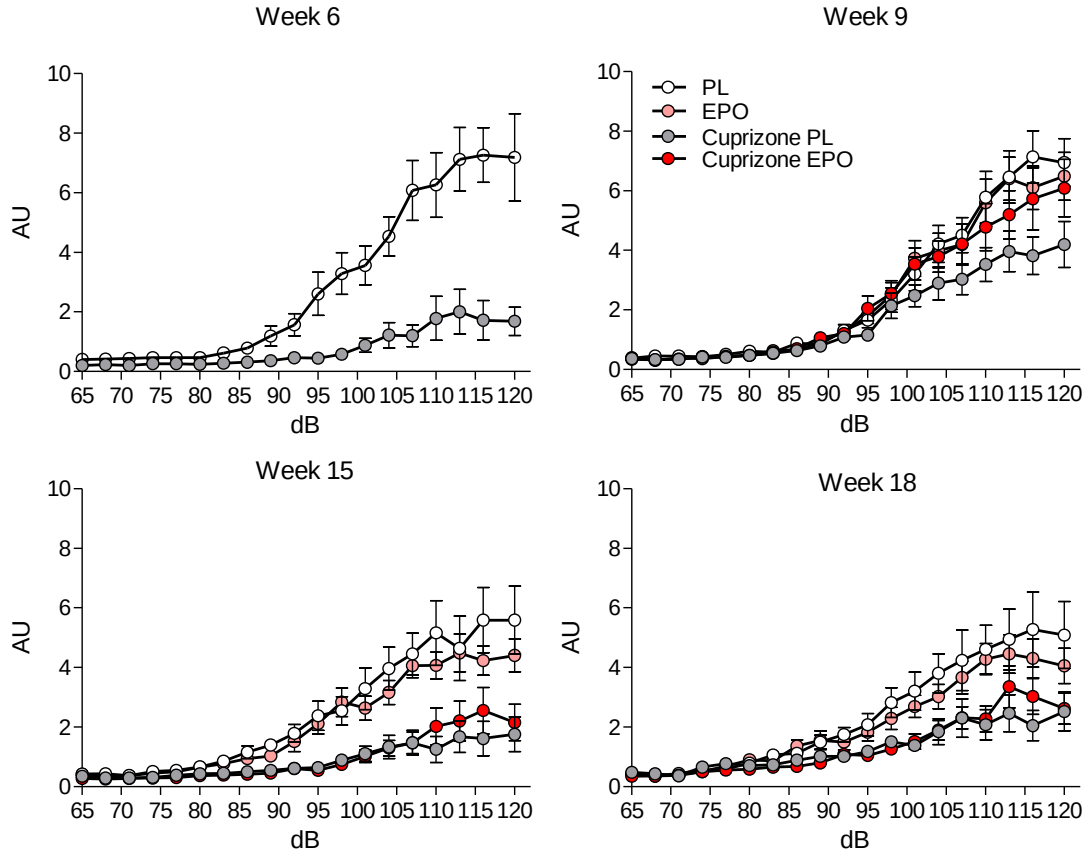

Figure 17: Effect of EPO on remyelination. Assessment of hearing measured by the startle response of mice to acoustic stimuli ranging from 65 to 120 dB. This test was performed at weeks 6, 9, 15, and 18. N= 12-15; mean±SEM presented; PL=placebo; EPO=erythropoietin; AU = arbitrary unit.

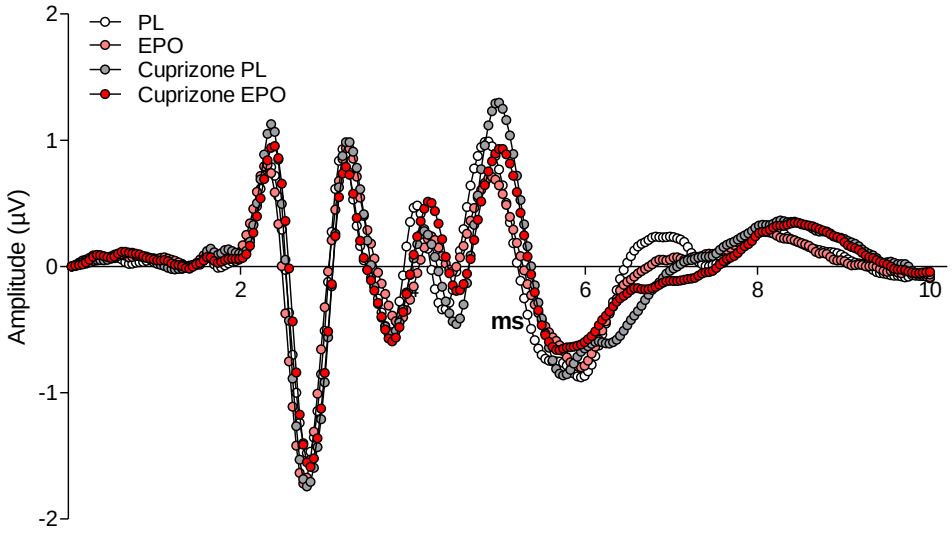

Figure 18: Effect of EPO on remyelination. Assessment of hearing by the recording of acoustic evoked brain stem responses to 20 Hertz stimuli at week 18; N=6. PL=placebo; EPO=erythropoietin.

3.2.2.4 Analysis of myelin proteins in the hippocampus and cortex

Besides investigating physical and behavioral parameter, changes related to myelin were assessed on protein level. The cortex and hippocampus were the regions of interest for myelin protein analysis. At week 9, after the first remyelination phase of 3 weeks, CNP, MOG (myelin oligodendrocyte glycoprotein) and MBP were significantly decreased in the cortex of cuprizone mice (Figure 19; Mann-Whitey U-test, PL vs. Cuprizone PL, $P<0.01$). PLP showed the same trend but failed to be significant. In contrast, all these myelin proteins were not affected in the hippocampus of cuprizone-fed mice at this time point (Figure 19). EPO did not show any effect.

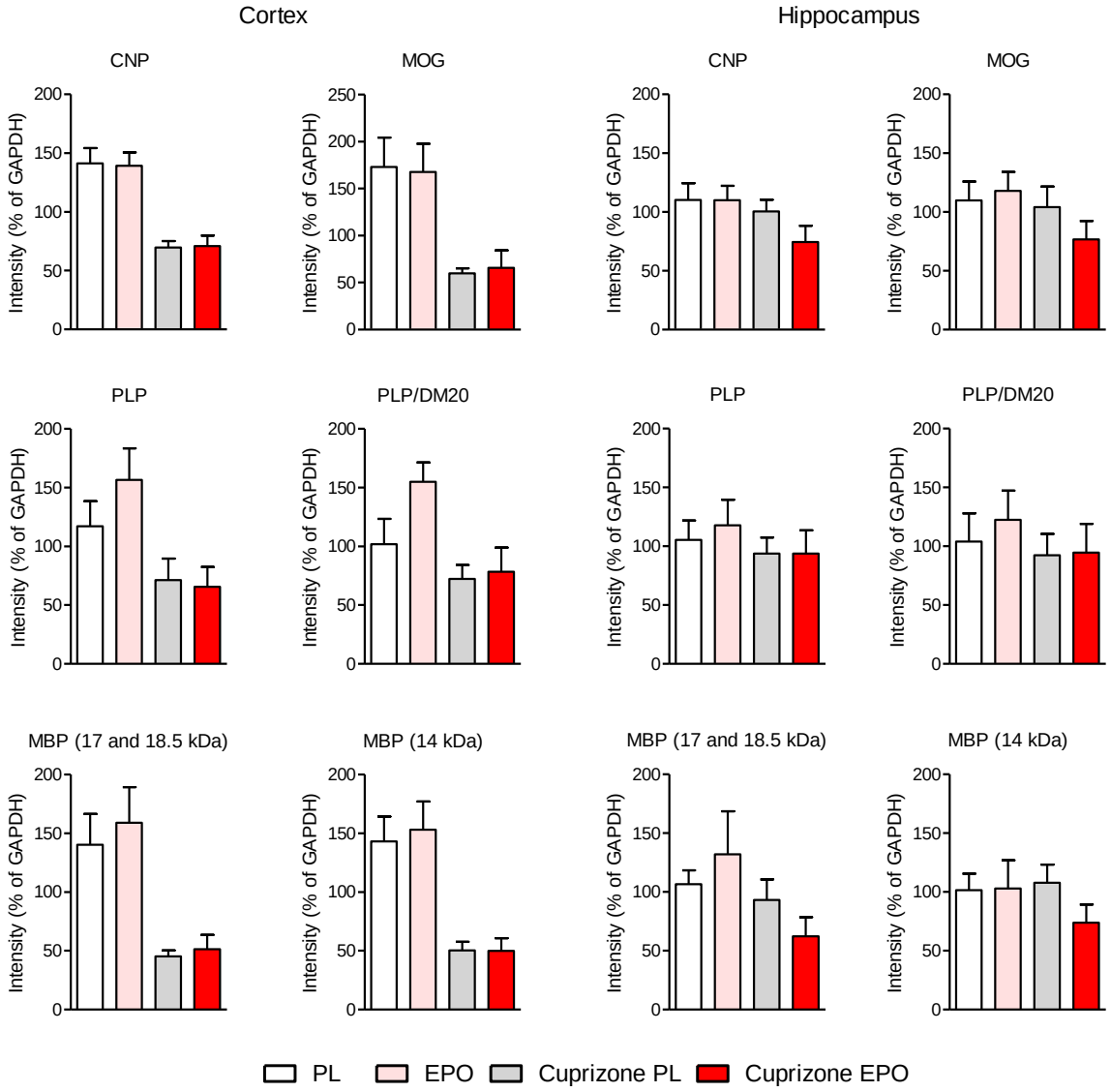

Figure 19: Effect of EPO on remyelination. Analysis of the myelin proteins: CNP (2'-3'-cyclic nucleotide 3'-phosphodiesterase), MOG (myelin oligodendrocyte glycoprotein), PLP (proteolipid protein) and MBP (myelin basic protein) in the cortex and hippocampus at week 9; N=7; mean±SEM presented; PL=placebo; EPO=erythropoietin.

At week 18, after the second recovery phase, all myelin proteins in both cortex and hippocampus were significantly reduced (Mann-Whitey U-test, PL vs. Cuprizone PL, P<0.01). No effect of EPO was present (Figure 20).

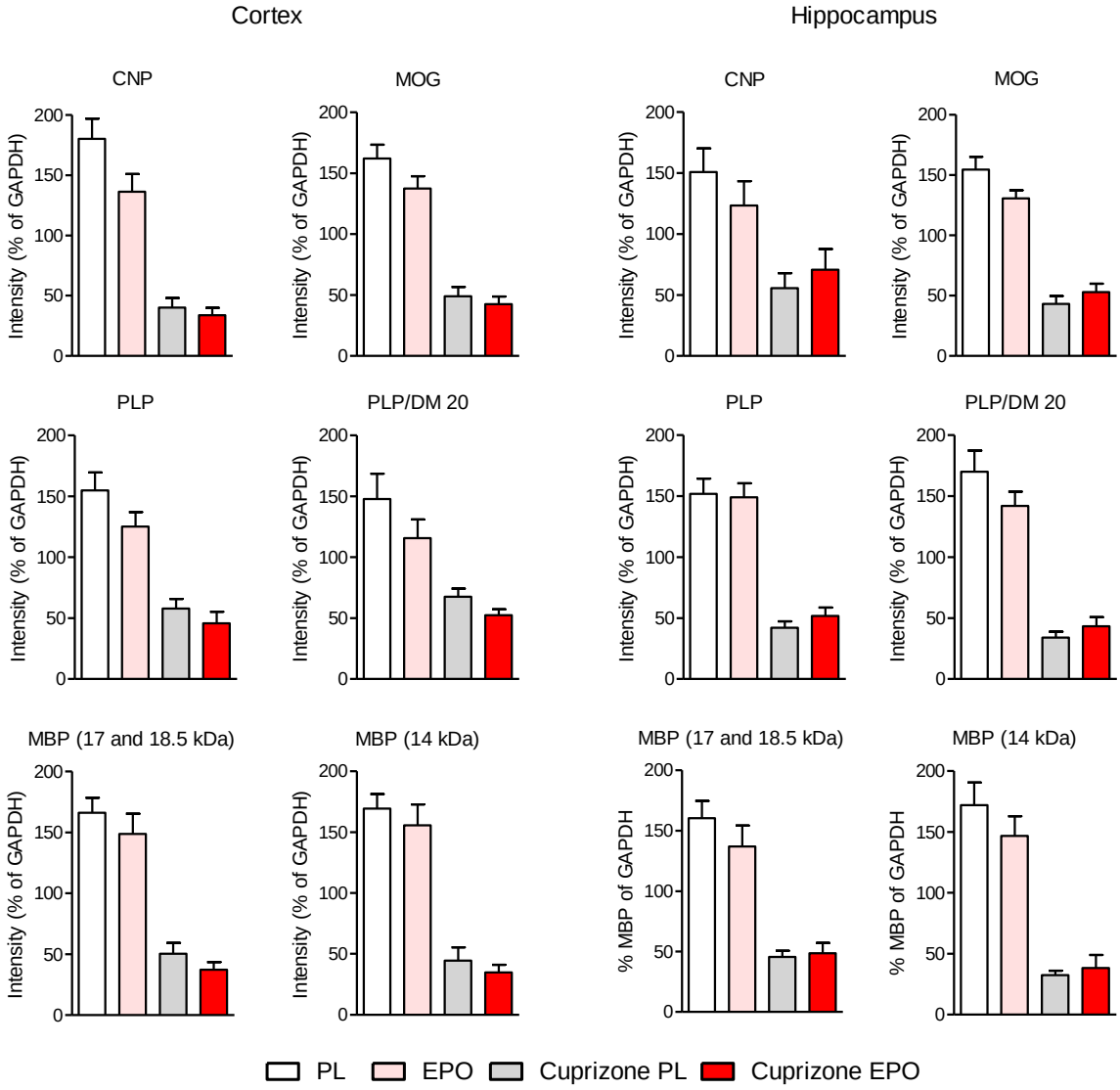

Figure 20: Effect of EPO on remyelination. Analysis of the myelin proteins: CNP (2'-3'-cyclic nucleotide 3'-phosphodiesterase), MOG (myelin oligodendrocyte glycoprotein), PLP (proteolipid protein) and MBP (myelin basic protein) in the cortex and hippocampus at week 18; N=8-10; mean±SEM presented; PL=placebo; EPO=erythropoietin.

3.2.2.5 Volumetrical analysis of cuprizone-fed mice

At the end of the experiment (week 18) MRI took place. Cuprizone-fed mice did not show any sign of brain atrophy as analyzed by T1-maps (Figure 22; Brain matter). In all cuprizone mice an obvious enlargement of the ventricular system was apparent (as illustrated in Figure 21), although it was not significant. High variations in the

measurement of the ventricular volume within the cuprizone groups became apparent (error bars in Figure 22). EPO had no additional effects in this analysis.

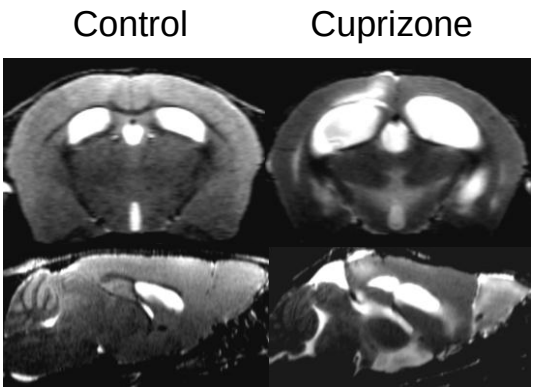

Figure 21: Effect of EPO on remyelination. T2-weighted sample image to illustrate the enlargement of the ventricular system of mice fed with 0.2% cuprizone. Images kindly provided by Susann Boretius.

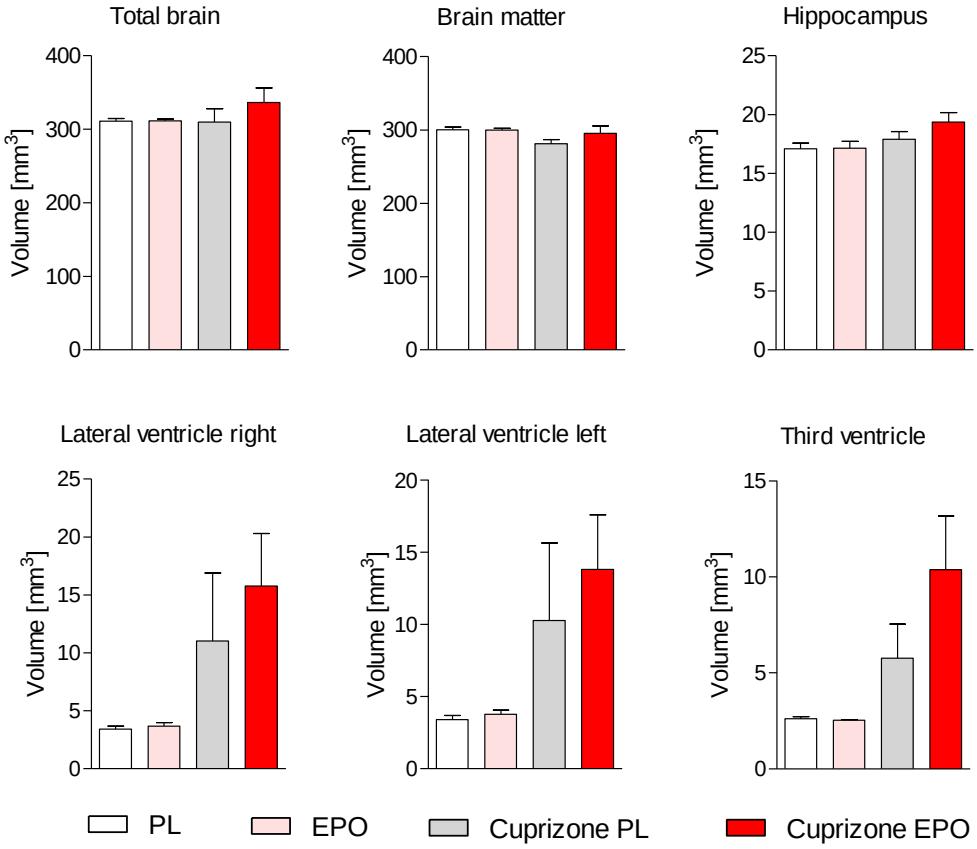

Figure 22: Effect of EPO on remyelination. Volumetrical analysis of the total brain, brain matter, hippocampus and ventricular system at week 18; N=6; mean±SEM presented; PL=placebo; EPO=erythropoietin.

In summary, the study of investigating the effect of EPO on remyelination showed that cuprizone feeding had a potent effect on the body weight of mice, vestibulomotor function, myelin protein levels in the brain and brain volumetrical parameters (ventricular system). EPO application had a slight effect on the body weight of mice during the second demyelination phase and significantly improved the performance in the beam balance task at week 15. No further beneficial effect of EPO was present.

3.2.3 Effect of EPO on demyelination

3.2.3.1 Basic observations under cuprizone and EPO treatment

The cuprizone diet was again applied for 6 weeks and was followed by a remyelination phase of 3 weeks. In weeks 4-6 of cuprizone feeding placebo/EPO treatment was applied (see experimental scheme in Materials and Methods section 2.5.3). The body weight of mice was significantly reduced by the cuprizone feeding (3-way ANOVA for repeated measures, $F_{(1,56)}$=235,61, P<0.001) and returned to comparable levels to the controls after 3 weeks recovery (Figure 23A). The haematocrit of EPO-treated mice in both the control and cuprizone group was significantly increased at week 6 (Mann-Whitey U-test, P≤0.001), directly after the termination of the treatment. Both groups reached normal levels after the recovery period (week 9; Figure 23B).

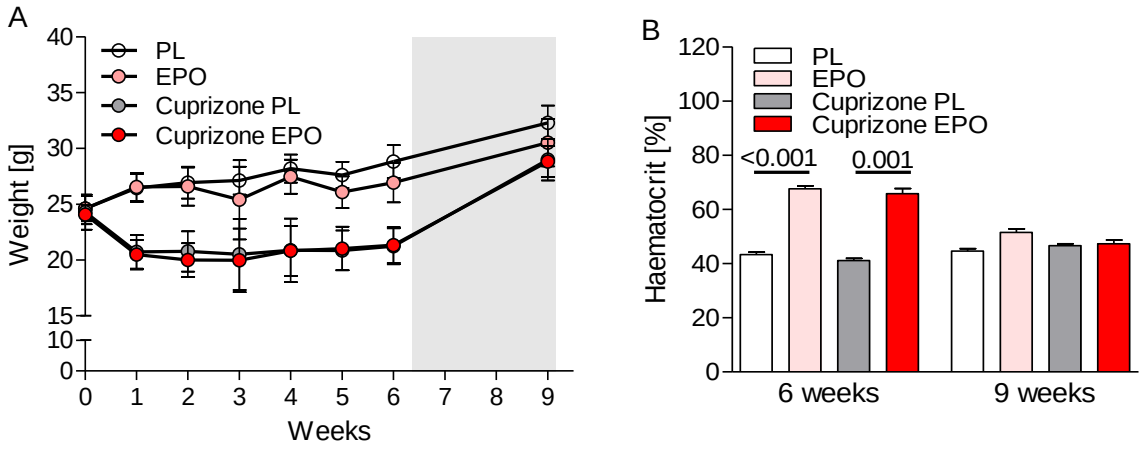

Figure 23: Effect of EPO on demyelination. (A) Body weight of mice. Cuprizone-fed mice had significantly lower body weight over time compared to controls (3-way ANOVA for repeated measures, $F_{(1,56)}$=235,61, P<0.001); N=15-26; mean±SD presented. Grey box indicates the recovery phase. (B) Haematocrit of mice at weeks 6 and 9; EPO significantly enhanced the haematocrit at week 6 (Mann-Whitey U-test, P≤0.001). N=6-15; mean±SEM presented; PL=placebo; EPO=erythropoietin.

3.2.3.2 Motor coordination and balance under cuprizone and EPO treatment

At baseline, before the cuprizone feeding started, the performance of mice on the rota-rod was comparable and all groups showed an improvement of the performance from day 1 to 2 (Figure 24, 3-way ANOVA for repeated measures, $F_{(2,100)}$=5.90, P=0.017). 6 weeks after cuprizone initiation all mice showed a comparable performance on the rota-rod and improvement over the 3 testing days (Figure 25A, 3-way ANOVA for repeated measures, $F_{(2,194)}$=12.57, P<0.001). No differences between groups were detected after the 3 week recovery phase (Figure 25B).

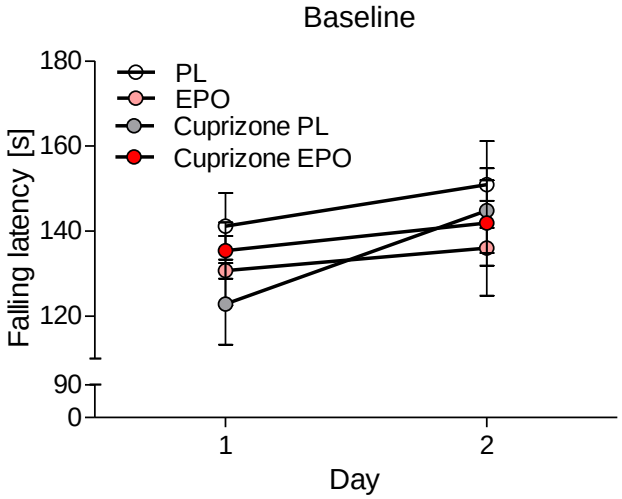

Figure 24: Effect of EPO on demyelination. Baseline performance in a 2-day rota-rod paradigm (acceleration 4-40 rpm). N=26; mean±SEM presented; PL=placebo; EPO=erythropoietin.

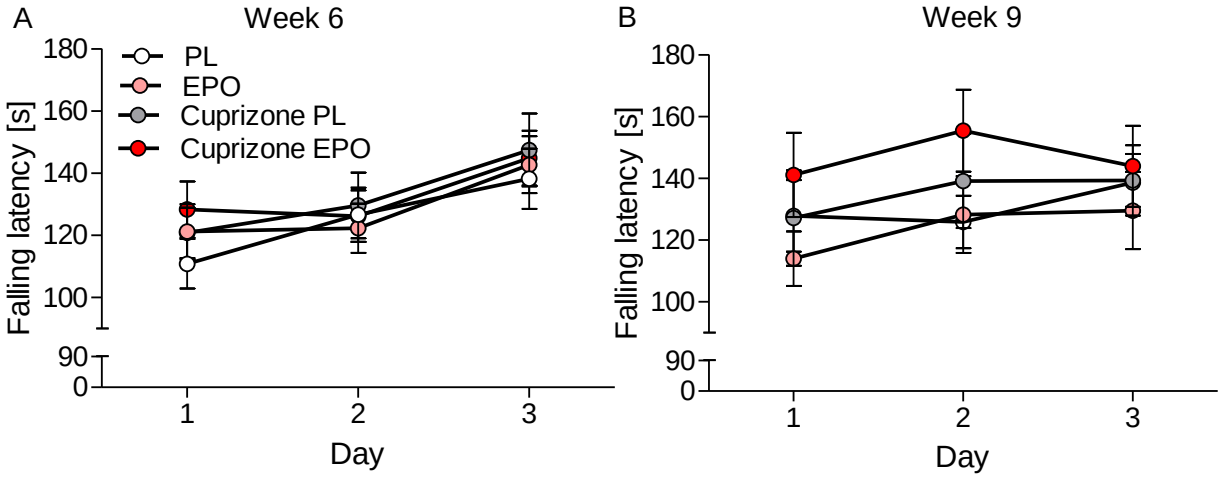

Figure 25: Effect of EPO on demyelination. Falling latency in a 3-day rota-rod paradigm (acceleration 4-40 rpm) at (A) week 6; all mice improved their performance over time (3-way ANOVA for repeated measures, $F_{(2,194)}$=12.57, P<0.001); N=24-26 and (B) week 9; N=15. Mean±SEM presented; PL=placebo; EPO=erythropoietin.

In the beam balance task, all mice at baseline showed a comparable duration to cross the 10 and 8 mm beam (Figure 26). At week 6, the cuprizone-fed mice needed significantly longer time to cross the 10 and 8 mm beam (Mann-Whitey U-test, PL vs. Cuprizone PL, P<0.001). However, EPO-treated cuprizone mice improved their performance on the 10 mm beam and significantly on the 8 mm beam (Figure 27; Mann-Whitey U-test, P=0.004). At week 9, both cuprizone groups recovered and reached almost control levels without any additional effect of EPO (Figure 27).

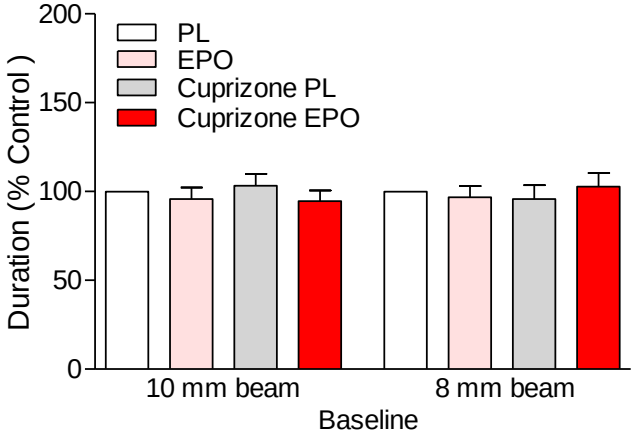

Figure 26: Effect of EPO on demyelination. Baseline performance on the 8 and 10 mm beam. The time to cross the beam (duration) was measured. N=24-26; mean±SEM presented; PL=placebo; EPO=erythropoietin.

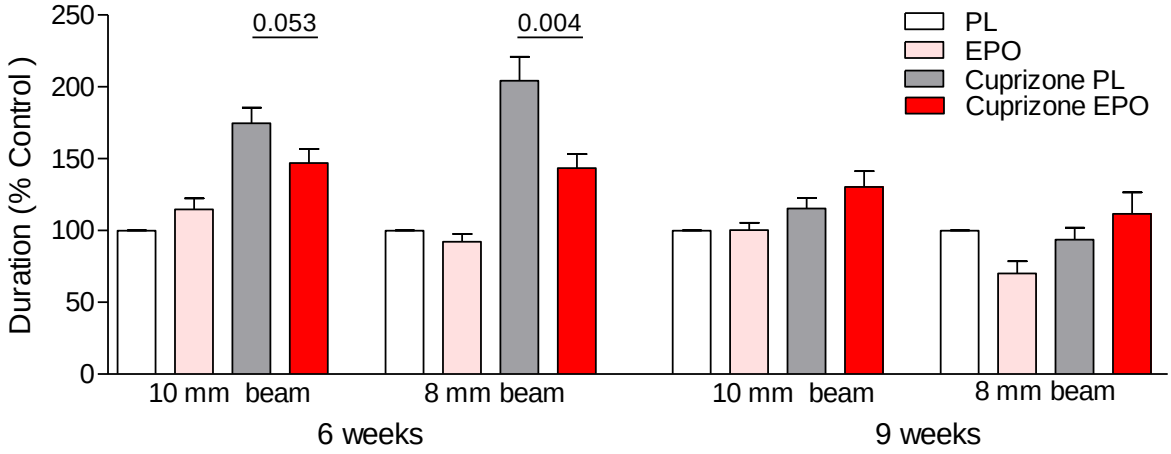

Figure 27: Effect of EPO on demyelination. Beam balance test performed on the 8 and 10 mm beam at weeks 6 and 9. At week 6, cuprizone mice showed a higher duration to cross the beam (Mann-Whitey U-test, PL vs. Cuprizone PL, P<0.001). N=14-26; mean±SEM presented; PL=placebo; EPO=erythropoietin.

3.2.3.3 Startle response of mice

To evaluate the startle response of mice in the current experimental conditions and to prove the previous observations, this test was performed again. A similar picture was present; whereas all groups showed a similar startle response at baseline (Figure 28), at week 6, cuprizone feeding significantly reduced the startle response of mice (Figure 29; 3-way ANOVA for repeated measures, $F_{(1,87)}$=61.65, P<0.001). This effect disappeared after 3 weeks recovery. No effect of EPO was present.

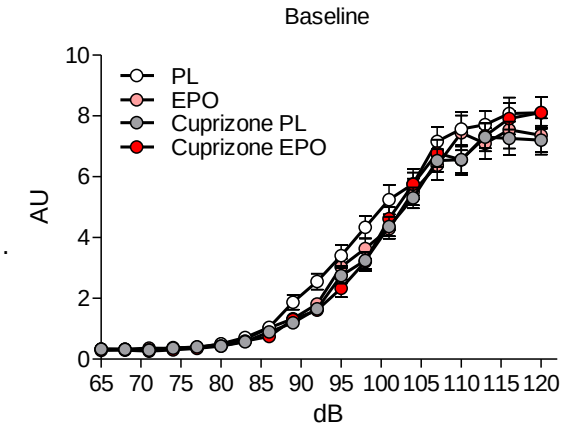

Figure 28: Effect of EPO on demyelination. Assessment of hearing at baseline. The startle response of mice to acoustic stimuli ranging from 65 to 120 dB was measured. N=26; mean±SEM presented; PL=placebo; EPO=erythropoietin; AU=arbitrary unit.

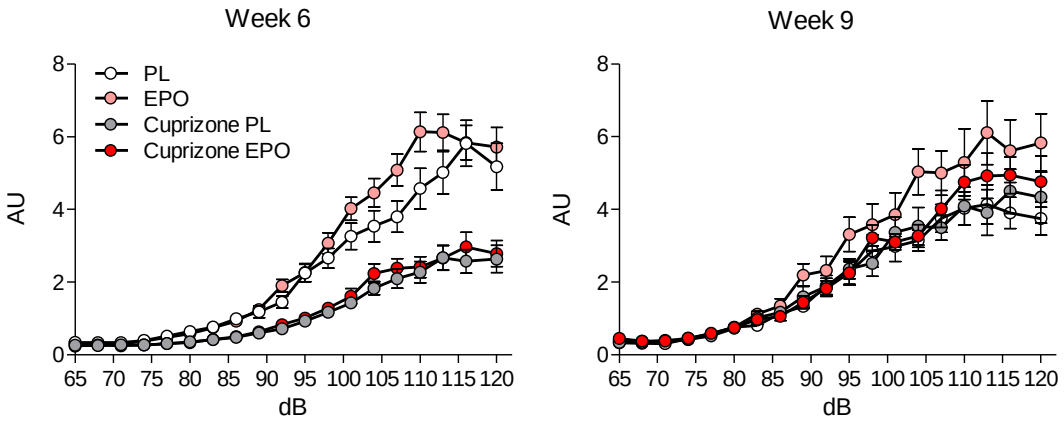

Figure 29: Effect of EPO on demyelination. Assessment of hearing at weeks 6 and 9 by measuring the startle response of mice to acoustic stimuli ranging from 65 to 120 dB. At week 6, cuprizone mice showed a significant reduced startle response (3-way ANOVA for repeated measures, $F_{(1,87)}$=61.65, P<0.001). N=15-26; mean±SEM presented; PL=placebo; EPO=erythropoietin; AU=arbitrary unit.

3.2.3.4 Volumetrical analysis of cuprizone-fed mice

At two time points, weeks 6 and 9, MRI was performed. As seen already in the previous experiment, cuprizone did not affect the brain matter of mice at any time point (Figure 30). Interestingly, the volume of the hippocampus of cuprizone mice was significantly reduced at week 6 (Mann-Whitey U-test, PL vs. Cuprizone PL, P=0.005) and returned back to control levels at week 9. The brain volume of the cuprizone/placebo mice was significantly enlarged at week 6 (Mann-Whitey U-test, PL vs. Cuprizone PL, P=0.005). The analysis of the ventricular system (lateral ventricle left and right and third ventricle) showed a huge increase of the ventricular volume of cuprizone mice at week 6 (Mann-Whitey U-test, PL vs. Cuprizone PL, P=0.005). This effect was significantly reduced by EPO (Figure 30). After a recovery of 3 weeks the ventricles were still enlarged without any further effect of EPO.

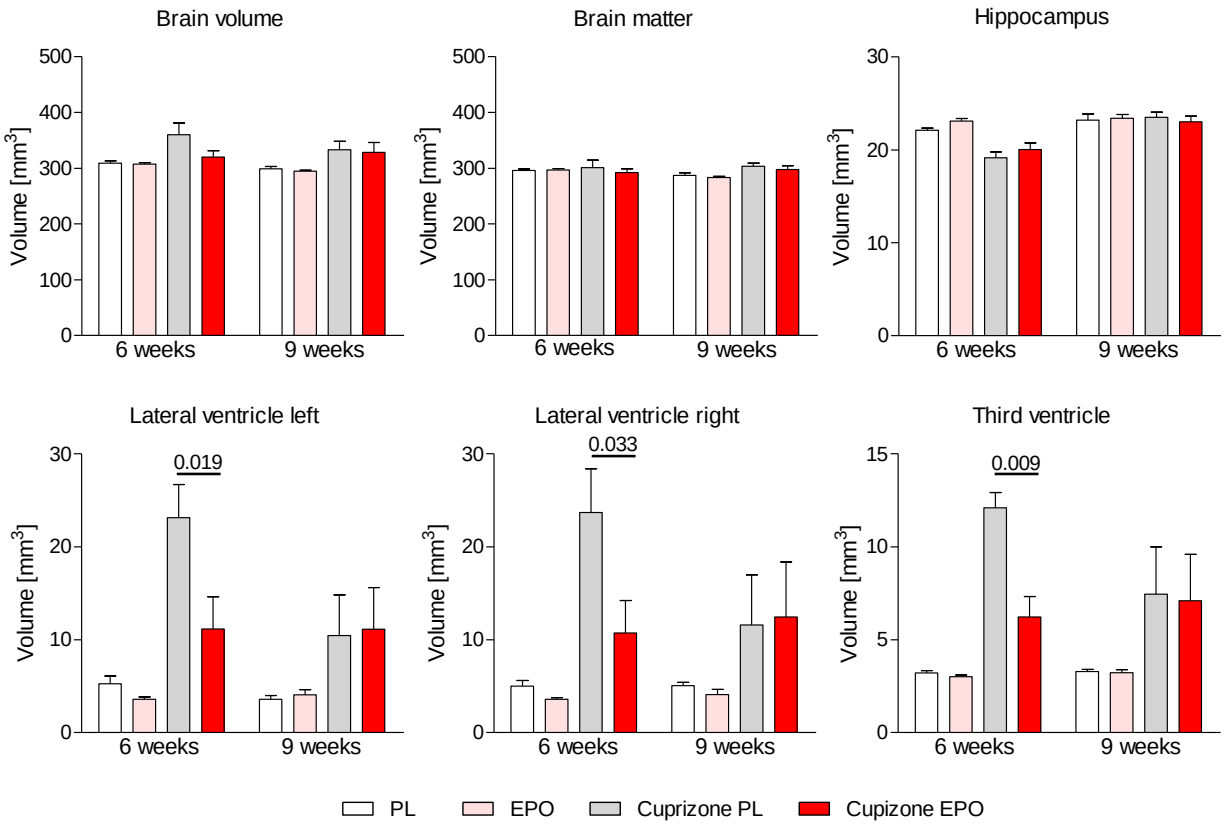

Figure 30: Effect of EPO on demyelination. Volumetrical analysis of the brain volume, brain matter, hippocampus, lateral ventricles and the third ventricle at weeks 6 and 9. N=4-6; mean±SEM presented; PL=placebo; EPO=erythropoietin.

Additionally, the %MTR, a measurement of the degree of myelination, was analyzed. This value was significantly decreased in cuprizone mice at week 6 (Mann-Whitey U-test, PL vs. Cuprizone PL, P=0.01) whereas the cuprizone/EPO group showed slightly higher levels (Figure 31). At week 9, this value was still not completely back to control levels in both the cuprizone placebo and EPO group.

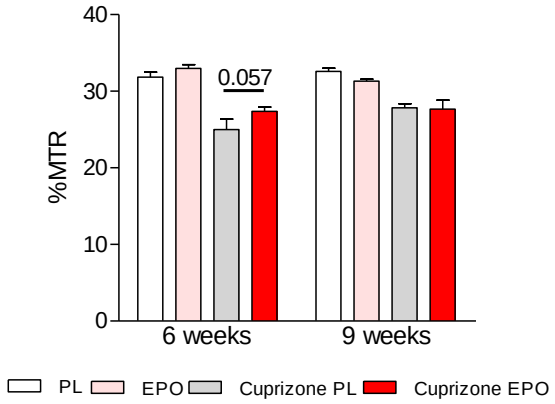

Figure 31: Effect of EPO on demyelination. Analysis of the % magnetization transfer ratio (%MTR) at weeks 6 and 9. N=4-6; mean±SEM presented; PL=placebo; EPO=erythropoietin.

3.2.3.5 Examination of mature and precursor oligodendrocytes at week 6

For a better understanding of the observed effect of EPO on behavioral and imaging parameters at week 6, this time point was selected to perform immunohistochemical analysis for oligodendrocytes, microglia and axonal degeneration. Oligodendrocytes were visualized by immunohistochemistry using the antibodies PDGFR-α and CC-1 (anti-APC). As illustrated in Figure 32, PDGFR-α nicely stains the cell body and processes of precursor oligodendrocytes in the brain sections whereas CC-1 (anti-APC) stains the cell body and cytoplasm of mature oligodendrocytes (Figure 33). Both were analyzed in the corpus callosum 6 weeks after cuprizone initiation. Precursor oligodendrocytes were significantly increased within the rostral and caudal part of the corpus callosum upon cuprizone feeding (Figure 32 and 34 upper panels; for both regions: Mann-Whitey U-test, PL vs. Cuprizone PL, P<0.001). No clear effect of EPO was observable, although a trend of a slight decrease of precursor oligodendrocytes was visible (Figure 34). Mature oligodendrocytes were heavily depleted in the entire corpus callosum (Figure 33 and 34 lower panels; for both regions: Mann-Whitey U-test, PL vs. Cuprizone PL, P<0.001). EPO was not able to counteract this effect (Figure 34).

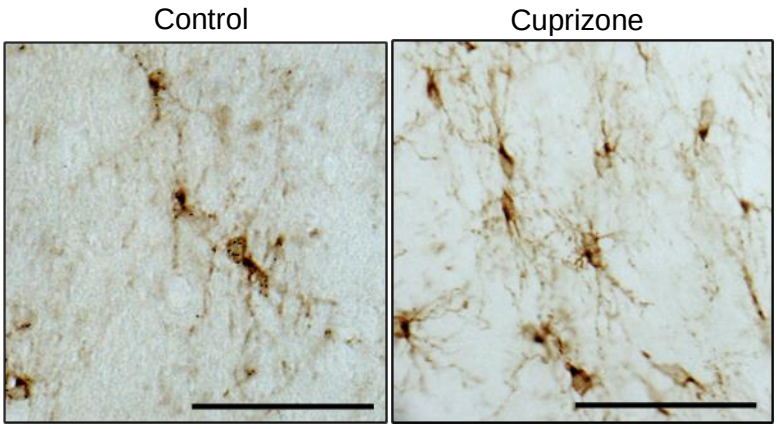

Figure 32: Effect of EPO on demyelination. Precursor oligodendrocytes stained by PDGFR-α in the corpus callosum of a control mouse (left) and a cuprizone mouse (right). Scale bar 50µm.

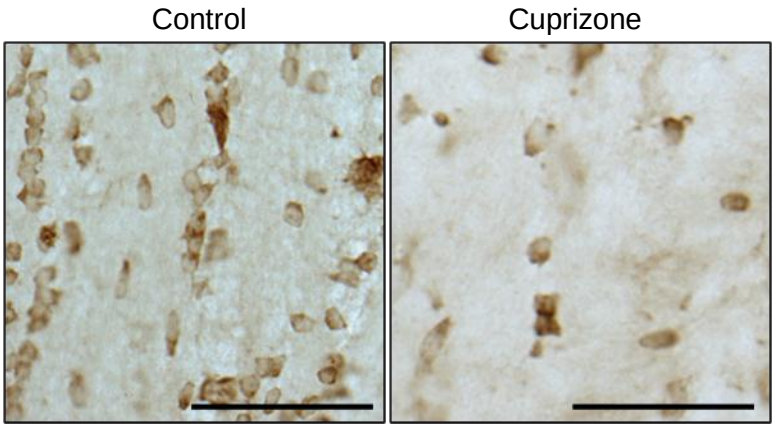

Figure 33: Effect of EPO on demyelination. Mature oligodendrocytes stained by CC-1 (anti-APC) in the corpus callosum of a control mouse (left) and a cuprizone mouse (right). Scale bar 50µm.

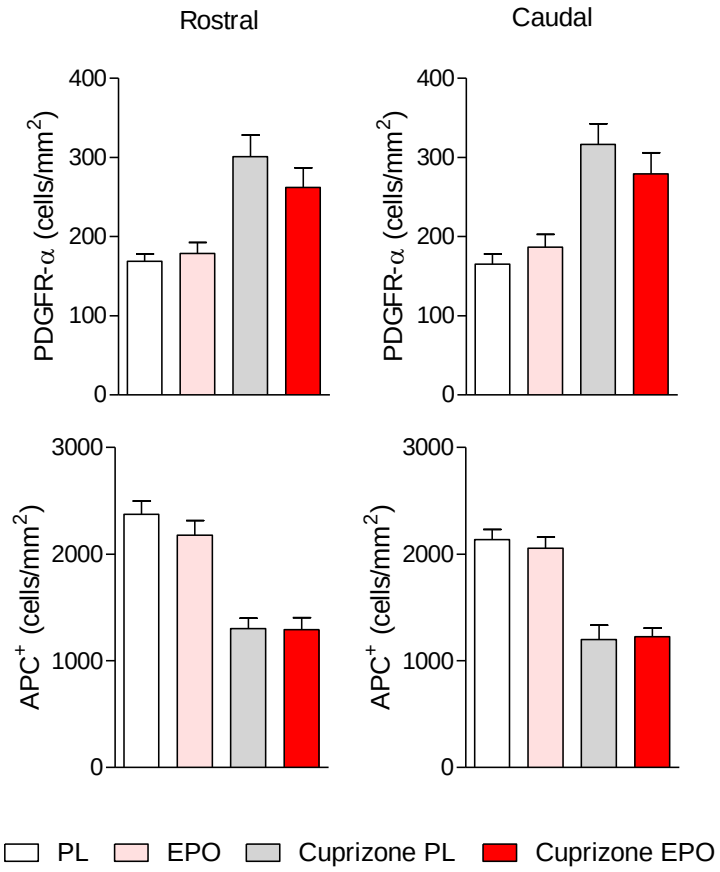

Figure 34: Effect of EPO on demyelination. Quantification of PDGFR-α$^+$ precursor (upper panels) and APC$^+$ mature oligodendrocytes (lower panels) in the rotral and caudal corpus callosum at week 6. Both cell types were significantly influenced upon cuprizone feeding (Mann-Whitey U-test, PL vs.Cuprizone PL, P<0.001). N=9-11; mean±SEM presented; PL=placebo; EPO=erythropoietin.

3.2.3.6 Analysis of microglia and axonal degeneration at week 6

At week 6, microglia were stained with IBA-1 and quantified within the corpus callosum. As illustrated in Figure 35, microglia in control mice were highly ramified (left), whereas cuprizone-fed mice changed their morphometrics to amoeboid-like cells (right). Quantification of these cells showed a dramatic increase in cuprizone mice in both regions of the corpus callosum (Figure 36; Mann-Whitey U-test, PL vs. Cuprizone PL, P<0.001). EPO decreased the number of microglia, slightly in the

rostral and significantly in the caudal corpus callosum (Figure 36; Mann-Whitey U-test, P=0.019).

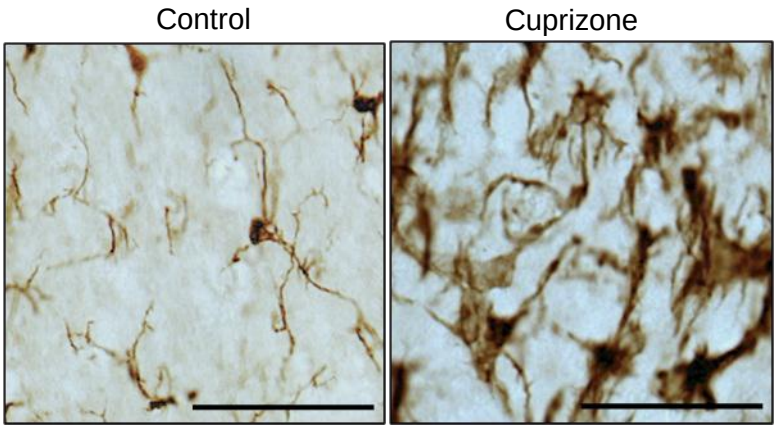

Figure 35: Effect of EPO on demyelination. Highly ramified microglia in the corpus callosum of control mice (right) and amoeboid-like microglia in cuprizone mice (left) at week 6. Scale bar 50µm.

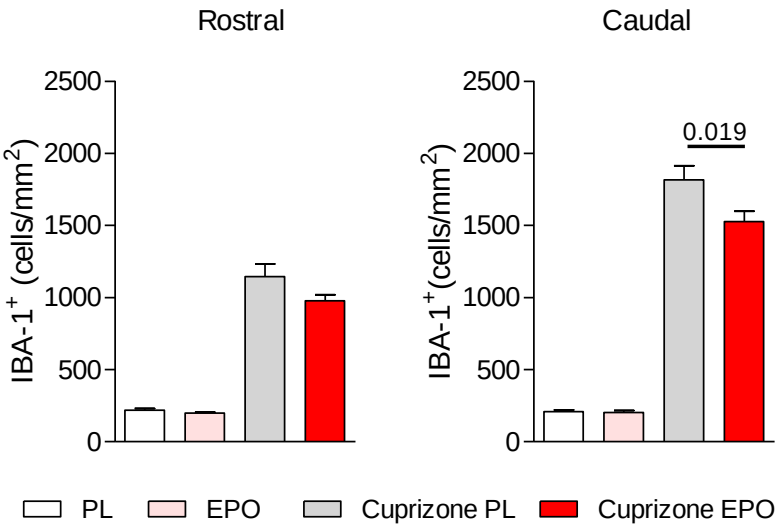

Figure 36: Effect of EPO on demyelination. Quantification of IBA-1$^+$ microglia in the rostral and caudal corpus callosum. Microglia were significantly elevated upon cuprizone feeding (Mann-Whitey U-test, PL vs. Cuprizone PL, P<0.001). N=7-11; mean±SEM presented; PL=placebo; EPO=erythropoietin.

Axonal degeneration can be analyzed on the immunohistochemical level using the APP antibody. Whereas no APP^+ spheroids were visible at week 6 in control mice (Figure 37 left), distinct accumulations were present in cuprizone mice (Figure 37 right; arrows). Quantification revealed a clear increase of APP^+ accumulations in the corpus callosum of cuprizone mice (Figure 38; Mann-Whitey U-test, PL vs. Cuprizone PL, $P<0.001$). A decrease of axonal degeneration was visible in the caudal and more pronounced in the rostral part of the corpus callosum upon EPO treatment (Figure 38).

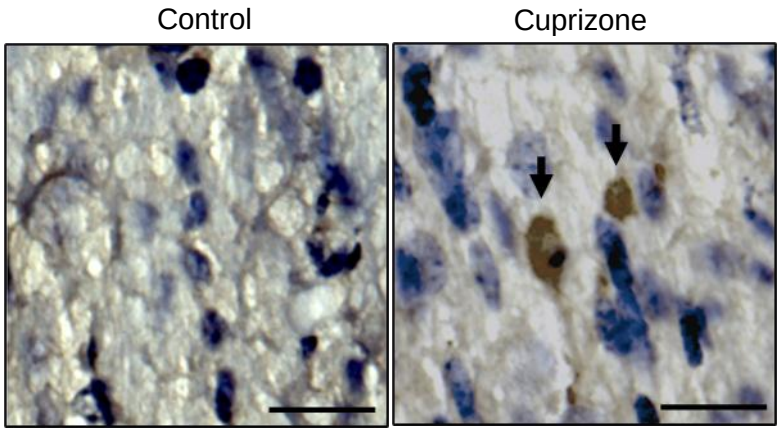

Figure 37: Effect of EPO on demyelination. APP^+ accumulations in the corpus callosum of control (left) and cuprizone (right) mice at week 6. Arrows point to positive accumulations. Scale bar 20µm.

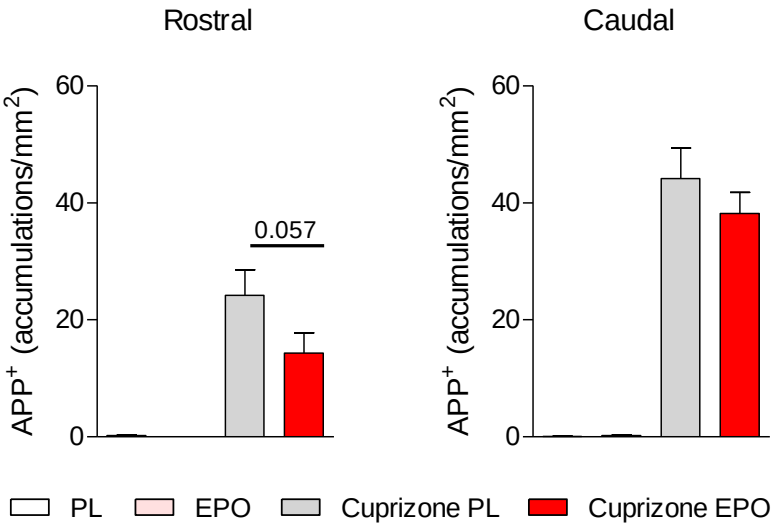

Figure 38: Effect of EPO on demyelination. Quantification of APP^+ accumulations in the rostral and caudal corpus callosum. Significant increase of axonal degeneration upon cuprizone (Mann-Whitey U-test, PL vs. Cuprizone PL, $P<0.001$). N=8-11; mean±SEM presented; PL=placebo; EPO=erythropoietin.

3.2.3.7 Expression of cytokines and mircoglia activity markers at week 6

To further evaluate the inflammatory component of the cuprizone model and potential EPO effects in this context, quantification of brain mRNA levels of cytokines and micoglial activity markers was performed. The analyzed cytokines, IL-1α and IL-1β, showed a strong upregulation upon cuprizone feeding (Figure 39; Mann-Whitey U-test, PL vs. Cuprizone PL, P<0.001). Similarly, two microglial activity markers, C1qA and Trem-2, showed the same pattern (Figure 39; Mann-Whitey U-test, PL vs. Cuprizone PL, P≤0.02). In contrast, TGF-β, a protective growth factor, was downregulated by cuprizone (Mann-Whitey U-test, PL vs. Cuprizone PL, P=0.026). Even though, in the most cases a small tendency of a counter regulation of EPO could be detected, there was no clear effect of EPO in this readout.

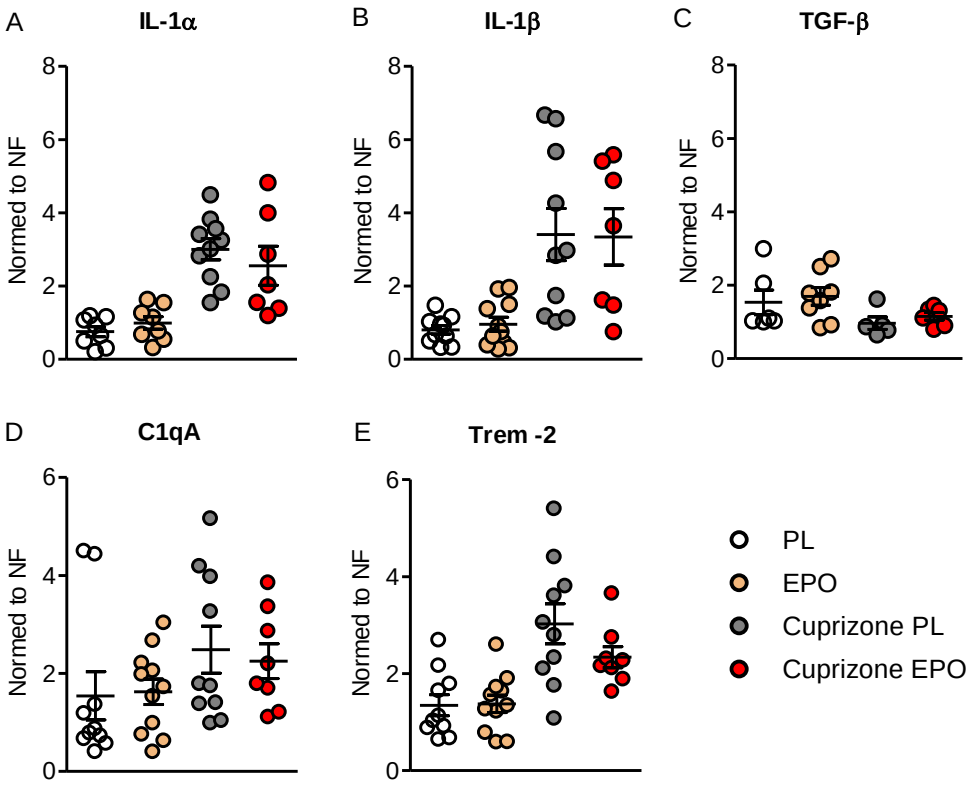

Figure 39: Effect of EPO on demyelination. Quantification of cytokines (IL-1α, IL-1β & TGF-β) and microglial activity marker (C1qA, Trem-2) on mRNA level at week 6. Expression levels are normalized to a normalization factor (NF) and significantly influenced by cuprizone (Mann-Whitey U-test, PL vs. Cuprizone PL, P<0.05). N=5-11; mean±SEM presented; PL=placebo; EPO=erythropoietin.

4 DISCUSSION

The present thesis investigated whether EPO modulates cuprizone-induced de- and/or remyelination processes in the corpus callosum, including related changes at the behavioral, imaging, immunohistochemical, mRNA expression and myelin protein levels. The selection of the cuprizone mouse model was based on several important characteristics. As elaborated in the introduction, the feeding of mice with the toxin cuprizone results in a marked demyelination of the corpus callosum, as well as other brain regions such as hippocampus, cortex and cerebellum. The advantage of this model, compared to EAE models, is to study myelination processes relatively isolated from direct immune-inflammatory influences. Moreover, the model has a recovery potential, allowing for investigation of events related to de- and remyelination. An intact BBB in cuprizone-fed mice excludes massive infiltration of peripheral immune cells. Two study designs were chosen to investigate the effect of EPO in the most clinical relevant manner: (1) EPO treatment started directly after the damage fully occurred (with the beginning of remyelination), or (2) EPO was given at an earlier time point when the first signs of damage appeared (during the demyelination phase). The hypothesis of the thesis was that EPO modulates the cuprizone-induced changes in all readouts analyzed.

4.1 Establishment of the cuprizone model

First the cuprizone mouse model had to be established. Oriented by the available publications about the cuprizone model (see Tables 1-5), 8 week old C57BL/6 male mice were used. In the first pilot experiment, the mice were fed with either normal food pellets or food pellets containing 0.2% cuprizone. This was done to make the application of cuprizone more precise and practical and avoid unnecessary dispersal of the toxin in the experimental room. Surprisingly, the feeding of mice with the cuprizone-containing food pellets resulted in neither the known cuprizone-induced decrease of body weight, nor in the demyelination of the corpus callosum. However, a toxicological analysis proved that cuprizone was present, intact and active in the food pellets (see Supplement 6.1). After a careful re-screening of the literature, it became clear that cuprizone was always administered with ground chow and was applied only once via drinking water (Zatta et al, 2005). Importantly, no publication explicitly stated that cuprizone has to be administered via ground chow.

A second pilot experiment was designed in which a small number of 6-7 week old mice were either exposed to ground chow containing 0.2 or 0.3% cuprizone or 0.2% cuprizone-containing food pellets. The higher dose was additionally used to control for the efficacy of different cuprizone doses. Younger mice were used to clarify if these mice were more susceptible to cuprizone intoxication. Monitoring of the body weight of mice clearly revealed a loss of body weight in mice fed with cuprizone mixed into ground chow, but not in the mice fed with cuprizone-containing food pellets, although these mice were even younger. A higher mortality rate of 0.3% cuprizone-fed mice indicated an increased severity of this dose. Furthermore, mice at an age below 8 weeks seemed to be highly susceptible to the toxin. With these data, it was concluded that there must be other routes of cuprizone uptake such as via e.g. skin or respiration to induce demyelination in mice. For all following experiments, 8 week old C57BL/6 male mice and 0.2% cuprizone mixed into standard ground chow were used.

4.2 Effect of EPO on remyelination

Two aspects were the focus of the experiments concerning the effect of EPO on remyelination: (1) The potential of EPO to support reparative mechanisms during remyelination after acute myelin damage and (2) after repeated myelin damage. The latter aspect was related to clinically relevant situations such as in a relapsing-remitting disease course in MS.

The body weight changed as expected even during the repeated de- and remyelination phase. Interestingly, the body weight of EPO-treated cuprizone mice decreased less in the second demyelination cycle compared to placebo-treated cuprizone mice, but this finding was not significant. Even in the second demyelination phase, no impairment in general motor performance could be found as evaluated by the accelerated rota-rod test. These two parameters (body weight and motor performance) show a general physical robustness of the mice even after a repeated cuprizone challenge. The measurement of haematocrit to monitor the effect of EPO on erythrocytes showed that cuprizone feeding did not interfere with this effect of EPO. Interestingly, as shown once before (Skripuletz et al, 2010b) the beam balance task turned out to be sensitive enough to detect cuprizone-induced changes in motor coordination and balance. What was even more striking was the fact that the task was able to reveal protective effects of EPO at week 15. This finding, together with

the observation that EPO led to a reduced loss of body weight in the second demyelination phase, suggests a protective effect of EPO in this experimental set-up.

Although a final explanation for reduced startle reactivity of mice upon cuprizone feeding is not yet possible, a deficit in the hearing ability of cuprizone-fed mice could be ruled out as a possible explanation. Additional analysis considering the influence of body weight of mice in this test did not explain the finding either. Interestingly, a reduced startle response was already seen in another study, though without further clarification of this observation (Xu et al, 2009). Furthermore, a higher number of mice showing freezing behavior to click stimuli was observed upon cuprizone intoxication, but the strength of the freezing was not specified (Franco-Pons et al, 2007). Cuprizone-induced demyelination that may lead to connectivity problems between brain regions and/or a generally poorer physical condition of the mice could be just two hypothetical explanations. Further analyses are needed to clarify the observed phenomenon.

Interestingly, the analysis of different myelin proteins after the first recovery period (week 9) showed a severe depletion of the proteins in the cortex, whereas remyelination in the hippocampus was already progressed and showed no differences between control and cuprizone groups. After the second recovery phase (week 18), all investigated myelin proteins were heavily reduced in both cortex and hippocampus. However, at both time points no effect of EPO was present. The differences between the cortex and hippocampus at week 9 could be explained, either by a different susceptibility of the brain regions to cuprizone or by a better recovery potential in the hippocampus. A hint of a different susceptibility to cuprizone between brain regions was given by a study showing more severe demyelination in the cortex compared to the corpus callosum (Skripuletz et al, 2008). The lack of a recovery of the myelin proteins in both the cortex and hippocampus at week 18 could be caused by an exhaustion of the myelin protein expression capacity by cuprizone at this time point. However, to support this statement, data at e.g. the 15 week time point would be needed to see the time course of the myelin protein expression. An expression analysis of myelin proteins in the cortex and hippocampus in the cuprizone model is not yet published and excludes a comparison of the presented

data to other studies. The raised statements above are therefore speculative but were not topics in question to be further analyzed in this study.
The absence of an EPO effect on myelin proteins is surprising, especially because in other models e.g. for juvenile brain trauma, an effect of EPO on myelin proteins was demonstrated (Sargin et al, 2009). Discrepancies compared to this study can be explained by different actions of EPO in different disease models and/or the age of mice at the time point of EPO treatment. In the study by Sargin et al (Sargin et al, 2009), EPO application took place in 4 week old mice, whereas in the current study the mice were 14 weeks old. Accumulating findings in our lab support the idea that age can play a role at the time of EPO application. In addition to this, other reasons for a lack of an EPO effect can be discussed. The analysis was restricted to the cortex and hippocampus; clearer results in this study may have come about by studying the myelin fraction of the brain. The time points of investigation were restricted to 9 and 18 weeks to analyze the effect of EPO on remyelination potential, but these may not be the most relevant ones to see EPO effects in this readout. In general, it could be further speculated that EPO application was not performed in the most relevant time window in this model. On the other hand, the specific cuprizone-induced damage of myelin proteins could perhaps not have been counteracted by EPO.

Enlarged ventricles are a common feature in the cuprizone model (Carlton, 1966; Carlton, 1967; Kesterson & Carlton, 1970). For instance, elevated ventricles were reported by the first and so far only cuprizone study of repeated feeding (Pattison & Jebbett, 1973). Although the design of this study differs compared to the present study, the influence of cuprizone on the ventricular system could be found here as well. EPO did not have an effect on this readout. However, the MRI analysis was restricted to the end-point of the experiment, making it difficult to draw any final conclusions regarding EPO action on this parameter.

To conclude, cuprizone had a potent effect on all parameters analyzed except the rota-rod performance of mice and acoustic evoked potentials. EPO showed a protective effect concerning body weight loss and vestibulomotor performance. However, analyses on an immunohistochemical and protein level at comparable time points are missing and make a conclusion of underlying mechanisms impossible. At

the end-point of this experiment (18 weeks), lack of an EPO effect in the MRI parameter, myelin protein analysis and beam balance task suggest that the cuprizone-induced damage at this time point may be too progressed or the recovery potential is still too fast to detect an EPO effect.

4.3 EPO effect on demyelination

In this experimental set-up, EPO had no influence on the weight loss of cuprizone-fed mice. The motor performance on the rota-rod confirmed the previous finding that mice fed with cuprizone do not have a severe motor phenotype. This has already led to the development of a more sophisticated motor task for this model by others (Liebetanz & Merkler, 2006). Interestingly, at week 6 EPO again improved the performance of cuprizone mice in the beam balance task, whereas at week 9 no differences were obtained between any groups showing a high recovery potential. Based on different time points investigated, direct comparison to the effect of EPO observed in the beam balance task in the previous experiment is difficult.

Volumetrical analysis at week 6 again showed no influence of cuprizone on brain matter. Interestingly, at this time point the hippocampal volume was reduced upon cuprizone feeding. In MRI images, as well as in histological sections, the hippocampus often appeared to be squeezed, which could be explained by the significant enlargement of the ventricular system by cuprizone. The ballooned ventricles may push the surrounding tissue, including the hippocampi, against the skull. The EPO-treated cuprizone mice had significantly smaller ventricles compared to the cuprizone/placebo mice.
So far, just one study intensively investigated the possible reasons for hydrocephalus in the cuprizone mouse model (Kesterson & Carlton, 1970). In this study, the authors suggested that hydrocephalus occurs secondary to the stenosis of the aqueduct of Sylvius, which may result from pressure exerted by the surrounding edematous tissue. The authors further claimed a normal secretion of cerebral spinal fluid. This is of course just one possible explanation and was unfortunately never in the interest of others to be further studied. However, EPO treatment during the demyelination phase may have dampened the degenerative effect of cuprizone on the brain tissue and therefore reduced the closure of the aqueduct of Sylvius. This could then explain the smaller ventricle volume.

Since the %MTR, a MRI readout, correlates with myelination in the corpus callosum (Merkler et al, 2005), the reduction of this value in cuprizone-fed mice at week 6 suggests demyelination occurring within the corpus callosum. EPO had the tendency to increase this value. This is in agreement with studies showing better myelin sheath preservation in different disease models by EPO (Gorio et al, 2002; Iwai et al, 2010; Kumral et al, 2007; Li et al, 2004; Liu et al, 2011; Vitellaro-Zuccarello et al, 2007; Yamada et al, 2011). Additionally, as shown before, immunohistochemical analysis revealed a severe depletion of mature oligodendrocytes by cuprizone within the corpus callosum without an additional effect of EPO. At the same time, precursor oligodendrocytes were significantly increased by cuprizone but only slightly reduced under EPO treatment. Indeed, studies which used other animal models found a clear effect of EPO on proliferation and maturation of oligodendrocytes (Iwai et al, 2010; Vitellaro-Zuccarello et al, 2007; Zhang et al, 2005; Zhang et al, 2010). The lack of an EPO effect on oligodendrocytes in the present study might be explained by the time point and brain region selected for the analysis. However, it could be more likely assumed that the mechanism of cell death induced by cuprizone feeding simply cannot be counteracted by EPO. This is supported by a recent publication, which showed an advantageous influence of vitamin D_3 treatment on demyelination in the cuprizone model but also failed to demonstrate an effect on mature oligodendocytes (Wergeland et al, 2011).

It is important to note that the experimental condition (animal model) and exact EPO application (dose, time point, age of mice) seem to fundamentally influence the outcome of EPO treatment.

The present study confirmed the known cuprizone-induced upregulation of microglia within the corpus callosum (Arnett et al, 2001; Gudi et al, 2009; Hiremath et al, 1998; Lindner et al, 2009; Mason et al, 2004; Merkler et al, 2005; Morell et al, 1998) and showed that EPO treatment counteracted this effect. Interestingly, this result was more prominent in the caudal than rostral region of the corpus callosum. A separate analysis of the rostral and caudal corpus callosum was based on findings of a different demyelination pattern through the corpus callosum (Stidworthy et al, 2003). However, no major differences in susceptibility to cuprizone between these two regions were apparent in the present study. An anti-inflammatory effect of EPO in oligodendrocyte cultures has been reported before (Genc et al, 2006) and is in

agreement with the general anti-inflammatory effect of EPO in several different models such as EAE (Agnello et al, 2002; Li et al, 2004), cortical lesions (Sargin et al, 2009), epilepsy (Jung et al, 2011), closed head injury (Yatsiv et al, 2005) and ischemia (Villa et al, 2003). The search for further mechanistic insight into EPO action in the cuprizone model related to cytokines or microglial activity markers failed to show any clear beneficial effect. This may result from several limitations of the cuprizone model (as discussed below) and from limitations of the available material for this analysis. The mRNA analysis was based on whole brain sections from perfused mice. Either native brain samples and/or a brain region-specific expression analysis of these markers could show a clearer result in this analysis.
Early axonal degeneration induced by cuprizone could be counteracted by EPO. So far, an effect of EPO on APP accumulation has not been reported. The EPO effect on axonal degeneration can either be direct or indirect via a reduction of the number of microglia. The anti-inflammatory and axon protective effect of EPO may explain, at least partly, better myelin preservation (%MTR) and better performance in the beam balance task.

In summary, this study showed that EPO improved the performance in the beam balance task and reduced or protected the severe enlargement of the ventricular system. Additionally, EPO reduced the number of microglia and for the first time, was found to reduce axonal degeneration in brain white matter tracts.

4.4 Limitations of the model

By carefully reviewing the cuprizone literature, one gets the impression that this model is well characterized and has only a few limitations. Indeed, the model is well characterized, especially concerning changes on the immunohistochemical level. However, in the presented experiments several difficulties became obvious that were not evident from the literature. (1) The model shows high variability, which became especially clear not only from the MRI but from the histological analysis as well. High within-group variability was observed. One reason for the variations could be the method of cuprizone application. The actual intake of cuprizone is dependent on how much they eat and therefore can vary a lot between the mice. Moreover, the aspect that cuprizone might be taken up via skin or respiration is an additional factor which may further raise the chances of variability. Especially regarding treatment trials, a

high variability means that a high number of mice need to be used for solid conclusions. The application of cuprizone via injections would be the most precise method of administration but is not reported so far. (2) The observation of intrinsic remyelination and a general fast recovery potential by the withdrawal of cuprizone in this model makes it difficult to predict the optimal time point for investigation. In this thesis it became clear that some effects of EPO may have been overlooked due to the possible lack of analyses at the optimal time points. A detailed analysis of a time series would be necessary but is animal consuming and labor intensive. Moreover, the fast recovery makes at least the investigation of treatment trials concerning neuroregeneration difficult. (3) Final conclusions of studies using the cuprizone model for pharmacological studies are limited because the mechanism of cuprizone damage on oligodendrocytes is not yet fully understood and subject to investigation (Liu et al, 2010).

4.5 Final conclusion

As outlined before, there are several limitations of the cuprizone model which should be carefully considered, especially before using this model for pharmacological trials in the future. For the first time, different aspects of EPO action on cuprizone-induced de- and remyelination were investigated in this thesis. In general, repeated cuprizone feeding was for the first time induced in C57BL/6 mice and showed a physical robustness (rota-rod and body weight) of the mice at the end-point of the experiment. However, from the myelin protein analysis, imaging readouts and beam balance performance, it could be speculated that the recovery potential of the model is either limited upon repeated cuprizone exposure or still has a high recovery potential. To clarify this aspect, analyses at several more time points would be needed. No major EPO effects were found in this experimental set-up. On the other hand, by investigating the effect of EPO on demyelination, a surprisingly clear protective effect of EPO was detectable even if not all readouts always reached clear significance. EPO ameliorated clinical readouts such as beam balance performance and enlargement of the ventricular system, which may partially be explained by a reduction of inflammation-associated axonal degeneration in the corpus callosum.

5 LITERATURE

Acs P, Kipp M, Norkute A, Johann S, Clarner T, Braun A, Berente Z, Komoly S, Beyer C (2009) 17beta-estradiol and progesterone prevent cuprizone provoked demyelination of corpus callosum in male mice. Glia 57**:** 807-814

Agnello D, Bigini P, Villa P, Mennini T, Cerami A, Brines ML, Ghezzi P (2002) Erythropoietin exerts an anti-inflammatory effect on the CNS in a model of experimental autoimmune encephalomyelitis. Brain Res 952**:** 128-134

Arishima Y, Setoguchi T, Yamaura I, Yone K, Komiya S (2006) Preventive effect of erythropoietin on spinal cord cell apoptosis following acute traumatic injury in rats. Spine (Phila Pa 1976) 31**:** 2432-2438

Armstrong RC, Le TQ, Flint NC, Vana AC, Zhou YX (2006) Endogenous cell repair of chronic demyelination. J Neuropathol Exp Neurol 65**:** 245-256

Arnett HA, Mason J, Marino M, Suzuki K, Matsushima GK, Ting JP (2001) TNF alpha promotes proliferation of oligodendrocyte progenitors and remyelination. Nat Neurosci 4**:** 1116-1122

Bakker DA, Ludwin SK (1987) Blood-brain barrier permeability during Cuprizone-induced demyelination. Implications for the pathogenesis of immune-mediated demyelinating diseases. J Neurol Sci 78**:** 125-137

Bartels C, Spate K, Krampe H, Ehrenreich H (2008) Recombinant Human Erythropoietin: Novel Strategies for Neuroprotective/Neuro-regenerative Treatment of Multiple Sclerosis. Ther Adv Neurol Disord 1**:** 193-206

Benetti F, Ventura M, Salmini B, Ceola S, Carbonera D, Mammi S, Zitolo A, D'Angelo P, Urso E, Maffia M et al (2010) Cuprizone neurotoxicity, copper deficiency and neurodegeneration. Neurotoxicology 31**:** 509-517

Bernaudin M, Marti HH, Roussel S, Divoux D, Nouvelot A, MacKenzie ET, Petit E (1999) A potential role for erythropoietin in focal permanent cerebral ischemia in mice. J Cereb Blood Flow Metab 19**:** 643-651

Blakemore WF (1972) Observations on oligodendrocyte degeneration, the resolution of status spongiosus and remyelination in cuprizone intoxication in mice. J Neurocytol 1**:** 413-426

Blakemore WF (1973a) Demyelination of the superior cerebellar peduncle in the mouse induced by cuprizone. J Neurol Sci 20**:** 63-72

Blakemore WF (1973b) Remyelination of the superior cerebellar peduncle in the mouse following demyelination induced by feeding cuprizone. J Neurol Sci 20**:** 73-83

Blakemore WF (1974) Remyelination of the superior cerebellar peduncle in old mice following demyelination induced by cuprizone. J Neurol Sci 22**:** 121-126

Boretius S, Kasper L, Tammer R, Michaelis T, Frahm J (2009) MRI of cellular layers in mouse brain in vivo. Neuroimage 47**:** 1252-1260

Brines M, Cerami A (2005) Emerging biological roles for erythropoietin in the nervous system. Nat Rev Neurosci 6**:** 484-494

Brines M, Grasso G, Fiordaliso F, Sfacteria A, Ghezzi P, Fratelli M, Latini R, Xie QW, Smart J, Su-Rick CJ et al (2004) Erythropoietin mediates tissue protection through an erythropoietin and common beta-subunit heteroreceptor. Proc Natl Acad Sci U S A 101**:** 14907-14912

Brines ML, Ghezzi P, Keenan S, Agnello D, de Lanerolle NC, Cerami C, Itri LM, Cerami A (2000) Erythropoietin crosses the blood-brain barrier to protect against experimental brain injury. Proc Natl Acad Sci U S A 97**:** 10526-10531

Byts N, Siren AL (2009) Erythropoietin: a multimodal neuroprotective agent. Exp Transl Stroke Med 1**:** 4

Cammer W (1999) The neurotoxicant, cuprizone, retards the differentiation of oligodendrocytes in vitro. J Neurol Sci 168**:** 116-120

Carlton WW (1966) Response of mice to the chelating agents sodium diethyldithiocarbamate, alpha-benzoinoxime, and biscyclohexanone oxaldihydrazone. Toxicol Appl Pharmacol 8**:** 512-521

Carlton WW (1967) Studies on the induction of hydrocephalus and spongy degeneration by cuprizone feeding and attempts to antidote the toxicity. Life Sci 6**:** 11-19

Carlton WW (1969) Spongiform encephalopathy induced in rats and guinea pigs by cuprizone. Exp Mol Pathol 10**:** 274-287

Carter RJ, Morton J, Dunnett SB (2001) Motor Coordination and Balance in Rodents. In Current Protocols in Neuroscience. John Wiley & Sons, Inc.

Chandran P, Upadhyay J, Markosyan S, Lisowski A, Buck W, Chin CL, Fox G, Luo F, Day M (2011) Magnetic resonance imaging and histological evidence for the blockade of cuprizone-induced demyelination in C57BL/6 mice. Neuroscience 202**:** 446-453

Chen SJ, Wang YL, Lo WT, Wu CC, Hsieh CW, Huang CF, Lan YH, Wang CC, Chang DM, Sytwu HK (2010) Erythropoietin enhances endogenous haem oxygenase-1 and represses immune responses to ameliorate experimental autoimmune encephalomyelitis. Clin Exp Immunol 162**:** 210-223

Chen ZY, Asavaritikrai P, Prchal JT, Noguchi CT (2007) Endogenous erythropoietin signaling is required for normal neural progenitor cell proliferation. J Biol Chem 282**:** 25875-25883

Clarner T, Parabucki A, Beyer C, Kipp M (2011) Corticosteroids impair remyelination in the corpus callosum of cuprizone-treated mice. J Neuroendocrinol 23**:** 601-611

Crawford DK, Mangiardi M, Xia X, Lopez-Valdes HE, Tiwari-Woodruff SK (2009) Functional recovery of callosal axons following demyelination: a critical window. Neuroscience 164**:** 1407-1421

Dame C, Fahnenstich H, Freitag P, Hofmann D, Abdul-Nour T, Bartmann P, Fandrey J (1998) Erythropoietin mRNA expression in human fetal and neonatal tissue. Blood 92**:** 3218-3225

Dasgupta S, Mazumder B, Ramani YR, Bhattacharyya SP, Das MK (2011) Evaluation of the role of erythropoietin and methotrexate in multiple sclerosis. Indian J Pharmacol 43**:** 512-515

Diem R, Sattler MB, Merkler D, Demmer I, Maier K, Stadelmann C, Ehrenreich H, Bahr M (2005) Combined therapy with methylprednisolone and erythropoietin in a model of multiple sclerosis. Brain 128**:** 375-385

Ehrenreich H, Degner D, Meller J, Brines M, Behe M, Hasselblatt M, Woldt H, Falkai P, Knerlich F, Jacob S et al (2004) Erythropoietin: a candidate compound for neuroprotection in schizophrenia. Mol Psychiatry 9**:** 42-54

Franco-Pons N, Torrente M, Colomina MT, Vilella E (2007) Behavioral deficits in the cuprizone-induced murine model of demyelination/remyelination. Toxicol Lett 169**:** 205-213

Fried W (1972) The liver as a source of extrarenal erythropoietin production. Blood 40**:** 671-677

Gao X, Gillig TA, Ye P, D'Ercole AJ, Matsushima GK, Popko B (2000) Interferon-gamma protects against cuprizone-induced demyelination. Mol Cell Neurosci 16**:** 338-349

Genc K, Genc S, Baskin H, Semin I (2006) Erythropoietin decreases cytotoxicity and nitric oxide formation induced by inflammatory stimuli in rat oligodendrocytes. Physiol Res 55**:** 33-38

Gorio A, Gokmen N, Erbayraktar S, Yilmaz O, Madaschi L, Cichetti C, Di Giulio AM, Vardar E, Cerami A, Brines M (2002) Recombinant human erythropoietin counteracts secondary injury and markedly enhances neurological recovery from experimental spinal cord trauma. Proc Natl Acad Sci U S A 99**:** 9450-9455

Groebe A, Clarner T, Baumgartner W, Dang J, Beyer C, Kipp M (2009) Cuprizone treatment induces distinct demyelination, astrocytosis, and microglia cell invasion or proliferation in the mouse cerebellum. Cerebellum 8**:** 163-174

Gudi V, Moharregh-Khiabani D, Skripuletz T, Koutsoudaki PN, Kotsiari A, Skuljec J, Trebst C, Stangel M (2009) Regional differences between grey and white matter in cuprizone induced demyelination. Brain Res 1283**:** 127-138

Harsan LA, Steibel J, Zaremba A, Agin A, Sapin R, Poulet P, Guignard B, Parizel N, Grucker D, Boehm N et al (2008) Recovery from chronic demyelination by thyroid hormone therapy: myelinogenesis induction and assessment by diffusion tensor magnetic resonance imaging. J Neurosci 28**:** 14189-14201

Hibbits N, Pannu R, Wu TJ, Armstrong RC (2009) Cuprizone demyelination of the corpus callosum in mice correlates with altered social interaction and impaired bilateral sensorimotor coordination. ASN Neuro 1

Hiremath MM, Saito Y, Knapp GW, Ting JP, Suzuki K, Matsushima GK (1998) Microglial/macrophage accumulation during cuprizone-induced demyelination in C57BL/6 mice. J Neuroimmunol 92**:** 38-49

Hoffmann K, Lindner M, Groticke I, Stangel M, Loscher W (2008) Epileptic seizures and hippocampal damage after cuprizone-induced demyelination in C57BL/6 mice. Exp Neurol 210**:** 308-321

Iocca HA, Plant SR, Wang Y, Runkel L, O'Connor BP, Lundsmith ET, Hahm K, van Deventer HW, Burkly LC, Ting JP (2008) TNF superfamily member TWEAK exacerbates inflammation and demyelination in the cuprizone-induced model. J Neuroimmunol 194**:** 97-106

Irvine KA, Blakemore WF (2006) Age increases axon loss associated with primary demyelination in cuprizone-induced demyelination in C57BL/6 mice. J Neuroimmunol 175**:** 69-76

Iwai M, Stetler RA, Xing J, Hu X, Gao Y, Zhang W, Chen J, Cao G (2010) Enhanced oligodendrogenesis and recovery of neurological function by erythropoietin after neonatal hypoxic/ischemic brain injury. Stroke 41**:** 1032-1037

Jelkmann W (1992) Erythropoietin: structure, control of production, and function. Physiol Rev 72**:** 449-489

Jelkmann W (2007) Erythropoietin after a century of research: younger than ever. Eur J Haematol 78**:** 183-205

Jewett DL, Williston JS (1971) Auditory-evoked far fields averaged from the scalp of humans. Brain 94**:** 681-696

Jung KH, Chu K, Lee ST, Park KI, Kim JH, Kang KM, Kim S, Jeon D, Kim M, Lee SK et al (2011) Molecular alterations underlying epileptogenesis after prolonged febrile seizure and modulation by erythropoietin. Epilepsia 52**:** 541-550

Jung M, Sommer I, Schachner M, Nave KA (1996) Monoclonal antibody O10 defines a conformationally sensitive cell-surface epitope of proteolipid protein (PLP): evidence that PLP misfolding underlies dysmyelination in mutant mice. J Neurosci 16**:** 7920-7929

Juul SE, Anderson DK, Li Y, Christensen RD (1998) Erythropoietin and erythropoietin receptor in the developing human central nervous system. Pediatr Res 43**:** 40-49

Kang SY, Kang JH, Choi JC, Lee JS, Lee CS, Shin T (2009) Expression of erythropoietin in the spinal cord of lewis rats with experimental autoimmune encephalomyelitis. J Clin Neurol 5**:** 39-45

Kesterson JW, Carlton WW (1970) Aqueductal stenosis as the cause of hydrocephalus in mice fed the substituted hydrazine, cuprizone. Exp Mol Pathol 13**:** 281-294

Kesterson JW, Carlton WW (1971) Histopathologic and enzyme histochemical observations of the cuprizone-induced brain edema. Exp Mol Pathol 15**:** 82-96

Klingmuller U (1997) The role of tyrosine phosphorylation in proliferation and maturation of erythroid progenitor cells--signals emanating from the erythropoietin receptor. Eur J Biochem 249**:** 637-647

Kondo A, Nakano T, Suzuki K (1987) Blood-brain barrier permeability to horseradish peroxidase in twitcher and cuprizone-intoxicated mice. Brain Res 425**:** 186-190

Konishi Y, Chui DH, Hirose H, Kunishita T, Tabira T (1993) Trophic effect of erythropoietin and other hematopoietic factors on central cholinergic neurons in vitro and in vivo. Brain Res 609**:** 29-35

Koury MJ, Bondurant MC, Graber SE, Sawyer ST (1988) Erythropoietin messenger RNA levels in developing mice and transfer of 125I-erythropoietin by the placenta. J Clin Invest 82**:** 154-159

Koutsoudaki PN, Skripuletz T, Gudi V, Moharregh-Khiabani D, Hildebrandt H, Trebst C, Stangel M (2009) Demyelination of the hippocampus is prominent in the cuprizone model. Neurosci Lett 451**:** 83-88

Kubicki M, McCarley RW, Shenton ME (2005) Evidence for white matter abnormalities in schizophrenia. Curr Opin Psychiatry 18**:** 121-134

Kumar S, Biancotti JC, Yamaguchi M, de Vellis J (2007) Combination of growth factors enhances remyelination in a cuprizone-induced demyelination mouse model. Neurochem Res 32**:** 783-797

Kumral A, Baskin H, Yesilirmak DC, Ergur BU, Aykan S, Genc S, Genc K, Yilmaz O, Tugyan K, Giray O et al (2007) Erythropoietin attenuates lipopolysaccharide-induced white matter injury in the neonatal rat brain. Neonatology 92**:** 269-278

Leist M, Ghezzi P, Grasso G, Bianchi R, Villa P, Fratelli M, Savino C, Bianchi M, Nielsen J, Gerwien J et al (2004) Derivatives of erythropoietin that are tissue protective but not erythropoietic. Science 305**:** 239-242

Li L, Jiang Q, Ding G, Zhang L, Zhang ZG, Li Q, Panda S, Kapke A, Lu M, Ewing JR et al (2009) MRI identification of white matter reorganization enhanced by erythropoietin treatment in a rat model of focal ischemia. Stroke 40**:** 936-941

Li W, Maeda Y, Yuan RR, Elkabes S, Cook S, Dowling P (2004) Beneficial effect of erythropoietin on experimental allergic encephalomyelitis. Ann Neurol 56**:** 767-777

Liebetanz D, Merkler D (2006) Effects of commissural de- and remyelination on motor skill behaviour in the cuprizone mouse model of multiple sclerosis. Exp Neurol 202**:** 217-224

Lim KO, Hedehus M, Moseley M, de Crespigny A, Sullivan EV, Pfefferbaum A (1999) Compromised white matter tract integrity in schizophrenia inferred from diffusion tensor imaging. Arch Gen Psychiatry 56**:** 367-374

Lin W, Kemper A, Dupree JL, Harding HP, Ron D, Popko B (2006) Interferon-gamma inhibits central nervous system remyelination through a process modulated by endoplasmic reticulum stress. Brain 129**:** 1306-1318

Linares D, Taconis M, Mana P, Correcha M, Fordham S, Staykova M, Willenborg DO (2006) Neuronal nitric oxide synthase plays a key role in CNS demyelination. J Neurosci 26**:** 12672-12681

Lindner M, Fokuhl J, Linsmeier F, Trebst C, Stangel M (2009) Chronic toxic demyelination in the central nervous system leads to axonal damage despite remyelination. Neurosci Lett 453**:** 120-125

Lindner M, Heine S, Haastert K, Garde N, Fokuhl J, Linsmeier F, Grothe C, Baumgartner W, Stangel M (2008) Sequential myelin protein expression during remyelination reveals fast and efficient repair after central nervous system demyelination. Neuropathol Appl Neurobiol 34**:** 105-114

Liu L, Belkadi A, Darnall L, Hu T, Drescher C, Cotleur AC, Padovani-Claudio D, He T, Choi K, Lane TE et al (2010) CXCR2-positive neutrophils are essential for cuprizone-induced demyelination: relevance to multiple sclerosis. Nat Neurosci 13**:** 319-326

Liu W, Shen Y, Plane JM, Pleasure DE, Deng W (2011) Neuroprotective potential of erythropoietin and its derivative carbamylated erythropoietin in periventricular leukomalacia. Exp Neurol 230**:** 227-239

Liu ZY, Chin K, Noguchi CT (1994) Tissue specific expression of human erythropoietin receptor in transgenic mice. Dev Biol 166**:** 159-169

Logue SF, Owen EH, Rasmussen DL, Wehner JM (1997) Assessment of locomotor activity, acoustic and tactile startle, and prepulse inhibition of startle in inbred mouse strains and F1 hybrids: implications of genetic background for single gene and quantitative trait loci analyses. Neuroscience 80**:** 1075-1086

Love S (1988) Cuprizone neurotoxicity in the rat: morphologic observations. J Neurol Sci 84**:** 223-237

Ludwin SK (1978) Central nervous system demyelination and remyelination in the mouse: an ultrastructural study of cuprizone toxicity. Lab Invest 39**:** 597-612

Makinodan M, Yamauchi T, Tatsumi K, Okuda H, Takeda T, Kiuchi K, Sadamatsu M, Wanaka A, Kishimoto T (2009) Demyelination in the juvenile period, but not in adulthood, leads to long-lasting cognitive impairment and deficient social interaction in mice. Prog Neuropsychopharmacol Biol Psychiatry 33**:** 978-985

Mana P, Linares D, Fordham S, Staykova M, Willenborg D (2006) Deleterious role of IFNgamma in a toxic model of central nervous system demyelination. Am J Pathol 168**:** 1464-1473

Marti HH (2004) Erythropoietin and the hypoxic brain. J Exp Biol 207**:** 3233-3242

Marti HH, Wenger RH, Rivas LA, Straumann U, Digicaylioglu M, Henn V, Yonekawa Y, Bauer C, Gassmann M (1996) Erythropoietin gene expression in human, monkey and murine brain. Eur J Neurosci 8**:** 666-676

Mason JL, Jones JJ, Taniike M, Morell P, Suzuki K, Matsushima GK (2000) Mature oligodendrocyte apoptosis precedes IGF-1 production and oligodendrocyte progenitor accumulation and differentiation during demyelination/remyelination. J Neurosci Res 61**:** 251-262

Mason JL, Langaman C, Morell P, Suzuki K, Matsushima GK (2001a) Episodic demyelination and subsequent remyelination within the murine central nervous system: changes in axonal calibre. Neuropathol Appl Neurobiol 27**:** 50-58

Mason JL, Suzuki K, Chaplin DD, Matsushima GK (2001b) Interleukin-1beta promotes repair of the CNS. J Neurosci 21**:** 7046-7052

Mason JL, Toews A, Hostettler JD, Morell P, Suzuki K, Goldman JE, Matsushima GK (2004) Oligodendrocytes and progenitors become progressively depleted within chronically demyelinated lesions. Am J Pathol 164**:** 1673-1682

Masuda S, Okano M, Yamagishi K, Nagao M, Ueda M, Sasaki R (1994) A novel site of erythropoietin production. Oxygen-dependent production in cultured rat astrocytes. J Biol Chem 269**:** 19488-19493

Matsushima GK, Morell P (2001) The neurotoxicant, cuprizone, as a model to study demyelination and remyelination in the central nervous system. Brain Pathol 11**:** 107-116

McMahon EJ, Cook DN, Suzuki K, Matsushima GK (2001) Absence of macrophage-inflammatory protein-1alpha delays central nervous system demyelination in the presence of an intact blood-brain barrier. J Immunol 167**:** 2964-2971

Merkler D, Boretius S, Stadelmann C, Ernsting T, Michaelis T, Frahm J, Bruck W (2005) Multicontrast MRI of remyelination in the central nervous system. NMR Biomed 18**:** 395-403

Messori L, Casini A, Gabbiani C, Sorace L, Muniz-Miranda M, Zatta P (2007) Unravelling the chemical nature of copper cuprizone. Dalton Trans**:** 2112-2114

Mitelman SA, Brickman AM, Shihabuddin L, Newmark RE, Hazlett EA, Haznedar MM, Buchsbaum MS (2007) A comprehensive assessment of gray and white matter volumes and their relationship to outcome and severity in schizophrenia. Neuroimage 37**:** 449-462

Miyake T, Kung CK, Goldwasser E (1977) Purification of human erythropoietin. J Biol Chem 252**:** 5558-5564

Mizuno K, Hida H, Masuda T, Nishino H, Togari H (2008) Pretreatment with low doses of erythropoietin ameliorates brain damage in periventricular leukomalacia by targeting late oligodendrocyte progenitors: a rat model. Neonatology 94**:** 255-266

Moharregh-Khiabani D, Blank A, Skripuletz T, Miller E, Kotsiari A, Gudi V, Stangel M (2010) Effects of fumaric acids on cuprizone induced central nervous system de- and remyelination in the mouse. PLoS One 5**:** e11769

Morell P, Barrett CV, Mason JL, Toews AD, Hostettler JD, Knapp GW, Matsushima GK (1998) Gene expression in brain during cuprizone-induced demyelination and remyelination. Mol Cell Neurosci 12**:** 220-227

Morishita E, Masuda S, Nagao M, Yasuda Y, Sasaki R (1997) Erythropoietin receptor is expressed in rat hippocampal and cerebral cortical neurons, and erythropoietin prevents in vitro glutamate-induced neuronal death. Neuroscience 76**:** 105-116

Nagai A, Nakagawa E, Choi HB, Hatori K, Kobayashi S, Kim SU (2001) Erythropoietin and erythropoietin receptors in human CNS neurons, astrocytes, microglia, and oligodendrocytes grown in culture. J Neuropathol Exp Neurol 60**:** 386-392

Nave KA (2010) Myelination and support of axonal integrity by glia. Nature 468**:** 244-252

Nilsson G (1950) A New Colour Reaction on Copper and Certain Carbonyl Compounds. Acta Chemica Scandinavica 4**:** 205

Noguchi CT, Asavaritikrai P, Teng R, Jia Y (2007) Role of erythropoietin in the brain. Crit Rev Oncol Hematol 64**:** 159-171

Norkute A, Hieble A, Braun A, Johann S, Clarner T, Baumgartner W, Beyer C, Kipp M (2009) Cuprizone treatment induces demyelination and astrocytosis in the mouse hippocampus. J Neurosci Res 87**:** 1343-1355

Pasquini LA, Calatayud CA, Bertone Una AL, Millet V, Pasquini JM, Soto EF (2007) The neurotoxic effect of cuprizone on oligodendrocytes depends on the presence of pro-inflammatory cytokines secreted by microglia. Neurochem Res 32**:** 279-292

Pattison IH, Jebbett JN (1971) Histopathological similarities between scrapie and cuprizone toxicity in mice. Nature 230**:** 115-117

Pattison IH, Jebbett JN (1973) Clinical and histological recovery from the scrapie-like spongiform encephalopathy produced in mice by feeding them with cuprizone. J Pathol 109**:** 245-250

Peterson RE, Bollier ME (1955) Spectrophotometric Determination of Serum Copper with Biscyclohexanoneoxalyldihydrazone. Analytical Chemistry 27**:** 1195-1197

Radyushkin K, El-Kordi A, Boretius S, Castaneda S, Ronnenberg A, Reim K, Bickeboller H, Frahm J, Brose N, Ehrenreich H (2010) Complexin2 null mutation requires a 'second hit' for induction of phenotypic changes relevant to schizophrenia. Genes Brain Behav 9**:** 592-602

Remington LT, Babcock AA, Zehntner SP, Owens T (2007) Microglial recruitment, activation, and proliferation in response to primary demyelination. Am J Pathol 170**:** 1713-1724

Sakanaka M, Wen TC, Matsuda S, Masuda S, Morishita E, Nagao M, Sasaki R (1998) In vivo evidence that erythropoietin protects neurons from ischemic damage. Proc Natl Acad Sci U S A 95**:** 4635-4640

Sargin D, Friedrichs H, El-Kordi A, Ehrenreich H (2010) Erythropoietin as neuroprotective and neuroregenerative treatment strategy: Comprehensive overview of 12 years of preclinical and clinical research. Best Pract Res Clin Anaesthesiol 24**:** 573-594

Sargin D, Hassouna I, Sperling S, Siren AL, Ehrenreich H (2009) Uncoupling of neurodegeneration and gliosis in a murine model of juvenile cortical lesion. Glia 57**:** 693-702

Sasaki R, Masuda S, Nagao M (2001) Pleiotropic functions and tissue-specific expression of erythropoietin. News Physiol Sci 16**:** 110-113

Sattler MB, Merkler D, Maier K, Stadelmann C, Ehrenreich H, Bahr M, Diem R (2004) Neuroprotective effects and intracellular signaling pathways of erythropoietin in a rat model of multiple sclerosis. Cell Death Differ 11 Suppl 2**:** S181-192

Savino C, Pedotti R, Baggi F, Ubiali F, Gallo B, Nava S, Bigini P, Barbera S, Fumagalli E, Mennini T et al (2006) Delayed administration of erythropoietin and its non-erythropoietic derivatives ameliorates chronic murine autoimmune encephalomyelitis. J Neuroimmunol 172**:** 27-37

Shingo T, Sorokan ST, Shimazaki T, Weiss S (2001) Erythropoietin regulates the in vitro and in vivo production of neuronal progenitors by mammalian forebrain neural stem cells. J Neurosci 21**:** 9733-9743

Siren AL, Ehrenreich H (2001) Erythropoietin--a novel concept for neuroprotection. Eur Arch Psychiatry Clin Neurosci 251**:** 179-184

Siren AL, Knerlich F, Poser W, Gleiter CH, Bruck W, Ehrenreich H (2001) Erythropoietin and erythropoietin receptor in human ischemic/hypoxic brain. Acta Neuropathol 101**:** 271-276

Skripuletz T, Bussmann JH, Gudi V, Koutsoudaki PN, Pul R, Moharregh-Khiabani D, Lindner M, Stangel M (2010a) Cerebellar cortical demyelination in the murine cuprizone model. Brain Pathol 20**:** 301-312

Skripuletz T, Lindner M, Kotsiari A, Garde N, Fokuhl J, Linsmeier F, Trebst C, Stangel M (2008) Cortical demyelination is prominent in the murine cuprizone model and is strain-dependent. Am J Pathol 172**:** 1053-1061

Skripuletz T, Miller E, Moharregh-Khiabani D, Blank A, Pul R, Gudi V, Trebst C, Stangel M (2010b) Beneficial effects of minocycline on cuprizone induced cortical demyelination. Neurochem Res 35**:** 1422-1433

Song SK, Yoshino J, Le TQ, Lin SJ, Sun SW, Cross AH, Armstrong RC (2005) Demyelination increases radial diffusivity in corpus callosum of mouse brain. Neuroimage 26**:** 132-140

Stidworthy MF, Genoud S, Suter U, Mantei N, Franklin RJ (2003) Quantifying the early stages of remyelination following cuprizone-induced demyelination. Brain Pathol 13**:** 329-339

Sugawa M, Sakurai Y, Ishikawa-Ieda Y, Suzuki H, Asou H (2002) Effects of erythropoietin on glial cell development; oligodendrocyte maturation and astrocyte proliferation. Neurosci Res 44**:** 391-403

Sun SW, Liang HF, Trinkaus K, Cross AH, Armstrong RC, Song SK (2006) Noninvasive detection of cuprizone induced axonal damage and demyelination in the mouse corpus callosum. Magn Reson Med 55**:** 302-308

Suzuki K, Kikkawa Y (1969) Status spongiosus of CNS and hepatic changes induced by cuprizone (biscyclohexanone oxalyldihydrazone). Am J Pathol 54**:** 307-325

Taylor LC, Puranam K, Gilmore W, Ting JP, Matsushima GK (2010) 17beta-estradiol protects male mice from cuprizone-induced demyelination and oligodendrocyte loss. Neurobiol Dis 39**:** 127-137

Thorne M, Moore CS, Robertson GS (2009) Lack of TIMP-1 increases severity of experimental autoimmune encephalomyelitis: Effects of darbepoetin alfa on TIMP-1 null and wild-type mice. J Neuroimmunol 211**:** 92-100

Torkildsen O, Brunborg LA, Milde AM, Mork SJ, Myhr KM, Bo L (2009a) A salmon based diet protects mice from behavioural changes in the cuprizone model for demyelination. Clin Nutr 28**:** 83-87

Torkildsen O, Brunborg LA, Thorsen F, Mork SJ, Stangel M, Myhr KM, Bo L (2009b) Effects of dietary intervention on MRI activity, de- and remyelination in the cuprizone model for demyelination. Exp Neurol 215**:** 160-166

Tsai PT, Ohab JJ, Kertesz N, Groszer M, Matter C, Gao J, Liu X, Wu H, Carmichael ST (2006) A critical role of erythropoietin receptor in neurogenesis and post-stroke recovery. J Neurosci 26**:** 1269-1274

Uranova NA, Vikhreva OV, Rachmanova VI, Orlovskaya DD (2011) Ultrastructural Alterations of Myelinated Fibers and Oligodendrocytes in the Prefrontal Cortex in Schizophrenia: A Postmortem Morphometric Study. Schizophrenia Research and Treatment 2011

Vandesompele J, De Preter K, Pattyn F, Poppe B, Van Roy N, De Paepe A, Speleman F (2002) Accurate normalization of real-time quantitative RT-PCR data by geometric averaging of multiple internal control genes. Genome Biol 3**:** RESEARCH0034

Venturini G (1973) Enzymic activities and sodium, potassium and copper concentrations in mouse brain and liver after cuprizone treatment in vivo. J Neurochem 21**:** 1147-1151

Villa P, Bigini P, Mennini T, Agnello D, Laragione T, Cagnotto A, Viviani B, Marinovich M, Cerami A, Coleman TR et al (2003) Erythropoietin selectively attenuates cytokine production and inflammation in cerebral ischemia by targeting neuronal apoptosis. J Exp Med 198**:** 971-975

Vitellaro-Zuccarello L, Mazzetti S, Madaschi L, Bosisio P, Gorio A, De Biasi S (2007) Erythropoietin-mediated preservation of the white matter in rat spinal cord injury. Neuroscience 144**:** 865-877

Voss EV, Skuljec J, Gudi V, Skripuletz T, Pul R, Trebst C, Stangel M (2012) Characterisation of microglia during de- and remyelination: can they create a repair promoting environment? Neurobiol Dis 45**:** 519-528

Wergeland S, Torkildsen O, Myhr KM, Aksnes L, Mork SJ, Bo L (2011) Dietary vitamin D3 supplements reduce demyelination in the cuprizone model. PLoS One 6**:** e26262

Werner SR, Saha JK, Broderick CL, Zhen EY, Higgs RE, Duffin KL, Smith RC (2010) Proteomic analysis of demyelinated and remyelinating brain tissue following dietary cuprizone administration. J Mol Neurosci 42**:** 210-225

Wetlesen CU (1957) Rapid spectrophotometric determination of copper in iron, steel and ferrous alloys. Analytica Chimica Acta 16**:** 268-270

Xiao L, Xu H, Zhang Y, Wei Z, He J, Jiang W, Li X, Dyck LE, Devon RM, Deng Y et al (2008) Quetiapine facilitates oligodendrocyte development and prevents mice from myelin breakdown and behavioral changes. Mol Psychiatry 13**:** 697-708

Xu H, Yang HJ, McConomy B, Browning R, Li XM (2010) Behavioral and neurobiological changes in C57BL/6 mouse exposed to cuprizone: effects of antipsychotics. Front Behav Neurosci 4**:** 8

Xu H, Yang HJ, Rose GM, Li XM (2011) Recovery of behavioral changes and compromised white matter in C57BL/6 mice exposed to cuprizone: effects of antipsychotic drugs. Front Behav Neurosci 5**:** 31

Xu H, Yang HJ, Zhang Y, Clough R, Browning R, Li XM (2009) Behavioral and neurobiological changes in C57BL/6 mice exposed to cuprizone. Behav Neurosci 123**:** 418-429

Yamada M, Burke C, Colditz P, Johnson DW, Gobe GC (2011) Erythropoietin protects against apoptosis and increases expression of non-neuronal cell markers in the hypoxia-injured developing brain. J Pathol 224**:** 101-109

Yang HJ, Wang H, Zhang Y, Xiao L, Clough RW, Browning R, Li XM, Xu H (2009) Region-specific susceptibilities to cuprizone-induced lesions in the mouse forebrain: Implications for the pathophysiology of schizophrenia. Brain Res 1270**:** 121-130

Yatsiv I, Grigoriadis N, Simeonidou C, Stahel PF, Schmidt OI, Alexandrovitch AG, Tsenter J, Shohami E (2005) Erythropoietin is neuroprotective, improves functional recovery, and reduces neuronal apoptosis and inflammation in a rodent model of experimental closed head injury. FASEB J 19**:** 1701-1703

Youssoufian H, Longmore G, Neumann D, Yoshimura A, Lodish HF (1993) Structure, function, and activation of the erythropoietin receptor. Blood 81**:** 2223-2236

Yu X, Shacka JJ, Eells JB, Suarez-Quian C, Przygodzki RM, Beleslin-Cokic B, Lin CS, Nikodem VM, Hempstead B, Flanders KC et al (2002) Erythropoietin receptor signalling is required for normal brain development. Development 129**:** 505-516

Yuan R, Maeda Y, Li W, Lu W, Cook S, Dowling P (2008) Erythropoietin: a potent inducer of peripheral immuno/inflammatory modulation in autoimmune EAE. PLoS One 3**:** e1924

Zanjani ED, Poster J, Burlington H, Mann LI, Wasserman LR (1977) Liver as the primary site of erythropoietin formation in the fetus. J Lab Clin Med 89**:** 640-644

Zatta P, Raso M, Zambenedetti P, Wittkowski W, Messori L, Piccioli F, Mauri PL, Beltramini M (2005) Copper and zinc dismetabolism in the mouse brain upon chronic cuprizone treatment. Cell Mol Life Sci 62**:** 1502-1513

Zhang J, Li Y, Cui Y, Chen J, Lu M, Elias SB, Chopp M (2005) Erythropoietin treatment improves neurological functional recovery in EAE mice. Brain Res 1034**:** 34-39

Zhang L, Chopp M, Zhang RL, Wang L, Zhang J, Wang Y, Toh Y, Santra M, Lu M, Zhang ZG (2010) Erythropoietin amplifies stroke-induced oligodendrogenesis in the rat. PLoS One 5**:** e11016

Zhang Y, Xu H, Jiang W, Xiao L, Yan B, He J, Wang Y, Bi X, Li X, Kong J et al (2008) Quetiapine alleviates the cuprizone-induced white matter pathology in the brain of C57BL/6 mouse. Schizophr Res 106**:** 182-191

6 SUPPLEMENT

6.1 Certificate of the toxicological analysis of cuprizone pellets

UNIVERSITÄTSMEDIZIN UMG GÖTTINGEN

Universitätsmedizin - 37099 Göttingen
Klinisch-toxikologisches Labor

Zentrum Pharmakologie und Toxikologie
Pharmakologisch-toxikologisches Servicezentrum (PTS)
Klinisch-toxikologisches Labor
Dipl.-Chem. Dr. Herbert Desel Leiter

Prof. Dr. Hannelore Ehrenreich
Max-Planck-Institut für Experimentelle Medizin
Klinische Neurowissenschaften
Hermann-Rein-Straße 3
37075 Göttingen

Dr. Herbert Desel Ansprechpartner
37099 Göttingen Postpost
Robert-Koch-Str. 40, 37075 Göttingen Adresse
0551-39 9613 Telefon
0551-38 31 881 Fax
hdesel@med.uni-goettingen.de E-Mail

12.09.2008 Datum

Toxikologische Untersuchung

Patientendaten	Untersuchungsmaterial	Befund-Nr
ohne	Asservat Futterprobe (Cuprizon-Pellets, 08.09.08)	8153
	Asservat Futterprobe (Kontroll-Pellets , 08.09.08)	
*	Asservat (Cuprizon-Vergleichssubstanz , 08.09.08)	
Pat. Nr.: Sub0162		

Grund der Untersuchung: Qualitätskontrolle eines Produktes

Befundbericht

Ergebnisse:

Asservat Futterprobe (Cuprizon-Pellets, 08.09.08):
Chemische Vorprobe (111):
Cuprizone: qualitativ nachgewiesen (*Substanz*)
Asservat Futterprobe (Kontroll-Pellets , 08.09.08):
Chemische Vorprobe (111):
Cuprizone: nicht nachweisbar (*Substanz*)
Asservat (Cuprizon-Vergleichssubstanz , 08.09.08):
Chemische Vorprobe (111):
Cuprizone: qualitativ nachgewiesen (*Substanz*)

Nachweismethoden:

(111) Chemische Vorprobe

1 von 2

Beurteilung:

In der Probe der Vergleichssubstanz und in der Probe des Cuprizon-Pellets konnte Cuprizon mittels der von Messori L et al. (2007) beschriebenen Methode als blauer Cuprizon-Kupfer-Komplex nachgewiesen werden.

In der Probe der Kontrollpellets wurde mit gleicher Methodik kein Cuprizon nachgewiesen.

Für eine detaillierte Erläuterung und Diskussion der Unteruchungsergebnisse insbesondere hinsichtlich auch einer pH-Abhängigkeit der Cuprizon-Kupfer-Komplex-Bildung, stehen wir Ihnen gern zur Verfügung. Bitte rufen Sie uns an (39-14465, -9613).

Dr. Herbert Desel, Dipl.-Chem.
Facharzt für Pharmakologie und Toxikologie
Klinischer Toxikologe GTFCh

Hartmud Neurath
Chemiker

Das Klinisch-toxikologische Labor des PTS nimmt regelmäßig mit Erfolg an Ringversuchen der GTFCh (www.gtfch.org) zur Qualitätssicherung der Untersuchungsverfahren teil.

www.klintox.de - Informationen zum Klinisch-toxikologischen Labor

6.2 Accepted first-author and co-author publications

6.2.1 Publication of first-authorship 1

Nora Hagemeyer, Susann Boretius, Christoph Ott, Axel von Streitberg, Henrike Welpinghus, Swetlana Sperling, Jens Frahm, Mikael Simons, Pietro Ghezzi, Hannelore Ehrenreich (2012). Erythropoietin attenuates neurological and histological consequences of toxic demyelination in mice. *Molecular Medicine, [Epub ahead of print].*

Due to copyright reasons, please check the journals homepage:
http://www.molmed.org/pdfstore/11_457_Hagemeyer.pdf

6.2.2 Publication of first-authorship 2

Nora Hagemeyer[*], Sandra Goebbels[*], Sergi Papiol[*], Anne Kästner, Sabine Hofer, Martin Begemann, Ulrike C. Gerwig, Susann Boretius, Georg L. Wieser, Anja Ronnenberg, Artem Gurvich, Stephan H. Heckers, Jens Frahm, Klaus-Armin Nave, Hannelore Ehrenreich (2012). A myelin gene causative of a catatonia-depression syndrome upon aging. *EMBO Molecular Medicine* ***4****, 6.*

*These authors contributed equally to this work

Due to copyright reasons, please check the journals homepage:
http://onlinelibrary.wiley.com/doi/10.1002/emmm.201200230/pdf

6.2.3 Publication of co-authorship 1

Hannes Treiber, **Nora Hagemeyer**, Hannelore Ehrenreich, Mikael Simons (2011). BACE1 in central nervous system myelination revisited. *Molecular Psychiatry **17**, 3.*

Due to copyright reasons, please check the journals homepage:
http://www.nature.com/mp/journal/v17/n3/pdf/mp2011140a.pdf

6.2.4 Publication of co-authorship 2

Bartosz Adamcio, Swetlana Sperling, **Nora Hagemeyer**, Gail Walkinshaw and Hannelore Ehrenreich (2010). Hypoxia inducible factor stabilization leads to lasting improvement of hippocampal memory in healthy mice. *Behavioural Brain Research **208**,1.*

Due to copyright reasons, please check the journals homepage:
http://ac.els-cdn.com/S0166432809006755/1-s2.0-S0166432809006755-main.pdf?_tid=fa128822b5b6eeedc664b13cf9fcf1a6&acdnat=1338370927_e255be0cbd65ecca8bcbf10ebb3a4f4d

6.3 Curriculum vitae

Personal data

Name	Nora Hagemeyer
Address	Max Planck Institute of Experimental Medicine Hermann-Rein-Straße 3 37075 Göttingen
Date of birth	April, 7th 1983
Place of birth	Göttingen, Germany
Nationality	German
E-mail	norahagemeyer@gmx.de

Education

since 2008	PhD student - Center for Systems Neuroscience, Graduate School for Neuroscience and Molecular Biosciences, Göttingen, Germany Supervisor: Prof. H. Ehrenreich, Division of Clinical Neuroscience, Max Planck Institute of Experimental Medicine, Göttingen, Germany
Nov 2007	Diploma in Biology, University of Bremen, Germany
Jun 2002	German „Abitur“ at the Georg-Christoph-Lichtenberg Gesamtschule, Göttingen, Germany